PHOTOCHEMICAL AND PHOTOPHYSICAL STUDIES OF A FEW BISCHROMOPHORIC SYSTEMS

THESIS SUBMITTED TO
COCHIN UNIVERSITY OF SCIENCE & TECHNOLOGY
IN PARTIAL FULFILLMENT OF THE REQUIREMENTS
FOR THE DEGREE OF
DOCTOR OF PHILOSOPHY
IN CHEMISTRY
UNDER THE FACULTY OF SCIENCE

BY

GISHA GEORGE

COCHIN UNIVERSITY OF
SCIENCE AND TECHNOLOGY

DEPARTMENT OF APPLIED CHEMISTRY
COCHIN UNIVERSITY OF SCIENCE & TECHNOLOGY
COCHIN-22, KERALA, INDIA

JANUARY 2010

CERTIFICATE

This is to certify that the work embodied in the thesis entitled:

"Photochemical and Photophysical Studies of a Few Bischromophoric Systems"

has been carried out by Ms. Gisha George under my supervision at the Department of Applied Chemistry, Cochin University of Science & Technology and the same has not been submitted elsewhere for a degree.

(P. A. Unnikrishnan)

Kochi-22   **Thesis Supervisor**
January 11, 2010

DECLARATION

I hereby declare that the work presented in this thesis entitled: **"Photochemical and Photophysical Studies of a Few Bischromophoric Systems"** is original and was carried out by me independently under the supervision of Dr. P. A. Unnikrishnan, Lecturer in Organic Chemistry, Department of Applied Chemistry, Cochin University of Science and Technology, Kochi-682 022, India, and has not been included in any other thesis submitted previously for the award of any other degree.

Gisha George

Kochi-22
January 11, 2010

Acknowledgements

Gisha George

CONTENTS

i

Chapter 4. **Investigation of Photophysical Properties of a few Bispyrene systems**

Chapter 5.   Synthesis of a Few Bisdibenzobarrelene Systems

Preface

The thesis entitled **"Photochemical and Photophysical Studies of a Few Bischromophoric Systems"** is divided into 5 chapters.

In **Chapter 1**, photochemistry and photophysics of bisaromatic systems is discussed in the context of more complex multichromophoric systems. **Chapter 2** presents synthesis and photochemical studies of a few bisaromatic systems and effect of structure and geometry on their reactivity. **Chapter 3** deals with synthesis, structural investigation and examination of the effect of structure and geometry on photochemistry and photophysics of bisanthracene systems. **Chapter 4** deals with the investigation of photophysical properties of a few bispyrene systems. In **Chapter 5**, synthesis of a few bisdibenzobarrelene systems is dicussed.

Chapter 1: Photochemistry and Photophysics of Multichromophoric Compounds: Fundamental Concepts and Applications

Large, well-defined multichromophoric arrays are receiving much attention due to the control they offer over energy and electron transfer processes in restricted space. Despite the progress that has been made in the synthesis of complex molecules, formation of multichromophoric arrays in single molecule of high symmetry is a challenge on its own. Covalent multichromophoric arrays are connected through linkers in such a manner that they can be rigid or non-rigid controlling orientation of the chromophoric groups. By contrast, better models for quantitative study of energy transfer are provided by rigid covalently linked donor-bridge-acceptor systems in which the chromophores are held with well-defined distances and orientation.

A brief introduction on the state of the art on multichromophoric systems is included in **Chapter 1**. Intramolecular energy transfer is reviewed from several perspectives, such as the generally accepted mechanism and molecular structure dependence. Identification of the research problem and outline for its execution are also mentioned herein. A brief description of bischromophoric systems and the objectives of the present investigation and identification of the research problem and its significance are also presented.

Chapter 2: Synthesis and Photochemical Studies of a few Bisaromatic systems: Structure - Activity Relationships

In **Chapter 2**, we discuss the synthesis of bischromophoric molecules containing benzene, naphthalene, anthracene and pyrene as donor and acceptor linked through cyclopentanone units (Chart **1**). Some unique molecules such as bischromophores linked by rigid bridges were designed to serve as models for studying excited state interaction between constituent chromophore residues.
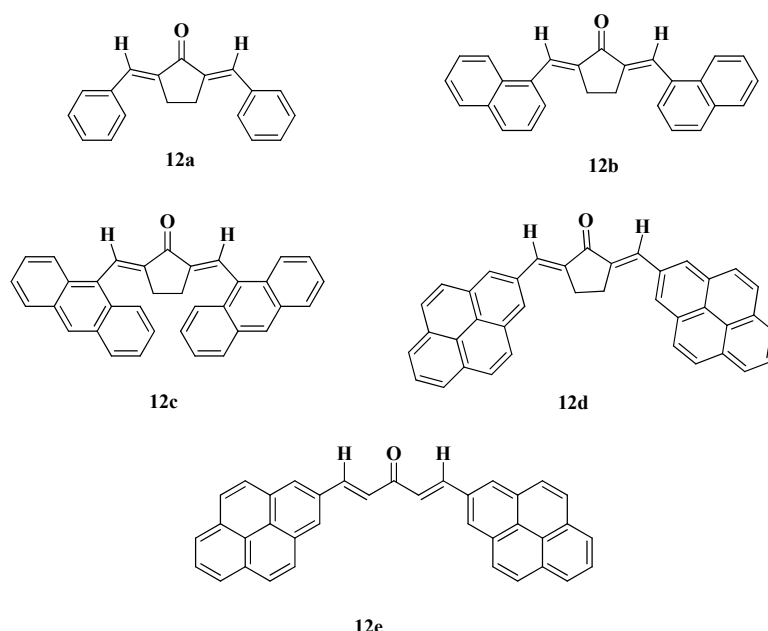
Chart I

Though these molecules appear similar, they exhibit remarkable structural variety. Absorption and NMR spectral data supports extended conjugation in these systems. In continuation, we examined the photochemistry of the above diarylidenecycloalkanones. Photochemical studies have shown that *cis-trans* isomerisation takes place for bisphenyl and bisnaphthyl compounds, while bisanthracene and bispyrene were unreactive towards photolysis. Several reasons can be cited to account for the dichotomous behaviour of these closely related bisaromatics:

1. With anthracene and pyrene residues present, excited state energy of the compounds may not be sufficient to initiate *cis-trans* isomerisation. Exciton coupling is expected to further reduce the excited state energy.

2. Excimer formation may be acting as an energy wastage process.

3. Adverse steric interaction between cyclopentanone methylene and aromatic residues may be preventing rotation around the double bond.

4. The carbonyl group may be responsible for preventing rotation around the double bond.

Chapter 3: Synthesis, Photochemical and Photophysical Studies of Bisanthracenes - Geometry Effects

Our attempts to determine the actual reason for prevention of *cis-trans* isomerisation of bisanthracenes such as those discussed in **Chapter 2** are described in **Chapter 3**. In order to unravel the exact factor preventing the reaction of bianthracenylidenecyclopentanones, we synthesized a series of bisanthracene compounds of increasing cycloalkanone ring size (Chart **II**) and examined their geometry and photophysical properties. Slight variation in the nature of spacers brought drastic changes in the geometry of these bisanthracenes. We have systematically investigated the effects of geometry in deciding photophysical and photochemical properties of bisanthracenes.

Hence, this chapter describes our attempt to understand the effect of geometry and nature of chromophore in determining those properties. Where appropriate, model compounds were designed, synthesized and examined to test the veracity of our postulates.
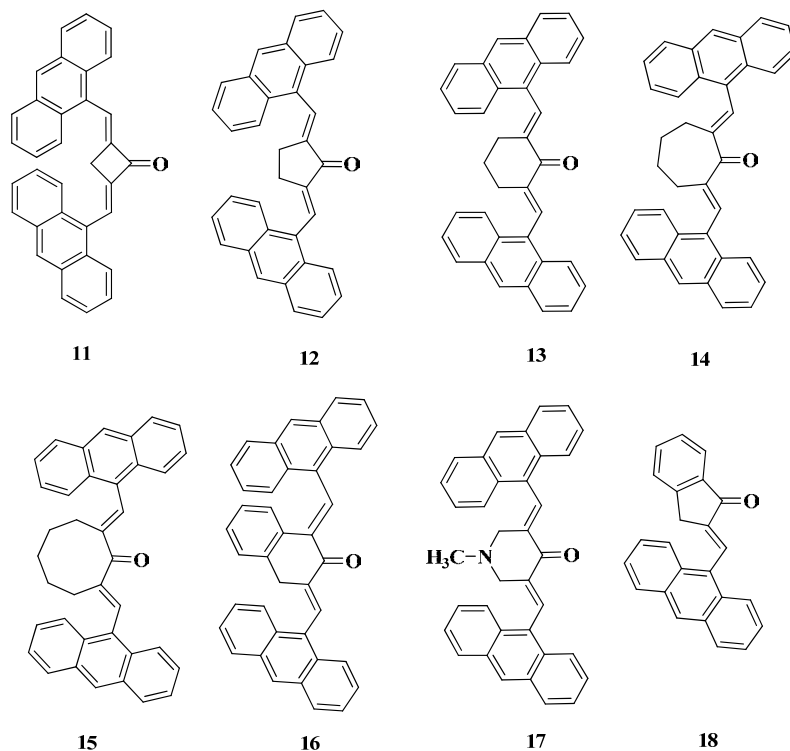
Chart II

Photochemical and photophysical properties of these bisanthracenes exhibited dramatic variation that is attributable to the relative geometry of the significant components: two anthracene and the cycloalkanone building blocks. Geometry of **12, 14** and **15** were established on the basis of single crystal X-ray analysis and molecular modelling studies. In **12** and **13**, the two anthracene components maintain cofacial orientation while the anthracene units are perpendicular to the enone component in **14** and **15**. While significant ground state as well as excited state interactions between

components were apparent for **12** and **13**, negligible interactions were observed for **14** and **15**. Interestingly, while **11-13** did not undergo any change upon irradiation, **14** and **15** underwent interesting rearrangement to give ring-expanded products. We conclude that, *cis-trans* isomerisation is the key step in determining photoreaction of these types of compounds.

n=0,1,2,3
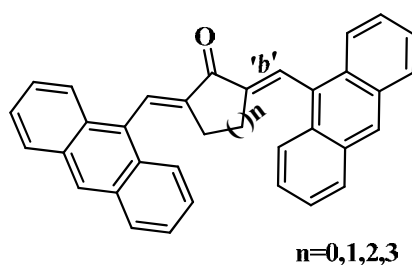
Figure 1

Constrained geometry prevented **11-13** from undergoing photochemical rearrangement involving rotation around bond '*b*' while such constraints are absent for **14** and **15**. Our investigations on suitable model compounds **16**-**18** ruled out the role of exciton coupling and consequent lowering of excited state energy, adverse interaction between methylene group and aromatic residues, and possibility of excimer formation in controlling the photochemistry of these bisanthracenes.

Chapter 4: Investigations on Photophysical Properties of a few Bispyrene Systems

As an extension to our studies on effects of geometry on photochemical and photophysical behaviour of bisanthracenes, we synthesised a few bispyrene systems (Chart **III**) with a view to examine their photochemical and photophysical behaviour. In this chapter, we present an overview of their interesting properties and a detailed analysis of the results

obtained. Due to poor solubility of these compounds in most solvents, we could not examine their photochemistry.
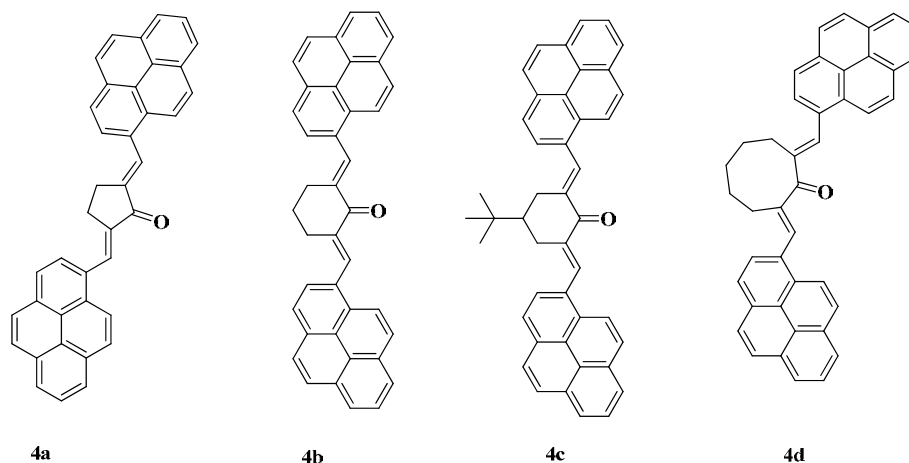
Chart III

The photophysical observations with bispyrene compounds **4a-d** were highly interesting. We noted significant solvatochromic behaviour in the case of bispyrene system with cyclopentanone spacer. Pyrene is one of the most widely used neutral fluorescence probes. Photophysical observations of bispyrene systems confirmed the conclusions regarding the bisanthracenes on the effect of cycloalkanone ring size on geometry and photophysical behaviour of bisaromatic compounds. Fluorescence emission studies and lifetime studies on **4a** confirmed its highly conjugated single excited state. Increasing ring size of spacer from cyclopentanone greatly affected the properties of other bispyrene systems. Solvatochromic shifts of pyrene excimer fluorescence were obtained in both polar and non-polar solvents.

Chapter 5: Synthesis of a few Bisdibenzobarrelene Systems

Fifth chapter of the thesis deals with the synthesis and photochemical studies of several bisdibenzobarrelenes. Dibenzocyclooctatetraene and

dibenzosemibullvalene are the photoproducts obtained respectively through the singlet excited state and triplet excited state of dibenzobarrelenes. So, examining the photochemical behaviour of novel bisdibenzobarrelenes with alkenone spacer is interesting. Our attempts on examining the photochemistry of bisdibenzobarrelenes are reported in this chapter. This chapter can also be considered as an extension to our studies on effects of geometry on photochemical and photophysical behaviour of bischromophoric systems. Structure of various bisbarrelenes examined by us is given in Chart **IV**.
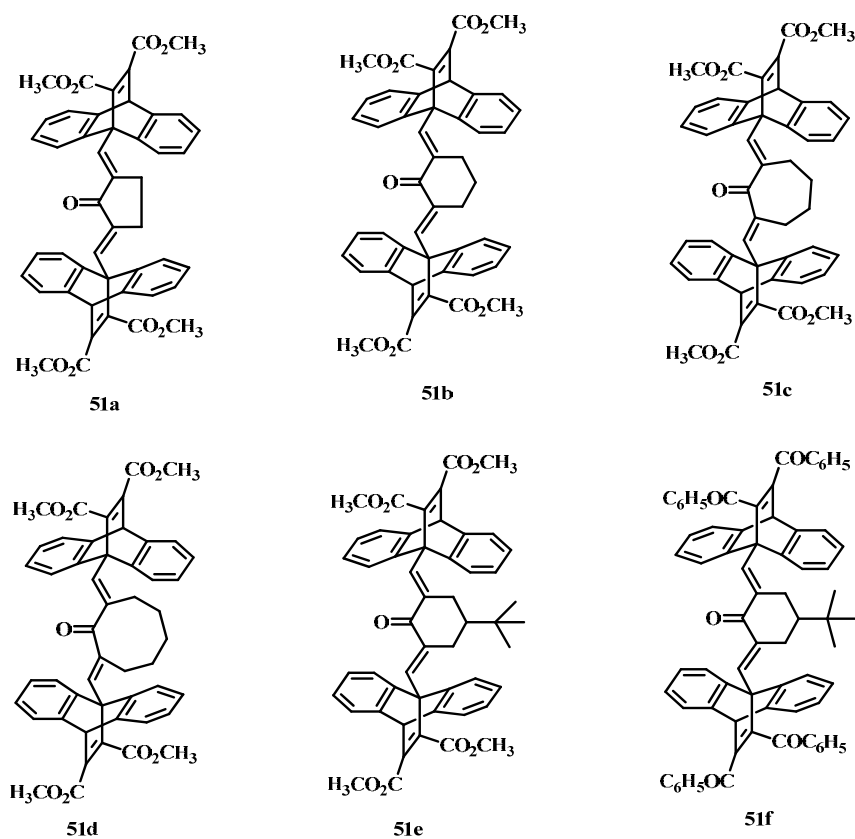
Chart IV

The bisdibenzobarrelenes were found to be mostly stable under irradiation conditions employed by us. They exhibited negligible

fluorescence.   Hence, we conclude that fast radiationless decay from the excited state is preventing them from undergoing photoreaction.

Note: *The numbers given to various compounds herein correspond to those given in respective chapters.*

PHOTOCHEMISTRY AND PHOTOPHYSICS OF MULTICHROMOPHORIC COMPOUNDS: FUNDAMENTAL CONCEPTS AND APPLICATIONS

1.1. Abstract

The present chapter gives an overview of multichromophoric compounds, which includes photophysical properties and mechanism of energy transfer in these systems. A survey including several selected examples of multichromophoric arrays is presented. Furthermore, a brief description of bischromophoric systems and the objectives of the present investigation are also discussed.

1.2. Introduction

Large, well-defined multichromophoric arrays are receiving much attention due to the control they offer over the energy and electron transfer processes in restricted space. Formation of these arrays can be accomplished by either covalent coupling of chromophore building blocks into a single molecule or by the self assembly of interacting monochromophoric species where they are held together by relatively weak non-covalent interactions like hydrogen bonds, van der Waals interactions, electrostatic interactions, metal ion co-ordination and donor-acceptor interactions or π-stacking.[1,2] Different interactions of monochromophoric systems are shown in Figure 1.1.

Isolated Organic Molecules

Aggregated Superstructure

Solid State

Aggregated Superstructure

Linked Organic Molecules
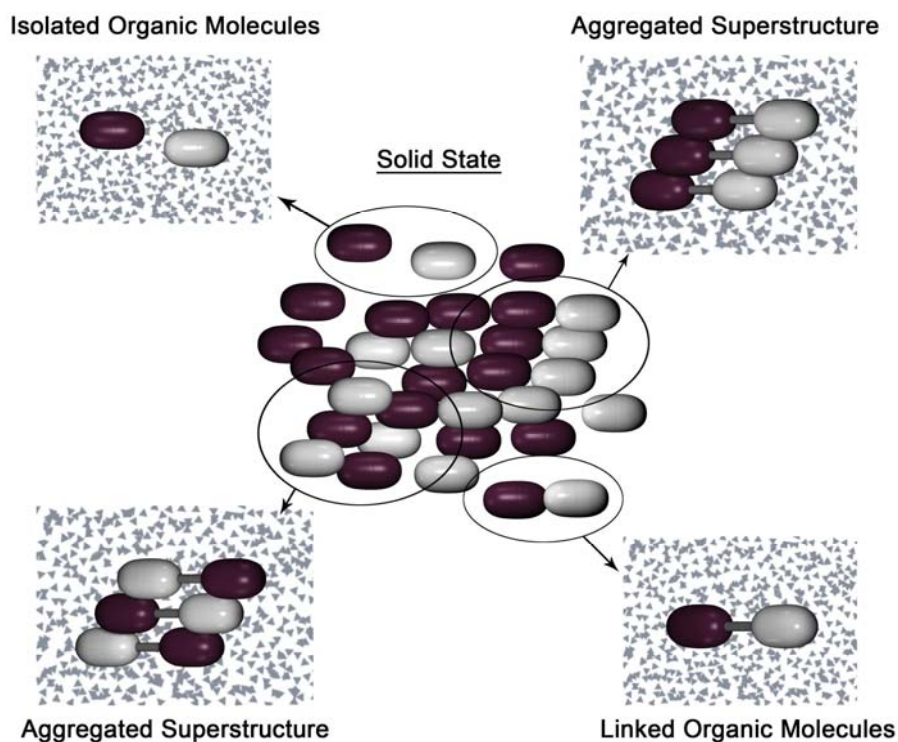
Figure 1.1: *Schematic representation of the morphology of a donor-acceptor system.*

The combined strength of these relatively weak intermolecular interactions, possessing different degrees of strength, directionality and dependence on distance and angles, determines the final architecture of the assembly. The close proximity of, or the interactions between multicomponent arrays as well as between individual segments that make up such arrays; can significantly affect their photophysical properties. The individual chromophores are weakly coupled electronically, such that the key optical, redox, and vibrational properties of a dimer (and larger arrays) are essentially the sum of those of the individual molecular components.

Despite the progress that has been made in the synthesis of complex molecules,[3] formation of multichromophoric arrays in single molecule of high symmetry is a challenge on its own. From mechanistic studies of the

intramolecular energy transfer process, it has been clearly demonstrated that factors at the molecular level, such as the nature of the chromophores, interchromophoric distance and orientation, and so on, play important roles in affecting the energy transfer process. In addition to the relative orientation of chromophores and size of the chromophoric system, nature of the linker also dictates the properties. Covalent multichromophoric arrays are connected through linkers in such a manner that they can be rigid or non-rigid controlling orientation of chromophoric groups. Molecules with flexible spacers (Figure 1.2), such as methylene-linked **1**[4] and ester-linked **2**[5] can adopt many conformations and hence, the measured rate constant for intramolecular energy transfer is an average over many conformations. Another disadvantage associated with flexible spacers is that several mechanisms can operate at the same time.
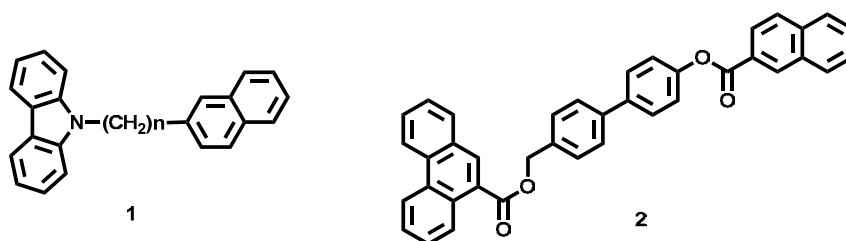
Figure 1.2: *Molecules with flexible spacers*

On the other hand, better models for quantitative study of energy transfer are provided by rigid covalently linked donor-bridge-acceptor systems in which the chromophores are held with well-defined distances and orientation. In order to regulate the orientation among chromophores by means of both covalent and non-covalent approaches, more convenient methods are still required to organize the chromophores in various well-defined manners. Therefore, large well-defined, chemically similar structures have been prepared by us from smaller molecules connecting through covalent

linkers. Slight variations in the nature of spacers have brought drastic changes in the orientation of the structures. This thesis addresses the photochemical and photophysical properties of such bischromophoric systems, and also is an attempt to understand the effect of molecular geometry and nature of chromophore in determining those properties. We investigated the effects of geometry in a more systematic way. Though orientation effects are well studied in covalent donor-acceptor arrays, the determination of geometry of aggregates is currently a tremendously active field; the influence of organizational effects on the photophysics within a superstructure is rarely the topic of interest.

Investigations of such well defined bischromophoric arrays might give information on the relation between the properties of these arrays and those of monochromophoric building blocks. Extrapolation of this knowledge by applying these relations to even larger architectures might facilitate relating molecular and material properties conceivable. A variety of techniques to study photophysical properties are available (e.g. UV/Vis and fluorescence spectroscopy, CD/ORD spectroscopy, non-linear optical techniques like electric field induced second harmonic generation (EFISHG)[6,7,8] and hyper Rayleigh scattering (HRS),[9,10,11] sub-picosecond transient spectroscopy, time resolved microwave conductivity (TRMC)[12,13] etc.

1.3. Photophysical Processes

Two different chromophores in close proximity with complementary electronic properties often exhibit photophysical processes that are not found in either of the pure materials. Two of the most fundamental and potentially useful photophysical reactions are energy transfer and electron (or charge) transfer. These transfer reactions form the heart of natural photosynthesis and are fundamental to the operation of artificial organic systems for solar light harvesting antennae complexes and photovoltaics. In this section the basic

principles of photoinduced energy and electron transfer reaction will be briefly discussed.

1.3.1. Electron Transfer Process

Electron transfer[14] occurs upon illumination of a chromophore pair. For electron transfer, either the donor or the acceptor may be photoexcited. In a system consisting of an electron donating moiety (D) and an electron accepting group (A), upon photoexcitation, an electron transfer can occur from the donor to the acceptor moiety, resulting in the creation of a charge-separated (CS) state (consisting of the corresponding radical cation and anion), from which charge recombination can take place to bring the system back to the ground state. Electron transfer can occur when the change in free energy for charge separation (ΔG_0) is negative. As a first approximation, this is achieved when the excited-state energy exceeds the energy difference between the oxidation potential of the donor [$E_{ox}(D)$] and the reduction potential of the acceptor [$E_{red}(A)$]. For donor-acceptor systems in solutions, the likelihood of an electron transfer reaction can be predicted by analysing the various contributions to the free energy (ΔG_0) according to Scheme 1.1, which also contains terms for the spatial separation of the ions and their solvation.[15]

$$\Delta G_{cs} = e\left[E_{ox}(D) - E_{red}(A)\right] - E_{oo} - \underbrace{\frac{e^2}{4\pi\varepsilon_o\varepsilon_s R_{cc}}}_{} - \underbrace{\frac{e^2}{8\pi\varepsilon_0}\left(\frac{1}{r^+} + \frac{1}{r^-}\right)\left(\frac{1}{\varepsilon_{ref}} - \frac{1}{\varepsilon_s}\right)}_{}$$

$$\underbrace{\qquad\qquad\qquad}_{\text{"polar driving force term"}} \quad \underbrace{\qquad}_{\text{"coulombic term"}} \quad \underbrace{\qquad\qquad}_{\text{"solvation term"}}$$

Scheme 1.1

The parameters involved in Scheme 1.1 are the electron charge (-*e*), the vacuum permittivity (ε_0), the relative permittivities of the solvent (ε_s)

and the reference solvent (ε_{ref}) used to determine the redox potentials, the centre-to-centre distance of positive and negative charges in the chromophores (R_{cc}), and the radii of the positive and negative ions ($r+$ and $r-$). The driving force ($-\Delta G_0$) can be directly linked to the kinetics of the reaction by the theory proposed by Marcus.[16]

1.3.2. Energy-Transfer Mechanism in Multichromophoric Systems

Multichromophoric systems can exhibit interesting optical and electronic properties due to the interactions between chromophore units that are near to each other. This may result in electron energy (exciton) transfer over the system, a process that constitutes the physical working mechanism in various kinds of relevant complex molecular aggregates, such as photosynthetic and autofluorescent proteins,[17,18] light-harvesting assemblies[19] and conjugated polymers.[20]

In absence of orbital overlap, electron energy transfer between nearby chromophores is generally caused by the transition dipole moment coupling, an interaction whose strength (U) decreases with the third power of the interchromophoric distance. The rate of the transfer process, however, is constrained by static (energy and geometry fluctuations) and dynamic (coupling to phonons) disorder in the system (Δ), which counter-balances the effect of dipole coupling on the optical properties of the assembly. Two limiting situations can be distinguished according to the U/Δ ratio. For large U/Δ values (i.e., large coupling strength due to short interchromophoric distances, low disorder), coherent energy transfer between adjacent chromophores holds, whose individual electronic functions superimpose to yield new exciton states delocalised over the entire system. The underlying basic principle is schematically represented in Figure 1.3.[21]
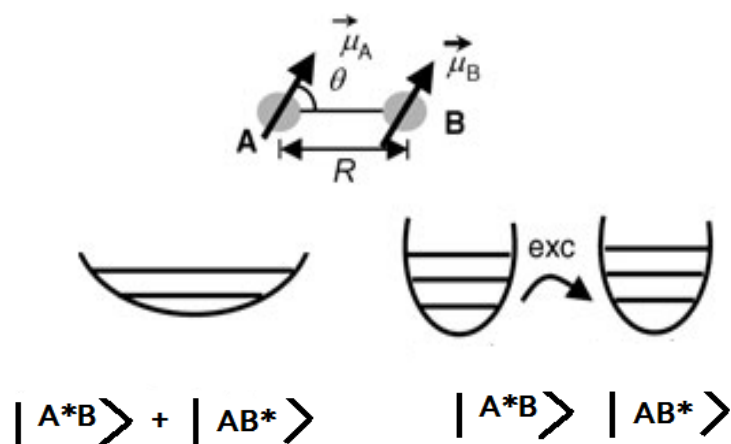
Figure 1.3: *Two limiting energy-transfer processes occurring on close-by molecules; a) In the strong coupling regime, the assembly behaves as a new single quantum system, and the energy is delocalised over the entire system. b) In the weak coupling regime, the molecules behave as separate entities preserving their spectral properties. Incoherent energy transfer occurs from a donor to an acceptor molecule.*

Accordingly, the assembly behaves as a new single-quantum system, whose optical properties significantly differs from those of the separate chromophores and critically depends on the orientation of the interacting dipoles. Whereas a head-to-tail alignment (*J* configuration) leads to an enhancement of the excited-state radiative rate (superradiance) together with red-shifted absorption and emission, a parallel transition dipole arrangement (*H* configuration) results in blue-shifted absorption followed by suppression of fluorescence emission.[21] On the other extreme, very low U/Δ^{21} values (i.e., small coupling strength due to large interchromophoric distances, high disorder) lead to Forster-type incoherent energy transfer between nearby chromophores (Figure 1.3), vibrational relaxation in the excited unit (donor) occurring before transfer to the adjacent chromophore (acceptor).[22] To attain optimal excitonic behaviour in multichromophoric assemblies, a well-defined close packing of the chromophores is thus required.

1.4. Applications of Multichromophoric Systems

It has been estimated that the average yearly incidence of solar radiation at the earth's surface amounts to several orders of magnitude more energy than is consumed by its population.[23] Clearly, harnessing this energy is an important endeavour that will reduce our dependence on fossil fuels. Indeed, our own existence depends on light-harvesting by the plethora of photosynthetic organisms in the biosphere. These organisms have evolved intricate and extremely efficient mechanisms for the transduction of light into chemical energy in the form of ATP.[24] The most studied of all photosynthetic systems, is probably that of purple bacteria.[25] The high resolution X-ray crystal structure of the photosynthetic unit (PSU) reveals a central reaction centre (RC) that is surrounded by light harvesting (LH) complexes (Figure 1.4).[26]
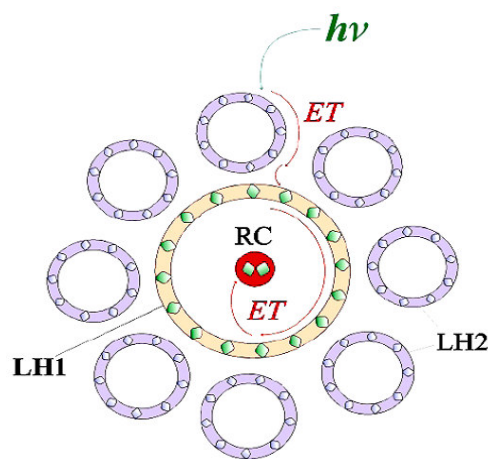
Figure 1.4: *Schematic representation of bacterial light-harvesting complexes (LH1 and LH2), showing the different protein-embedded light-absorbing porphyrinic pigments arranged in circles around the reaction centre (RC). The path of energy transfer (ET) is indicated by arrows.*

Here the photoactive molecules are rarely covalently bound but rather carefully positioned by supramolecular interactions. The solar light is captured in the two pigment-protein light-harvesting complexes and preserved

by circulating the energy within the cyclic arrays of bacteriochlorophyll molecules.

The LH1 complex is composed of a ring-shaped assembly of chlorophyll and carotenoid moieties embedded in a protein matrix that immediately surrounds the reaction centre. Similar ring-shaped assemblies, somewhat further removed from the reaction centre, make up the LH1 and LH2 complexes.[25] The role of these chlorophyll-containing assemblies is that of an antenna, absorbing photons that strike the relatively large surface area that they cover. Remarkably, the energy of any photon that strikes any of the several hundred chlorophylls within the extensive light harvesting system is transferred to the reaction centre with unit efficiency.[25] Following the initial charge separation reaction in the heart of the reaction centre, the photogenerated positive and negative charges are moved apart to suppress the recombination reaction. The energy of the resulting long-lived charges is subsequently used to drive biochemical processes within the bacteria. The conversion of solar light into valuable energy by natural or artificial photosynthesis is an appealing and intriguing process, making it an interesting topic for researchers in biology, physics and chemistry.[27] The most important, well-studied and illustrative system citing the application of multichromophoric system in nature is the photosynthetic reaction system in purple bacteria.[25]

In natural photosynthetic systems, by employing elaborate light harvesting antenna complexes, low intensity sunlight (280-900 nm) is efficiently absorbed and energy is funnelled to the reaction centres. The important mechanistic information extracted from studies on natural processes[28] led to ideas for the design of artificial reaction systems to mimic and possibly improve the solar energy conversion process based on photo induced electron transfer between electron donor and acceptor systems.[29] Therefore in analogy to natural multichromophoric system, a large number of multichromophoric systems have been synthesized. The preparation of

macromolecular assemblies composed of numerous light-collecting chromophores that transfer their energy to a single energy 'sink' at the core has been achieved in a number of diverse and creative ways. The underlying basic principle is schematically represented in Figure 1.5.
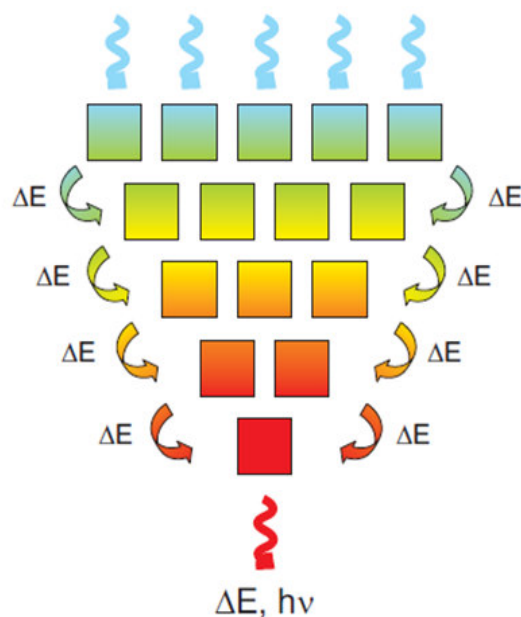
Figure 1.5: *Schematic representation of absorption of light by an array of chromophores is followed by sequential and directional energy transfer that leads the excitation energy to a reaction centre.*

The first examples are emerging where many chromophores with donor and acceptor electronic properties self-assemble into larger architectures by noncovalent bonding. Though electron and energy transfer processes continue to drive the synthesis of more complex systems, more recent focus has shifted towards other applications and functionalities of these structures. Major applications of these systems include: (1) self-assembly and self-organization of chromophoric arrays and aggregates into phototransistors and photonic devices; (2) self-assembled chromophoric squares for sensors, sieves, and catalysts; (3) spatially separated arrays of chromophores as sensors; (4) covalently bound arrays of different chromophores as photonic materials; and

(5) the development of molecular photonic devices such as solar cells, photonated molecular wires, light-emitting diodes, organic electronic components. All these takes place by absorbing light of specific wavelengths and undergoing excited-state energy and or charge transfer reactions. The versatile, optical, redox and photochemical properties of chromophores makes them ideally suited as components of the above molecular devices.

To introduce photoexcitation at a specific site, the array requires the use of accessory pigments. The ideal accessory pigment would exhibit the following features: (1) absorb strongly in the trough between the B and Q bands, (2) exhibit a singlet excited-state lifetime (preferably monophasic) that is sufficiently long to support highly efficient energy transfer, (3) undergo energy transfer without deleterious excited state quenching reactions, (4) exhibit a high level of stability, (5) provide compatibility with the synthetic building block approach, and (6) exhibit sufficient solubility for chemical processing.

In those arrays, photochemical processes, especially photo-induced energy and electron transfer are significantly affected by both electronic properties (excitation energy and redox potentials) and structural elements (the interchromophoric distance, orientation, and nature of the bridge) are critical parameters that control the kinetics of charge transfer reactions in molecular systems.

In the following paragraphs some illustrative examples of carefully designed multichromophoric systems with covalent/non-covalent linkers are explained. A covalent linker between the chromophores facilitated study of interactions between different photoactive and electroactive chromophores in close proximity.

Several elegant multi-porphyrin covalent arrays[30] have been prepared and used to study energy transport. Synthetic porphyrin-based arrays with well-defined architectures provide essential models for probing the mechanisms of energy and electron transfer analogous to those occurring in

biological systems and can serve as molecular photonic devices. They are important because of their striking photophysical and electrochemical properties, their remarkable stability, and their predictable and rigid structure. The multiporphyrin arrays are soluble in various organic solvents, have controlled interporphyrin distances, incorporate porphyrins in predetermined metallation states, and have visible absorption spectra that are nearly the sum of spectra of the component parts. Their applications include nonlinear optics, catalysts, sensors, actuators, molecular sieves and therapeutics. Arrays with large numbers of porphyrins provide an ideal vehicle for studying energy migration processes underlying photosynthetic light harvesting phenomena.

Multichromophoric arrays, usually comprising photoactive porphyrin building blocks coupled to a quenching core, have been specifically engineered for the study of novel photophysical processes achievable with high powered laser sources. In this area, numerous biomimetic analogues of light-harvesting centers have been synthesized and scrutinized. A shape-persistent cyclic array of six zinc porphyrins provides an effective host for a dipyridyl substituted free base porphyrin, yielding a self-assembled structure for studies of light harvesting which is shown in Figure 1.6.[31]

Energy transfer occurs essentially quantitatively from uncoordinated to pyridyl-coordinated zinc porphyrins in the cyclic array. Energy transfer from the coordinated zinc porphyrin to the guest free base porphyrin is less efficient and is attributed to a Forster through-space process.
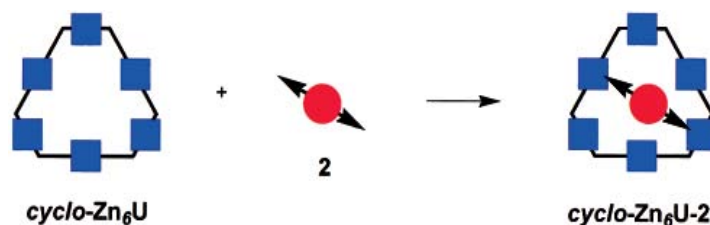
Figure 1.6: *Pyridyl coordinated Zinc Porphyrins. Blue squares indicate zinc porphyrins; red sphere indicates free base porphyrin.*

As for another example, covalent arrays of five or more porphyrins[32] in various metallation states with diphenylethyne spacer (Figure 1.7)[33] provide rigid centre to centre distances, is constructed from readily available tetraarylporphyrin building blocks, and appears to be of appropriate length for efficient light-harvesting. This synthetic approach enables incorporation of peripherally-functionalized, facially-encumbered, free base porphyrins or metalloporphyrins in rigid but soluble molecular architectures. The diphenylethyne spacer providing rigid centre to centre distances, is constructed from readily available tetraarylporphyrin building blocks, and appears to be of appropriate length for efficient light-harvesting. A key feature of this synthetic strategy is that the tetraarylporphyrins are intrinsic building blocks and comprise an integral part of the array scaffolding. This approach should provide a robust pathway to larger arrays resembling those found in the natural photosynthetic systems.
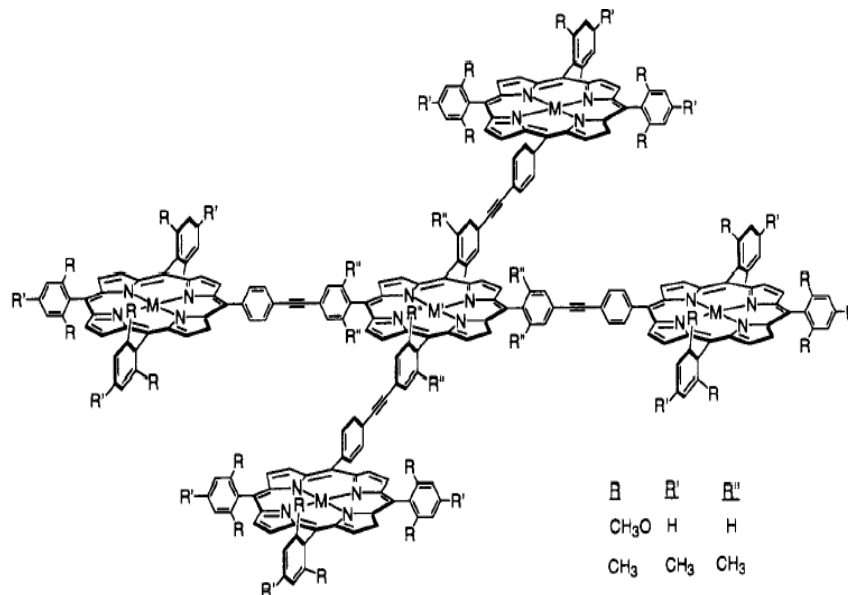
Figure 1.7: *Pentameric arrays of porphyrins through dibutadiyne-linkage where M=Zn and M'=H, H.*

Another example of the use of self assembled donor-acceptor multichromophoric porphyrin based systems is shown by Wasielewski *et al.* They have shown that zinc 5,10,15,20-tetrakis (perylenediimide) porphyrin (ZnTPP-PDI$_4$)[34] molecules (Figure 1.8), self-assemble into ordered nanoparticles both in solution and in the solid state driven by van der Waals stacking of the PDI molecules.

Photoexcitation of the nanoparticles results in quantitative charge separation in 3.2 ps to form ZnTPP$^+$ PDI$^-$ radical ion pairs in which the radical anion rapidly migrates to stacked PDI molecules that are on average 5 layers removed from the site of their generation as evidenced by magnetic field effects on the yield of the PDI triplet state that results from radical ion pair recombination. These field effects also show that the electron hopping rate within the PDI stacks is about 2×10^{10} s^{-1}. These nanoparticles can exhibit charge transport properties that combine important features from both photosynthetic and semiconductor photoconversion systems. So these molecular systems can be used as components of photonic devices.
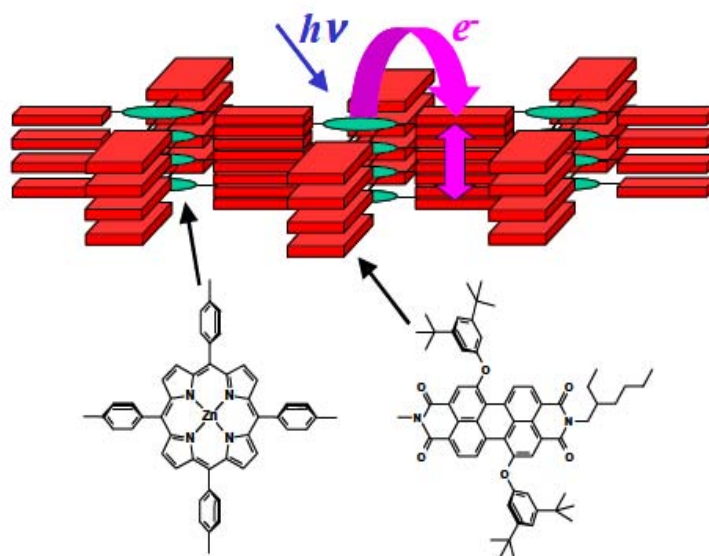
Figure 1.8*: Structure and cartoon of the self-assembled nanoparticles, ZnTPP-PDI$_4$.*

Porphyrin-Fullerene Linked Dyads[35] and Triads constitute highly efficient photosynthetic energy transfer systems. The type of linkage is still of major influence, in particular control over the rigidity of the linker deepened the knowledge as the orientation of the donor and acceptor could be fixed.[36] Synthetically more demanding is the extension of the lifetime of the created charges by the incorporation of additional chromophores in the system, much like in the natural photosynthetic reaction centre.[37] This has led to the creation of appealing, complex structures and demonstrates the large degree of control that has been achieved in fine tuning energy levels towards tailoring the outcome of the photophysical processes.

Of the many examples that can be found in literature, only two are briefly mentioned here as an illustration of the state-of-the art in this field.

The hexadic porphyrin-C_{60} compound described by Kuciauskas *et al.* shows how an artificial system can benefit from knowledge obtained from the natural photosynthetic reaction centre (Figure 1.9).[38] In a fullerene-containing triad, efficient stepwise charge separation[39] along a well-designed redox gradient can be realized regardless of the solvent environment, whereas this takes place only occasionally in conventional systems. The four zinc porphyrins in $(P_{ZP})_3$-P_{ZC}-P-C_{60} are used as a light-harvesting antenna. Subsequently, an energy transfer reaction occurs from the excited state of the zinc porphyrin to the free base porphyrin. Finally, a charge transfer reaction results in the formation of the $(P_{ZP})_3$-P_{ZC}-P^+-C_{60}^- radical ion pair. Such control over reaction pathways results in an exceptional enhancement of the lifetime of the photoinduced charges.

It should be mentioned that these effects are the small reorganization energy in electron-transfer and its consequences resulting from the fullerene's unique structure and symmetry, which are ultimately responsible for its high degree of delocalization and structural rigidity. Energy transfer rate constants depend on both the distance and driving force in a series of homologous porphyrin-fullerene linked systems. The fundamental information on energy

transfer obtained here will be helpful for the design of artificial photosynthetic systems.
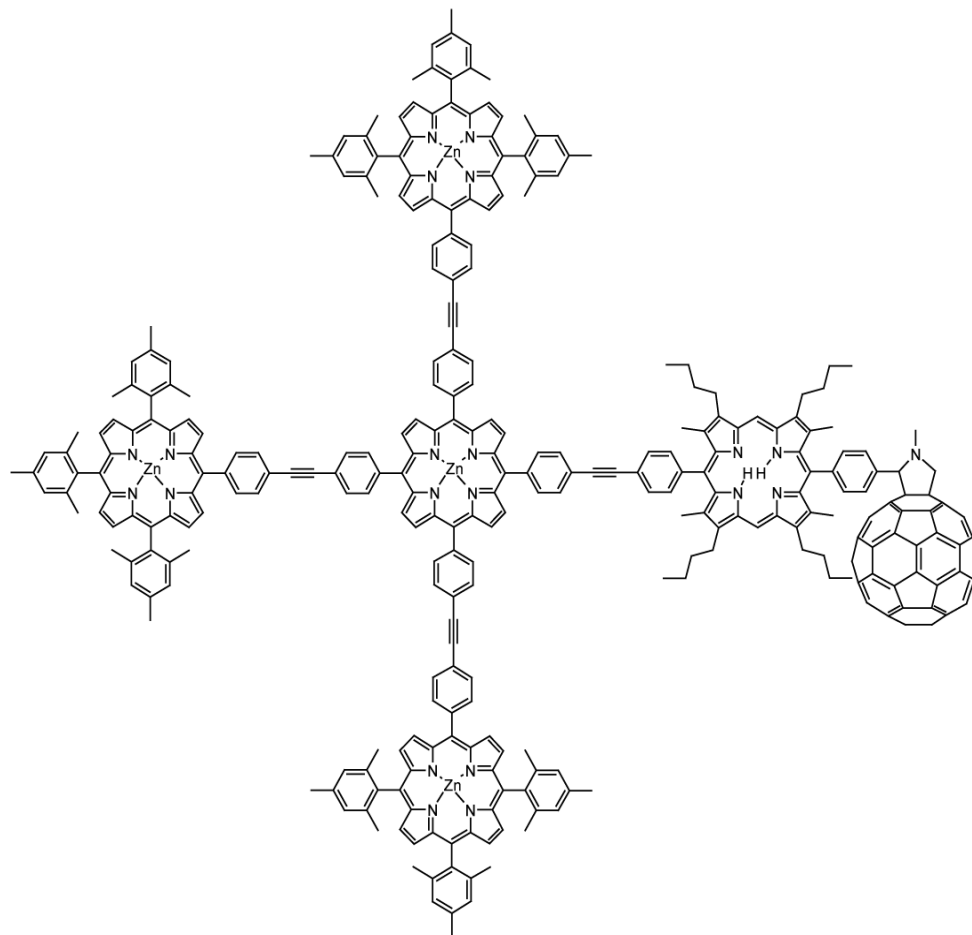
Figure 1.9: *Example of multichromophoric covalent Porphyrin-Fullerene array, (P$_{ZP}$)$_3$-P$_{ZC}$-P-C$_{60}$.*

Analogous to covalently coupled arrays, the porphyrin/fullerene couple is the most intensely studied supramolecular donor-acceptor system (Figure 1.10). In contrast to the covalent analogs, resolving the structure of the supramolecular architecture is typically the main goal[40] and the actual photophysical processes are only rarely studied in detail.[41]
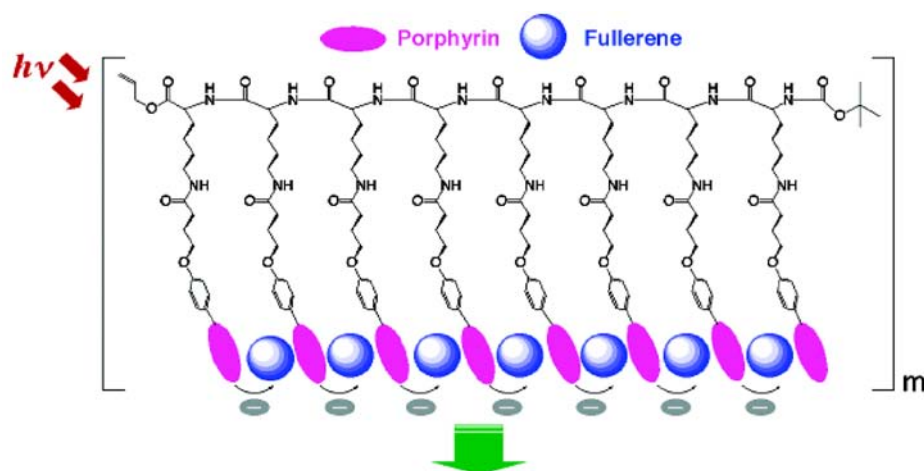
Figure 1.10*: Example of supramolecular porphyrin/fullerene structure.*

Boron-dipyrromethene (BODIPY) dyes,[42] which are widely applied as fluorescent sensors[43] and labelling reagents,[44] have remarkable properties such as high absorption coefficient, high fluorescence yield, and excellent photostability, etc.[45] The long wavelengths BODIPYs, in particular, have advantages over many other popular long wavelength dyes in these aspects. For example, in the long wavelength region, BODIPYs have a higher molar absorption coefficient than porphyrins and better photostability than cyanine dyes, etc. Thus, BODIPYs should be very competitive candidates in the design of light-harvesting systems.[46]

Boron-dipyrromethene based light-harvesting system containing three kinds of BODIPY dyes is shown in Figure 1.11 (yellow-green BODIPY, pink BODIPY, and purple BODIPY with the absorption maximum at 501, 568, and 647 nm, respectively) to absorb the light energy in corresponding regions. Its intense absorption from the visible to near infrared region covers the strong radiation scope of sunlight. Furthermore, its good photostability, solubility, and efficient energy transfer (99%) within it make these compounds promising as light-harvesting systems.
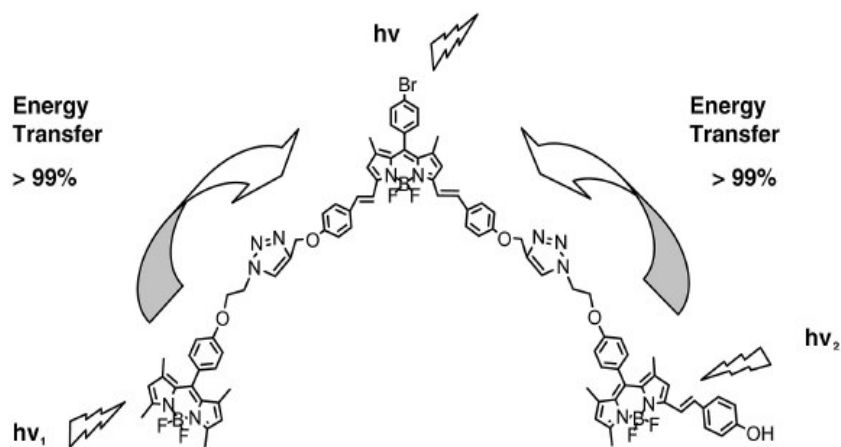
Figure 1.11: *A light-harvesting system containing three kinds of BODIPY fluorophores.*

Perylene Bisimide–Porphyrin shown in (Figure 1.12)[47] is another important multichromophoric system developed by Wasielewski and co-workers. Here two porphyrin donor components are rigidly attached to a perylene bisimide moiety.
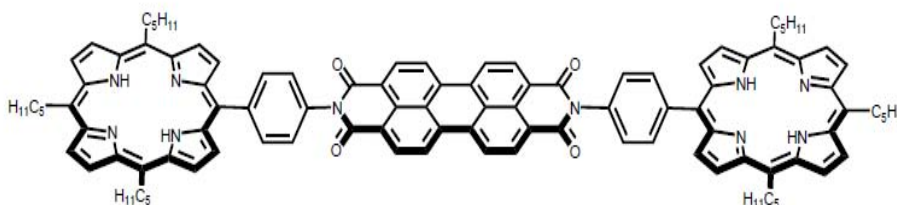
Figure 1.12: *Perylene Bisimide–Porphyrin multichromophoric system.*

Excitation of the porphyrins within this molecular switch results in single or double reduction of the acceptor unit depending on the light intensity. So it can be considered as a light-intensity dependent molecular biphotonic switch. Perylene bisimides are especially suitable for this purpose due to their strong and furthermore tunable absorption in the visible region, bright photoluminescence with quantum yields up to unity, chemical inertness

and low triplet yield, and exceptional photostability.[48]   Moreover perylene bisimides show excellent *n*-type semiconductivity and they have been utilized in various electronic and optical applications such as photovoltaic cells, dye lasers, light-emitting diodes, field-effect transistors, electrophotographic devices, industrial pigments and solar collectors. Recently, their ability to form supramolecular light-harvesting architectures by $\pi - \pi$-stacking, hydrogen-bonding or metal-ion-coordination has been explored.

        Another chromophore-rich environment is offered by man-made **Dendrimers.**[49] In these multichromophoric systems the relative position and orientation of the chromophores can be fixed in space (Figure 1.13).
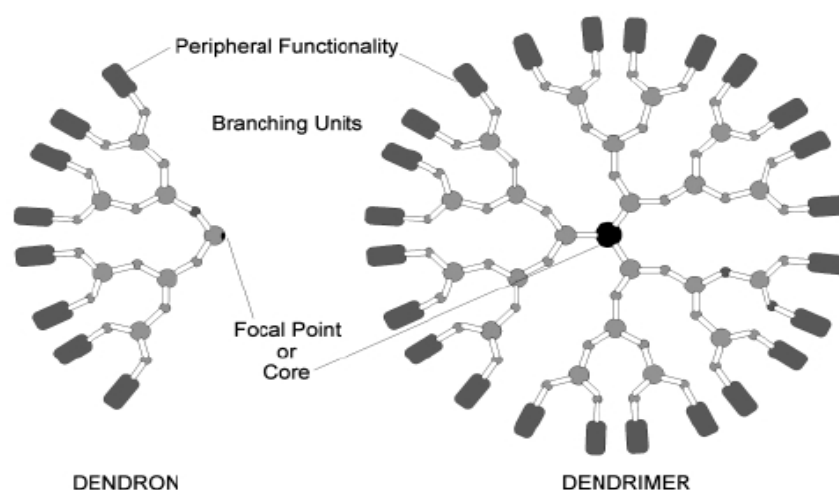
Figure 1.13: *Schematic diagram of the structure of a dendron and a dendrimer, highlighting the focal point or core (black) surrounded by rings of branching units (gray circles) and end-groups (rectangles).*

        Dendrimer synthesis indeed allows changing the number, relative position and orientation of attached chromophores in a controlled way. Dendritic structures offer a unique opportunity to vary the physical and electronic properties independently. The ability to independently vary the physical and electronic properties arises from the fact that in higher dendrimer generations it is only the surface groups which are in contact with the

environment. Many different forms of light-sensitive building blocks have been used in dendrimer construction, yielding macromolecules with interesting and diverse photophysical properties. In fact, traits of natural light-harvesting antenna systems themselves have been identified and studied.

A number of fascinating dendritic derivatives have been synthesized and studied by the groups of Mullen and De Schryver. Dendrimeric systems having many aromatic molecules, such as polyphenylbenzenes and perylene-3,4-dicarboximides, have been used to elucidate the details of energy transport within complex covalent structures as well as the photophysics of single molecules having multiple chromophores.

The encapsulation of lanthanide ions (Ln^{3+})[50] by dendritic ligands is a possible application for optical signal amplification. The impetus for this application originated from the self-quenching of fluorescence by lanthanide ions, such as erbium, when they are clustered together in the solid state. This self-quenching limits their effectiveness as signal amplifiers for optical fibre communications, since the poor solubility of Ln^{3+} ions in substrates such as silica leads to the formation of ion clusters.
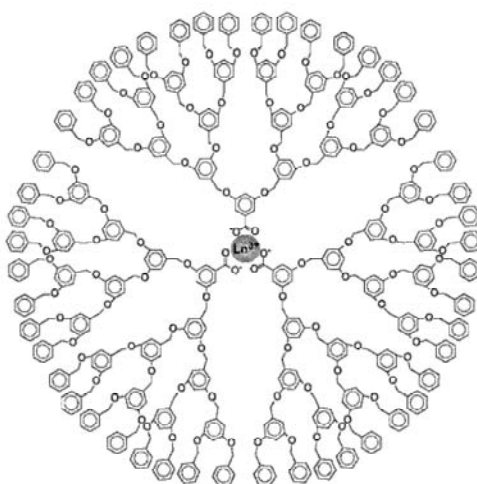
Figure 1.14: *Structure of a lanthanide-cored poly(benzyl ether) dendrimer.*[50]

Encapsulation of individual Er^{3+} and Tb^{3+} ions within a dendritic shell (Figure 1.14) was expected to lead to their site isolation, thereby increasing interchromophoric distance and decreasing the self-quenching effect. Indeed, this site isolation was realized by self-assembly of suitably functionalized carboxylate-cored dendrons around the lanthanide ion, and the resulting assemblies possessed all the characteristics desired for use in signal amplification.

During the course of photophysical studies on these ionically bound supramolecular assemblies, it was found that irradiation at wavelengths where the dendrimer backbone absorbed (280–290 nm) resulted in strong luminescence from the lanthanide core. Apparently, energy absorbed by the peripheral dendrimer shell was efficiently transferred to the luminescent Ln^{3+} at the focal point by a mechanism postulated to be of the Förster type. At these wavelengths, energy transfer to Tb^{3+} was found to be more efficient than in the case of Er^{3+}, likely due to the better overlap of dendrimer emission with Tb^{3+} absorption. This channeling of excitation energy from a dendrimer shell to a single core unit was termed the 'antenna effect'. Interestingly, it was also found that this energy transfer phenomenon was critically dependent on the substitution pattern within the dendritic shell. The findings made with the dendrimer antennas can be extended to the design of single-layer multichromophoric light-emitting diodes. The dendritic framework provides for both the energy transfer interaction and the site-isolation of different chromophores, enabling them to fluoresce simultaneously.[51]

Thus far, studies of energy transport in arrays consisting of many chromophores have been focused largely on polymers, self-assembled structures made from single chromophores and dendrimeric metal complexes. Relevant examples include the trinuclear ruthenium complex prepared by Scandola and Bignozzi which showed a remarkable photovoltaic performance in dye-sensitized solar cells (DSSCs) due to its high absorptivity. As example, a ruthenium polypyridine complex connected to a high absorber, either a

difluorobora-zaindacene or a zinc phthalocyanine proved to be efficient sensitizers in DSSCs. The underlying basic principle behind the operation of this multichromophoric system is schematically represented in Figure 1.15.[52]
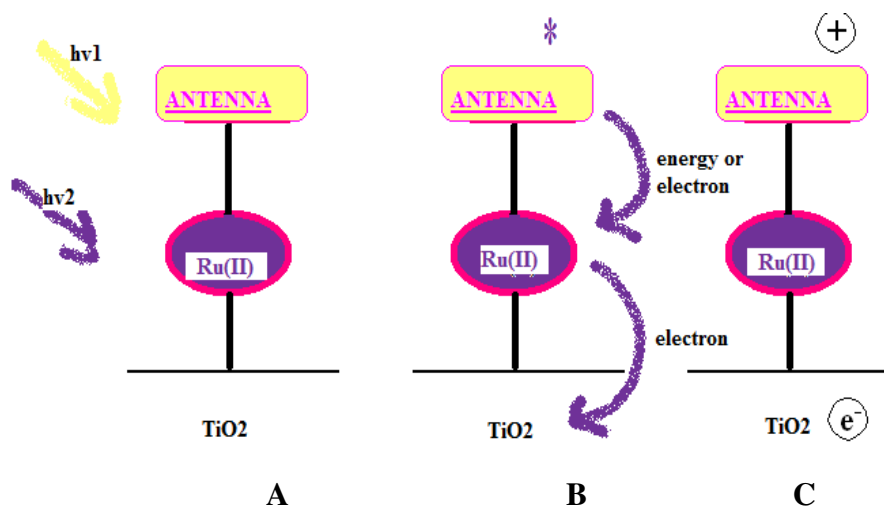
Figure 1.15: *Operation of Dyads.*

In the above case, light excitation of the ruthenium complex with a photon of energy hν1 results in electron injection in the conduction band of TiO_2. This step can be followed by a hole shift to the nearby antenna (leading to state C). Light excitation of the antenna with a photon of energy hν2 can undergo energy or electron transfer to the ruthenium complex. In the case of electron transfer, the reduced ruthenium complex can also inject an electron into TiO_2. In the case of energy transfer, the sensitized ruthenium complex excited state can subsequently inject an electron into the conduction band of TiO_2.

Multichromophoric cyclodextrins[53] are good models for the study of *excitation energy transport* (within a limited number of chromophores) and *antenna effect* (*i.e.* energy transfer from the appended antenna chromophores to an encased acceptor). They are of major interest for mimicking the photosynthetic light-harvesting antennae because the circular arrangement of

the chromophores is reminiscent of the light harvesting complexes of photosynthetic bacteria (LH1 and LH2). The underlying basic principle behind the operation of this multichromophoric system is schematically represented in Figure 1.16.
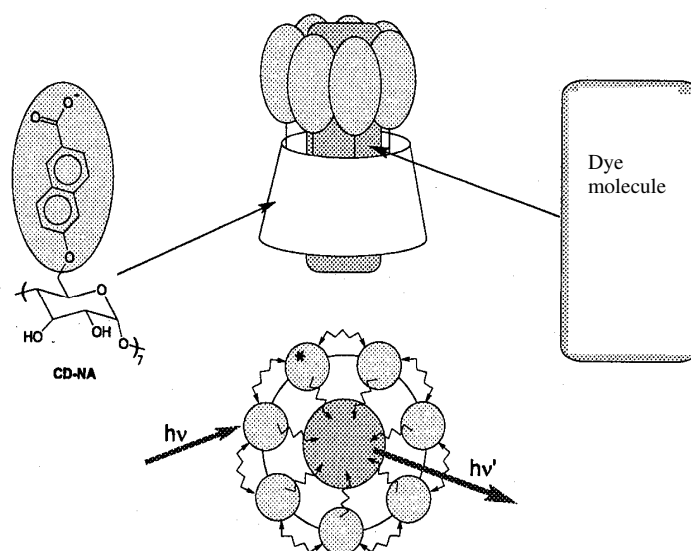
Figure 1.16: *Schematic representation of complex between β-CD-PT7 and a dye molecule, Bottom picture shows transfer of energy between chromophores and from chromophores to dye molecule.*[54]

In search of better mimics, Jullien and co-workers studied a number of naphthyl substituted β-cyclodextrins (β-CDs) containing up to 14 chromophore units.[55] The structural rigidity of these systems held the naphthyl chromophores in spatially well-defined positions and in close proximity with each other. This led to efficient energy hopping between the naphthyl units in these molecules. Multichromophoric cyclodextrins can also be used as *nanoreactors* for inducing selective photoreactions within the cavity by energy transfer from the antenna chromophores, and as *fluorescent nanosensors* of cationic surfactants or other cationic species.

A β-cyclodextrin bearing seven push-pull chromophores exhibits interesting linear and nonlinear optical properties. For example,

heptachromophoric β-cyclodextrin[56] (β-CD-PT7) with appended pyridin-2'-yl-1,2,3-triazole groups (Figure 1.17) exhibit great diversity in cation-induced photophysical effects.
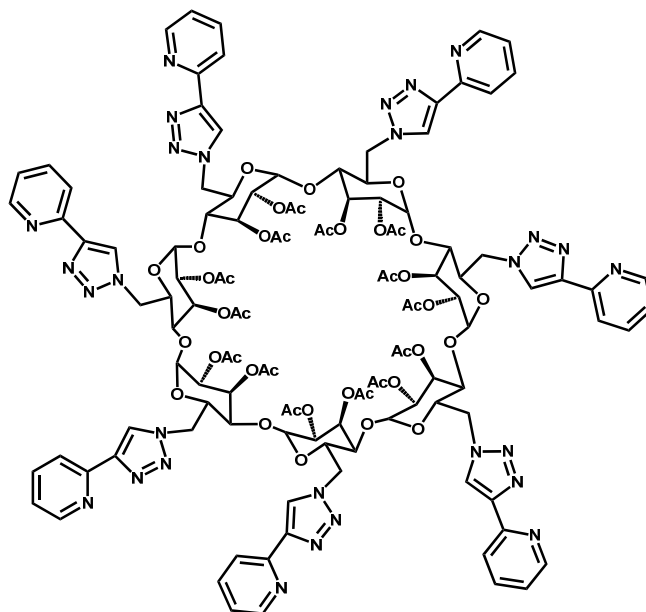
Figure 1.17: *β-CD-PT7*

Calixarenes, the cyclic oligomeric products formed from phenol and formaldehyde condensation, occupy a unique position in the annals of 'supramolecular chemistry'- the chemistry of non-covalent bonds. Multichromophoric system can be developed from this system by arranging the chromophores in a circular fashion. Calixarene-based multichromophoric systems that undergo changes in fluorescence emission upon ion binding are of great interest, especially as molecular sensors.

Calix[4]arenes[57] bearing more than two chromophores, have mainly been designed for the selective detection of metal ions. The luminescence properties of metal complexed calixarene derivatives, as investigated by Pochin *et al.,* show different phosphorescent behaviour for different metal ions. Furthermore, due to the alignment of four aromatic units in calix[4]arenes, Reinhoudt *et al.* were able to demonstrate that donor/acceptor

substituted derivatives exhibit nonlinear optical behaviour in a poled polymer matrix. Reinhoudt and co-workers devised new calixarenes having resorc[4]arene (Figure 1.18)[58] as the molecular building block. They described them as "molecular cages" since these molecules are able to recognise neutral molecules.
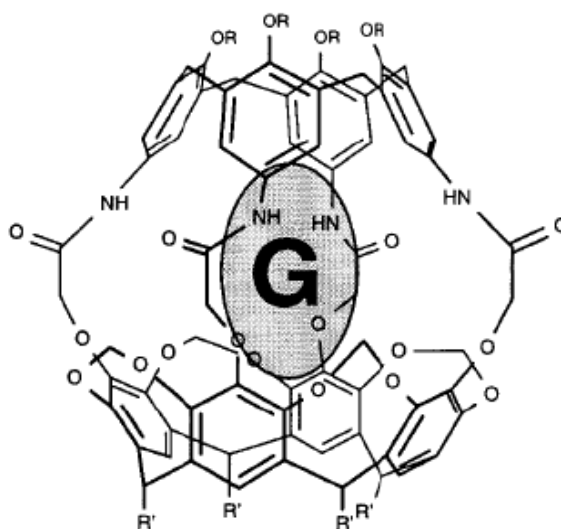
Figure 1.18: *Resorc[4]arene*

Multichromophoric cyclotriphosphazenes show unusual excited state photophysical properties arising from highly pre-organized trinuclear excimer formation. Cyclotriphosphazene (CTP) is a well known hexatopic core (Figure 1.19)[59] which can be easily pre-functionalized *via* substitution reactions on the corresponding hexachloride $(NPCl_2)_3$, especially with heteroatom nucleophiles. Cyclotriphosphazene can be used as a rigid hexavalent scaffold for constructing multichromophoric modules having unusual and interesting photophysical properties. When a relatively large chromophore is used, the structural rigidity of the CTP ring leads to a preferred conformation in which three chromophores reside on either side of the CTP plane forcing them into close proximity. Such a pre-organization

leads to facile intramolecular charge transfer in the excited state and a near complete trinuclear excimer formation.

Taking advantage of this conformational bias, these hexachromophoric CTP derivatives can be used for light harvesting studies.
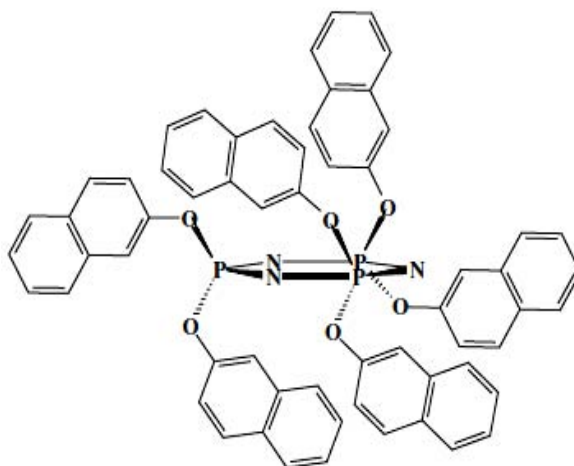
Figure 1.19: *Cyclotriphosphazenes*

Phthalocyanines are a class of azaporphyrins where the isoindolic rings are bridged by four nitrogen atoms, which augment absorption at longer wavelengths than the porphyrin derivatives. These dyes are extensively studied not only due to their favorable photophysical properties but also due to the ease at which their redox potentials and solubility in water can be tuned in accordance with their peripheral substitution. Metallation with zinc, gallium and aluminium increases the singlet oxygen generating efficiency of these dyes. Aluminium disulphonated phthalocyanines, under the commercial name Photosens (Figure 1.20) are under various phases of clinical trials for the treatment of skin, breast, lung, bladder, pancreatic, brain and gastrointestinal malignant cancers.[60]
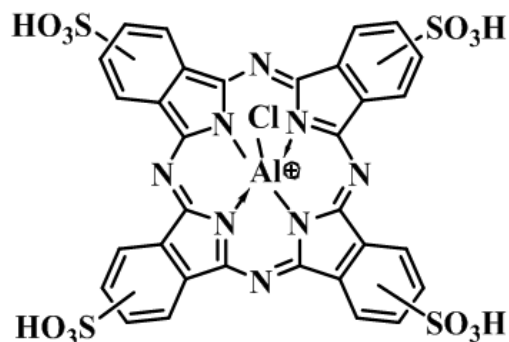
Figure 1.20: *Photosens*

Early studies on multichromophoric systems were carried out with polymers that were substituted at intervals with chromophoric units. However, due to their inherent flexibility and thus a number of different coiled conformations, these polymers turned out to be poor mimics of the natural photosynthetic reactors.

As the doping host, polyfluorene possesses extraordinary "light harvesting" ability, resulting in higher per-particle brightness as compared to dye-loaded silica nanoparticles of similar dimensions. Fluorescent dye-doped polyfluorene nanoparticles were prepared by a reprecipitation method, and energy transfers between the host polymer and the guest molecules were studied by steady state and time-resolved fluorescence measurements. A combined energy diffusion and Förster transfer model was determined to adequately describe the energy transfer efficiency in the doped nanoparticles. Both the steady-state fluorescence spectra and time-resolved fluorescence measurements indicate highly efficient energy transfer from the host polymer to the acceptor dye molecules. Energy transfer in the dye-doped nanoparticles was found to improve photostability, resulting in photostability estimated to be hundreds or thousands of times larger than dyes in solution. Fluorescence quantum yields of ~40% and a peak extinction coefficient of 1.5×10^9 $M^{-1}cm^{-1}$ were determined for aqueous suspensions of ~30 nm diameter

polymer nanoparticles doped with perylene or coumarin-6 (2 wt %). The combination of high brightness, highly red-shifted emission spectrum, and excellent photostability are promising for fluorescence imaging and multiplexing applications.

One-dimensional multichromophoric arrays can be designed to work as single unit; a typical example is single-molecule photonic wire. The general idea of such a device is illustrated in Figure 1.21.[61]
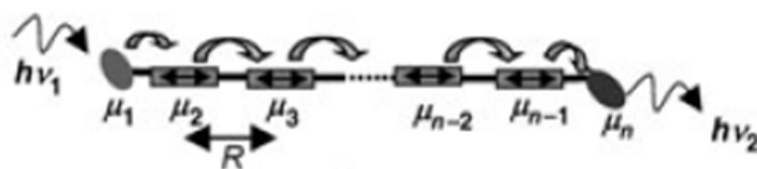
Figure 1.21: *Basic concept of a molecule-based photonic wire.*

Light is absorbed by one of the chromophores composing the wire and "transmitted" towards a collecting chromophore from which a final photon is emitted. This can be explained by considering the case of conjugated complex polymer given below (Figure 1.22).
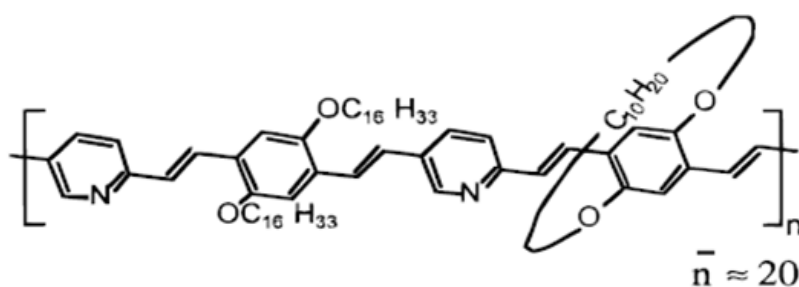
Figure 1.22: *Molecular structure of conjugated copolymer dPPV-PPyV.[61]*

The **dPPV-PPyV[61]** polymer has a molecular weight of ~22,000. This corresponds to ~20 monomer units, which can extend to as long as ~50 nm. According to the usual spectroscopic models for conjugated polymers, a

polymer of this size would have multiple conjugated segments, implying that the system is effectively multichromophoric. Accordingly, the absorption spectrum of the polymer is due to overlapping absorption bands from different conjugated segments of the polymer chain. In contrast, the emission may be due to emission from a small fraction of the total polymer chain, specifically the regions that correspond to local minima in the optical band structure. By analogy to other conjugated polymers, these regions should be efficiently populated on a picosecond time scale by intramolecular electronic energy transfer. Due to the co-operative behaviour of the different conjugated segments of the polymer, efficient intramolecular electronic energy transfer takes place in such systems. This dramatically increases the fluorescence intensity of multiple-chromophoric of the above conjugated polymer molecule.

A DNA-based unidirectional molecular wire[61] containing up to five different chromophores acts as one-dimensional multichromophoric array which behaves as a single unit (Figure 1.23). The given one-dimensional multimolecular array exhibiting weak excitonic interactions between neighbouring dyes works as molecular photonic wire.
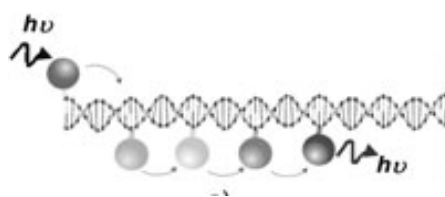
Figure 1.23: *DNA based photonic wire containing five different chromophores.*

Figure 1.23 is a cartoon of the DNA-based photonic wire designed for various experiments. Five chromophores with considerable overlap between subsequent absorption and emission spectra (Rhodamine green (RhG), tetramethylrhodamine (TMR), Atto 590, Atto 620 and Atto 680) were covalently attached to single-stranded DNA fragments of various lengths (60

or 20 bases) using 6C linkers. Hybridisation of the labelled DNA fragments to the complementary DNA strand (60 base pairs) results in a construct containing five different chromophores positioned at well-defined distances. The unique features of double-stranded DNA make it an ideally suited building block for nanoscaled molecular devices. With a persistence length of 50 nm, DNA constitutes a stiff scaffold for the chromophores. In addition, DNA offers many well-developed labelling strategies including hybridisation of labelled short complementary oligonucleotides and dye intercalation. Identical or different dyes can be easily incorporated at specific positions along the DNA strand, tuning in this way the directionality of the energy flow.

1.5. Bischromophoric Systems

As model systems we have investigated properties of a few bischromophoric systems. Bischromophoric systems are better-defined models for the processes occurring in multichromophoric systems. Upon excitation of a bischromophoric compound with conventional light source several processes can occur depending on the nature of the chromophores. However, it is recognized that considering a particular bischromophoric molecule as having "isolated" chromophores is, at best, an approximation. The degree of interaction can be expected to span a wide range, with the "isolated" and "completely mixed" characterizations at the extremes of the scale. Excitation of molecules containing more than one chromophores leads to intramolecular interaction such as excimer, exciplex and product formation.

A number of workers have studied the photophysics and photochemistry of bischromophoric molecules. In majority of these systems, the chromophores are connected via tethers which allow a large number of conformations. This study explores the photochemical and photophysical studies of a new bischromophoric system, the anthracene diadduct, in which a

large number of conformations are constrained. Figure 1.24 is a cartoon representation of our target bischromophoric system.
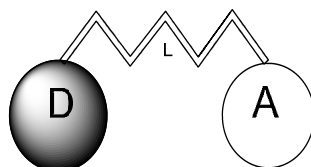
Figure: 1.24

Here **D** and **A** are two chromophores and **L** is a linker connecting the two. Such devices have potential applications as sensors, light harvesting antenna complexes, etc. In the ideal system, chromophores **D** and **A** should absorb and emit differently. It is also important to shut electronic communication between **D** and **A** in the ground state. When ground state electronic communication between **D** and **A** is effectively shut, the two chromophores will absorb independently. In other words, the absorption spectrum of such devices will be the sum of parts. However, both electron and energy transfer between **D** and **A** are possible in the excited state since such processes can take place through space.

1.6. Energy Transfer in Bischromophoric Systems

In a bischromophoric system where one chromophore (the energy donor, **D**) is in its excited state and the other (the energy acceptor, **A**) is in its ground state, energy transfer can occur such that the donor returns to its ground state simultaneously with the promotion of the acceptor to its excited state.[50] This transfer can occur by either a through-bond (Dexter) or through-space (Forster) mechanism. In the former, an electron exchange occurs from the S_1 state of the donor to the S_1 state of the acceptor, with a simultaneous exchange of an S_0 electron from acceptor to donor (Figure 1.25). This

electron exchange requires strong **D–A** orbital overlap and is therefore a short range (< 10 Å) interaction that diminishes exponentially with distance.

In contrast, the Förster mechanism does not require electron exchange and is rather a through-space dipole–dipole interaction. In this case, **D–A** orbital overlap is not necessary, allowing the chromophores to be separated by a relatively large distance (10–100 Å). The bridging moiety plays a crucial role in Dexter energy transfer, where rigidity and conjugation are the key parameters. The properties of the chromophores themselves (transition dipole moments and spectral overlap of donor emission and acceptor absorption) as well as the interchromophoric distance play the more important role in Förster energy transfer.
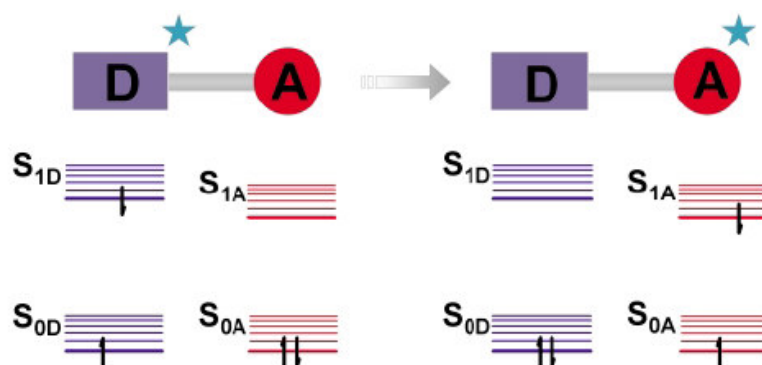
Figure 1.25: *The process of energy transfer involves the migration of excitation energy from an excited-state donor (D) to a nearby ground-state acceptor (A).*[50]

1.7. Photophysical Properties of Bischromophoric Systems

Since the first discovery by Forster and Kasper concerning complexes between the excited state and ground state aromatic hydrocarbons which were named excimers, numerous aromatic hydrocarbons have been found to exhibit excimer fluorescence and the results have been summarized in some reviews.[62] Their prominent feature is the broad and structureless fluorescence

band which is shifted 4000-6000 cm^{-1} to lower frequencies relative to the normal molecular fluorescence. This fluorescence has been observed both in fluid solutions and in solid state at atmospheric pressure, if the structure allows close overlap between the molecular planes. So the aromatic molecules which consist of two identical planar aromatic systems joined through a single carbon-carbon bond may exhibit spectra which are either very different from or virtually identical with the known spectrum of one half of the molecule. The mode of interaction between the chromophores responsible for the phenomena has largely, although not exclusively, through space interaction (TSI) and thus to be limited to molecules that adopt a "folded" conformation, which allows direct overlap between chromophores in the ground or excited state. Different possible TSI interactions are discussed below:

1. If the rings are coplanar, then resonance interaction is strong and the spectrum of the double molecule is vastly different from that of the isolated chromophores. The photophysical properties of bischromophores depend on the excited state complexes or molecular aggregates in the excited state.[63] These geometries correlate with distinct spectral emissions.
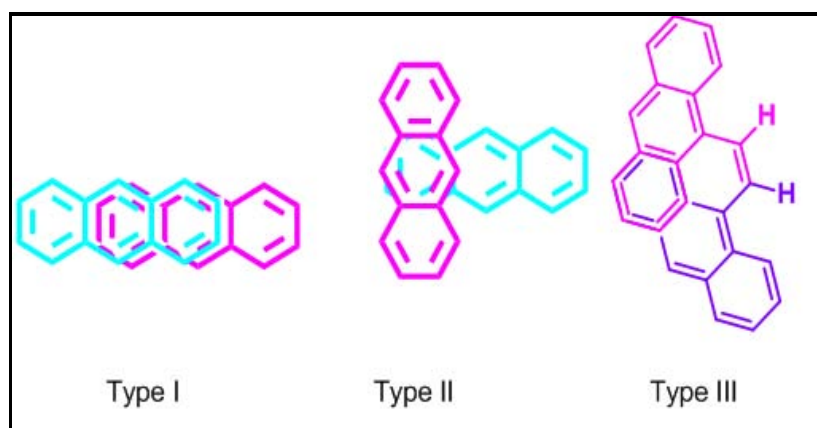
Figure 1.26: *Three possible interactions of bisanthracenes.*

For geometries in which the anthracene rings overlap with single phenyl unit (Type I) the emission has a peak in the 460 nm region. For geometries in which the anthracenes overlap by two phenyl units (Type II),

then it is more stable than above type and emission occurs at 570 nm region. For geometries in which the anthracenes overlap by three phenyl units (type III), emission occurs at 620 nm region (Figure 1.26).[63]

2. If the molecular planes are perpendicular, the systems are essentially non-interacting, within a π-electron approximation, and the double-molecule spectrum does not appear different from that of one ring of the system.[64] The binaphthyls were studied by Friedel and Orchin and the ultraviolet spectra in solution at room temperature indicated that resonance interaction was at a minimum for 1,1'-binaphthyl whose spectrum was quite similar to that of naphthalene. [65] 2,2'-binaphthyl on the other hand exhibited a spectrum which extended much further to the red than that of naphthalene, and in this case the steric inhibition of resonance was presumed to be at a minimum. In the first case steric hindrance made a perpendicular twist in the molecule, which was responsible for little resonance interaction between the two naphthyls in it. This twist was not present in the second case.

So the properties of absorption and luminescence emissions are important in analytical techniques as spectroscopy.

1.7.1. Conformational Dependence on Spectra - Exciton Coupling

In a system of N non interacting chromophores if one chromophore is excited by light, the energies of the other N-1 non interacting molecules are unchanged. Thus an array of N chromophores would have N-fold degeneracy, as any chromophores could be equally excited by the light. In biopolymers, however, the chromophores are in ordered arrays, and when electrons are excited they do interact. For example, if one chromophore is excited, its transition dipole may interact with the transition dipole of a neighbouring unexcited molecule. The net result is an exchange of excitation. The energy

of the transition will be perturbed by the potential which allows excitation energy of one molecule to migrate to another.

If one had only two identical chromophores in a crystal, and one was excited and the other was not, there could be resonance of the excitation between the two chromophores. It would be unclear, at any given time, which of the two chromophores was in the excited state. The exchange of excitation energy between the chromophores leads to two states, one of which has higher energy, and one of which has lower energy with respect to two isolated non interacting chromophores. In the case of an ordered array with two chromophores, the transition dipole of one of the isolated chromophores will be split into two transitions, one of which having lower energy and one of which having higher energy than the original transition. This splitting of one transition into two is called "exciton" splitting.[66]

Here for the above **D-A** system, absorption of two photons by a concentrated assembly of chromophores can lead to formation of a biexciton.

1.7.2. Effect of Conjugation on Spectra

Identical functional groups in different molecules will not necessarily absorb at exactly the same wavelength. For example consider the absorption spectra of butadiene. It gives absorption band at 217 nm (ε 21000). Here the magnitude of molar extinction coefficient for a particular absorption is directly proportional to the probability of the particular electronic transition; the more probable a given transition (slightly less energy required for the transition), the larger the extinction coefficient. The actual appearance of a simple conjugated diene with the chromophore will be similar to the above one. There are a large number of exceptions to the above rules, where special factors can operate. Transitions of identical functional groups in different molecules will not have *exactly* the same energy requirement because of different structural

environments (examples shown in Figure 1.27). Distortion of chromophores may lead to red or blue shifts, depending on the nature of the distortion.[67]
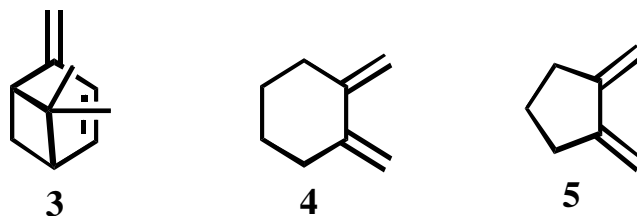
Figure 1.27: *Conjugated dienes with different constraints.*

The strained molecule verbenene **3** has an absorption maximum at 245.5 nm, whereas the usual calculation gives the value of 229 nm. The diene **4** might be expected to have a maximum at 273 nm; but the distortion of the chromophore, presumably out of planarity with consequent loss of conjugation, causes the maximum to be as low as 220 nm with a similar intensity (ε 5500). The diene **5**, in which coplanarity of the diene is more likely, gives a maximum at 248 nm (ε 15800) showing that this is so, although it still does not agree with the expected value.

It may be mentioned in this connection that the structural diversity exhibited by cyclic compounds having two or more exocyclic double bonds can provide an ideal platform for synthesizing several bischromphoric systems with tunable relative geometry of the chromophore components. We propose to utilize this possibility in the present investigation.

1.7.3. Effect of Cycloalkanone Ring Size in Spectra

S. A. Ahmed has reported that large cycloalkanone ring has more electron donating methylene groups, which led to increase the electron density of the carbonyl chromophore. So the absorption maximum of a particular bischromophore with cyclooctanone is higher than with cyclopentanone.[68,69]

1.7.4. Effect of Electronically Excited State in Spectra – Excimer Emission (Dual Emission Spectra)

The concentration quenching of fluorescence is a phenomenon that has been known for a long time. It was discovered only recently, on the other hand, that instead of quenching, many fluorescent organic compounds exhibit a change in the fluorescence spectrum; *i. e.* a new component becomes evident in such a spectrum with increasing concentration. Since no corresponding change is observed in the absorption spectrum, the new fluorescence component must be ascribed to an associate formed only ***after*** absorption of light in the electronically excited state. The term "excimers" has become widely accepted for associates of this type. So excimer is a dimer which is associated in the excited state and which is dissociative in the ground state.[70]

The role of the association of excited molecules as the cause of a change in the fluorescence spectrum with concentration was first recognized in the case of pyrene and some of its derivatives; and the formation of excimers is still most easily demonstrated for pyrene. A large aromatic π system exhibits dual emission. The formation of pyrene excimer requires encounter of an electronically excited pyrene with the second pyrene in the ground state. According to this definition the two pyrenes must be far enough away, so that the incident radiation can cause "localised excitation".[69] These locally excited molecules can cause "monomer" emission.

Mechanism of excimer formation together with the processes of fluorescence emission, the radiationless deactivation of the excited monomer and of the excimer, and the dissociation of the excimer leads to the following reaction as in Scheme 1.2.

$$A^* + A \; \underset{k_d}{\overset{k_a.c}{\rightleftharpoons}} \; (AA)^*$$

Scheme with arrows: k_a, k_1 from A^*; k_a^1, k_1^1 from $(AA)^*$ down to $A + h\nu\,A$, $(AA) + h\nu'\,(AA)$, then both to $A + A$.
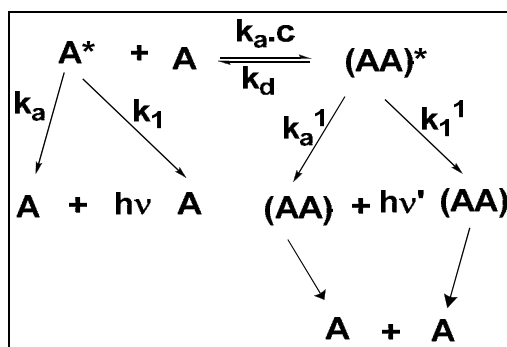
Scheme 1.2: *Mechanism of excimer formation.*

It is a bimolecular mechanism for the formation of the excimer by combination of an electronically excited molecule **A***(in the lowest excited singlet state) with an unexcited molecule **A** (in the singlet ground state). The observation of excimer emission indicates that diffusive encounters between pyrenes have occurred. There are instances that excimer emission is observed although there is no evidence that the pyrenes are separated in the ground state. These excited species are sometimes referred to as "static excimers" while those behaving as discussed earlier as "dynamic excimers". Forster and co-workers first recognised the role of association of the excited molecules as the cause of change in the fluorescence spectrum with concentration in the case of pyrene and some of its derivatives. In 1964, Stevens and Ban proposed a sandwich configuration of the excimer resulting from the mutual approach of the two components with their molecular planes parallel.

1.7.5. Charge Transfer Emission Spectra

The structures of the excited states of carbonyl compounds such as aldehydes and ketones have been studied most extensively.

Excited state reactions other than geometrical rearrangements can result in spectral changes. In the ground state the structure of carbonyl group contains an important contribution from the polar group. The position of absorption that involves nonbonding electrons is particularly sensitive to the

polarity of solvent used in the determination. If the group is more polar in the ground state than in the excited state, the non-bonding electrons are stabilised relative to the excited state by hydrogen bonding or electrostatic interaction with the polar solvent; the absorption is shifted to shorter wavelength. Conversely, if the group is more polar in the excited state, the absorption is shifted to longer wavelength with increasing solvent polarity.

The α,β-unsaturated ketone such as mesityl oxide (4-methyl-3-penten-2-one) shows λ_{max} 230 mμ, ε 12600 and λ_{max} 329 mμ, ε 41 in hexane and λ_{max} 243 mμ, ε 10,000 and λ_{max} 305mμ, ε 60 in water. These data indicate that the long wavelength n⟶π∗ absorption is shifted to shorter wavelength in the more polar solvent; thus the excited state would appear to be less polar than the ground state. That is the excited state is having contributions from C^--O^+ rather than C^+-O^- as in the ground state. The shift to longer wavelength observed in the π⟶π* transition of α,β-unsaturated ketones with increasing solvent polarity indicates that the excited state in this transition is more polar than in the ground state. For this transition the data have been interpreted as the promotion of an ethylenic π electron to a carbonyl π* orbital. Because the intramolecular effects such as these involve the transfer of charge from one atom to another, they are frequently called as *charge-transfer* spectra. Here **A-B** system with cycloalkenone linker can undergo intermolecular charge transfer depending on the size of cycloalkenone linkage.[71]

Same is the case with fluorescence emission spectra. Depending on the structures in the excited state and medium, emission spectra vary. Mataga and Murata reported fluorescence quantum yield and lifetime data for several CT complexes. They explored the effects of donor structure, temperature and solvent polarity on the emission and concluded that thermally equilibrated structures for the ground and excited states are quite different for CT complexes. They observed large Stokes shifts, which depend on structure and

medium. Dipole-dipole interactions between the solute and solvent molecules are proposed to be responsible for the large Stokes shift seen in polar solvents.

So such intramolecular charge transfer emission and absorption in bischromophoric molecule is through-bond interaction.

1.8. Photochemical Properties of Bischromophoric Systems

Light induced reactions are very important to life. So it is very important to know factors affecting photochemical reactions to make them useful for day to day life.

Photochemical reactions originate from the electronically excited states of molecules. Those electronically excited states may be singlet or triplet excited state. Normally a reaction occurs when a molecule gains the necessary activation energy to undergo change. Here in the case of photochemical reactions light provides the activation energy. This may lead directly to products (e.g. in dissociations or isomerisations) or it can react with another ground state molecule (e.g. in additions or substitutions) or more often to unstable or reactive chemical species (e.g. free radicals or radical cations) which then react further in secondary processes through dark reactions which lead ultimately to the final photoproducts.[72]

The sequence of photochemical reactions can be given as a succession of steps. It includes absorption of light, fluorescence, non-radiative deactivation, intersystem crossing and chemical reactions. The processes which occur between the absorption and emission of light can be illustrated by a Jablonski diagram (Figure 1.28).
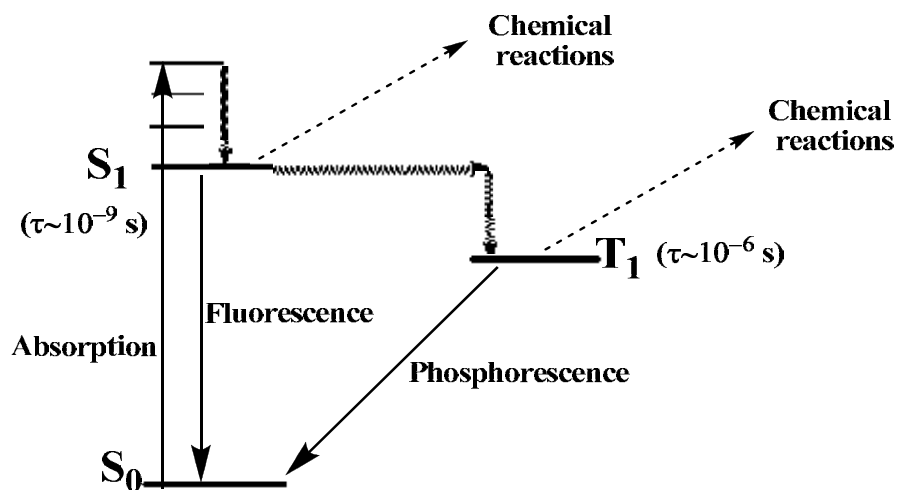
Figure 1.28: *Jablonski diagram illustrating the various photophysical and photochemical processes that occur upon excitation.*

Over the years organic photochemistry has matured to the stage where the consequences of excitation of the more common chromophores (*i.e.*, aromatics, ketones, esters, olefins, halogens, nitro, etc.) are reasonably well (though by no means completely!) understood. It is therefore logical that the next level of complexity be broached - the photochemical consequences of irradiating molecules containing two or more functional groups. Linking two chromophores by a non-absorbing chain is of great importance for the study of bimolecular interactions in dilute solutions.

For photochemical reactions to manifest in bischromophoric systems, intramolecular electronic energy transfer has to take place. Intramolecular electronic energy transfer processes in bischromophoric systems can be represented in terms of the process:

$$D^*\text{-}L\text{-}A \longrightarrow D\text{-}L\text{-}A^*$$
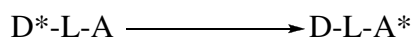
where the excitation energy is transferred from an excited donor D* chromophore moiety to a ground state acceptor moiety A, resulting in quenching of D* fluorescence and sensitization of A. L denotes a molecular

spacer bridge connecting the two chromophores. This bridge may play a role in promoting the transfer process. In all the EET processes, a resonance matching between the energy of the initial state of the system and that of its final state is required.

Another possibility is the intramolecular reaction of a component in the excited state with another component in the ground state. Dimerization arising through a [4+4] cycloaddition pathway in certain bisanthracenes is a typical example for such intramolecular photochemical reactions of bischromophoric systems.

The main photochemical reactions which have been reported in literature are explained below. Here we particularly discuss photochemistry of bisaromatic compounds connected through alkenone or alkene spacer. Arylanthrylethylenes or alkenones containing methyl, phenyl, 1-naphthyl and 9-anthryl as one substituent and anthryl group as the other, form an interesting group of bischromophoric systems. In these molecules, there is scope for strong interactions between low-lying excited state associated with the anthracene and arylethylene/arylalkenone moieties. Also anthracenes are unique in combining the advantages of having easily accessible absorption spectra, exhibiting monomer (and often excimer) fluorescence and high photoreactivity; they also have fairly good solubility in organic solvents and, although sometimes with difficulty, a variety of derivatives can be prepared.

Due to the above discussed peculiarities bisanthryls have been extensively investigated, so particularly, described here the photochemical reactions of bisanthryl alkenones. The observed reactions include geometrical isomerization, cycloaddition reactions, rearrangement reactions and dehydrocyclization reactions, which are described below.

1.8.1. Fundamental Photochemical Reactions

1.8.1.1. Geometrical Isomerization Reactions

Upon irradiation in dichloromethane solution, (9-anthry1)alkenes, in which the alkene is conjugatively substituted by either carbonyl or nitro groups, undergo reversible geometrical isomerization in dichloromethane solution. Here the *trans,trans*-(dianthryl)pentadienone **6** isomerizes photochemically in oxygen-saturated solution to give a mixture of *cis,trans*-isomer **7** and the *cis,cis-* isomer **8** (Scheme 1.3).
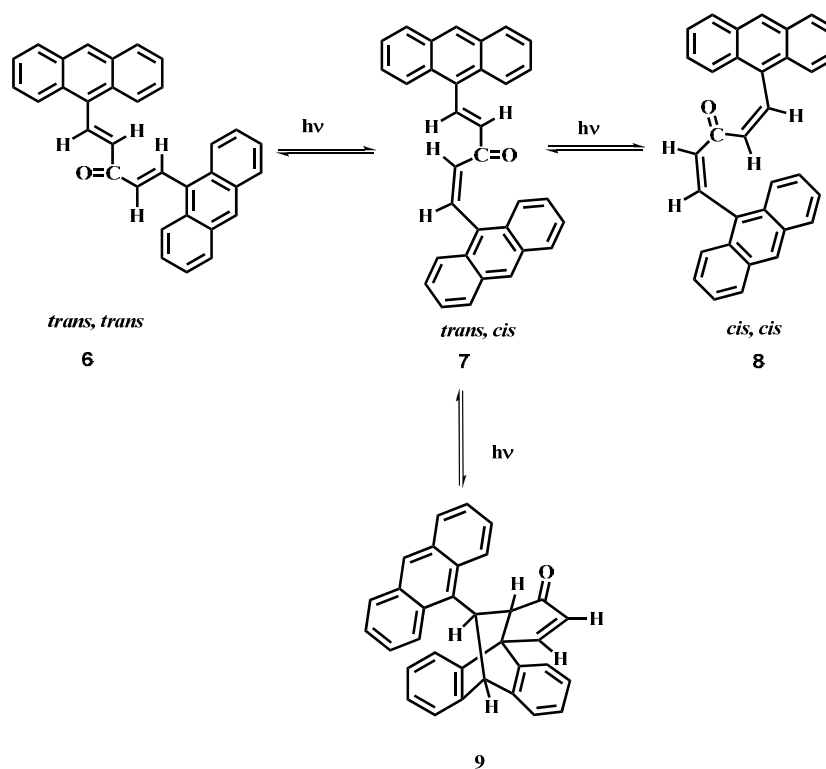
Scheme 1.3

However, irradiation under nitrogen smoothly leads *via* the *cis-trans* isomer **7** to the cyclomer **9.** Its formation involves the Diels-Alder addition of the *trans*-(9-anthryl)alkene double bond to the central ring of the other

anthracene moiety. The quenching by oxygen suggests that the [4π+2π] cycloaddition proceeds as a triplet-state reaction, while the geometrical isomerization involves the excited singlet state.[73]

1.8.1.2. Cycloaddition Reactions

The anthracene chromophore can undergo cycloaddition in which the central ring represents a 4π electron system or, more rarely, one of the lateral rings or any of the diene linkage acts as diene or dienophile. It can be either [4π + 2π] or [4π + 4π] cycloaddition reaction.

(*i*) Upon irradiation in dichloromethane solution, (9-anthryl)alkene**,** in which the alkene is conjugatively substituted by either carbonyl or nitro groups, undergoes reversible geometrical isomerization in dichloromethane solution. Geometrical isomerization and competing intramolecular cycloaddition reactions characterize the photochemistry of (9-anthryl)alkenes which contain an additional anthracene chromophore. Thus, irradiation of *trans*-1,3-di(9-anthryl)propene **10** in benzene smoothly gives the cycloaddition product **12**.[73]

A = Anthracene
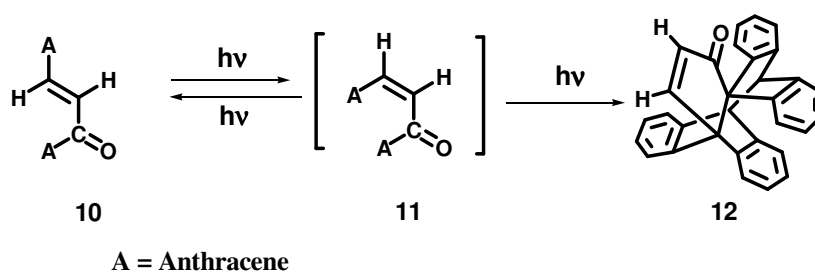
Scheme 1.4

(*ii*)   *cis*-1,2-di(9-anthryl)ethylene **13** undergoes geometrical isomerization to give *trans* isomer **15**, which is highly stable. The *cis* isomer

upon irradiation also undergoes [4π+ 2π] cycloaddition **14** and [4π+4π] cycloaddition **16** which is shown in Scheme 1.5.[74]
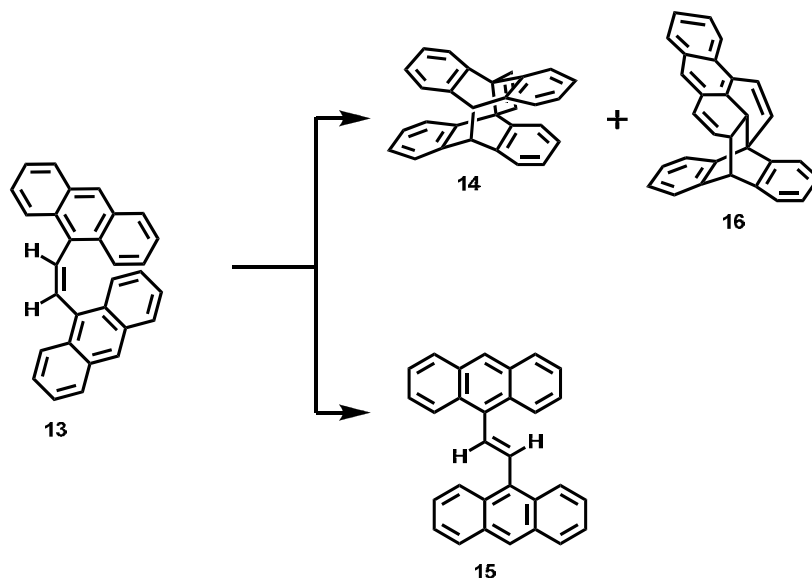
Scheme 1.5

(***iii***) *cis*-l-(9-anthryl)-2-benzoylethylene **18** can undergo [4π + 2π] cycloaddition followed by electrocyclic reaction and [1,5] prototropic shift as given in Scheme 1.6.
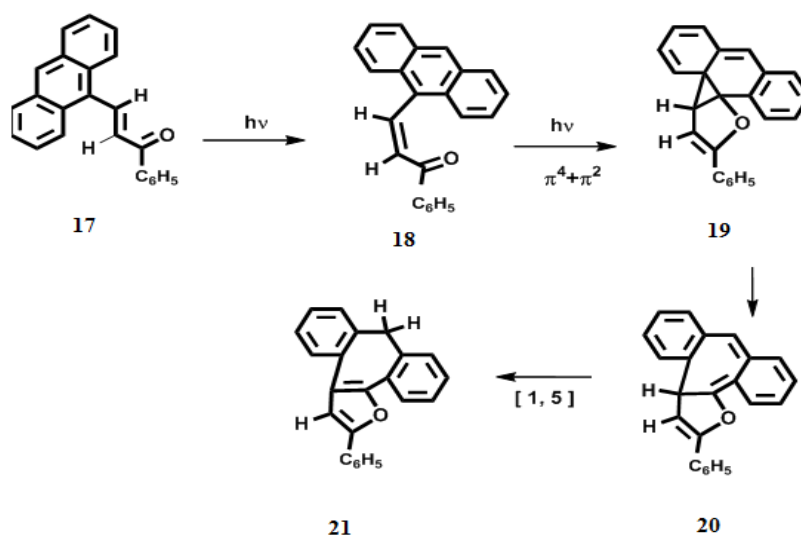
Scheme 1.6

In this case, photochemical isomerization of *trans* l-(9-anthryl)-2-benzoylethylenes **17** leading to 5H dibenzo[a,d]cycloheptenes proceeds smoothly, albeit with low quantum efficiency, as a process competing with geometrical *cis-trans* isomerization. The enlargement of the central ring of the anthracene system has been rationalized by a [4π+2π] cycloaddition leading to final product **21** *via* intermediates **19** and **20** are given in Scheme 1.6.[75]

(*iv*) Photochemistry of bis(9-anthryl)dimethylsilane: Bouas-Laurent and co-workers have reported the photocyclomerization of 9,9'-bisanthracenes[76] to generate a crowded derivative of silacyclopropane by irradiation of bis(9-anthryl)dimethylsilane.   Irradiation of bis(9-anthryl)dimethylsilane **22** generates a single photocyclomer **23** formed by [4π+2π] intramolecular 9,10: 1',2'-anthracene photodimerisation.[77]   The reaction is represented in Scheme 1.7 below.
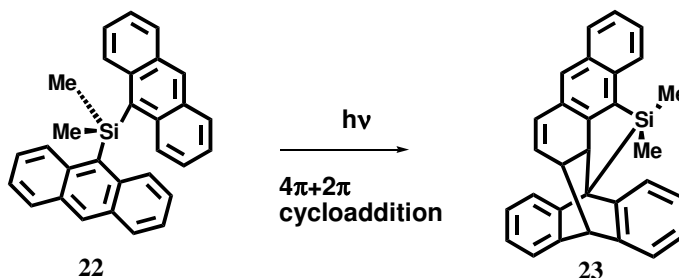
Scheme 1.7

1.8.1.3. Rearrangement Reactions

It can undergo rearrangement reaction as given in Scheme 1.8. The rearrangement of the anthracene derivative **24** by direct excitation to give the dearomatized product **25**, formally, also proceeds by way of β-bond cleavage and may be rationalized in terms of an intramolecular triplet sensitization by the cyclopentenone moiety. In the photoexcited state of anthracenes and

aromatic ketones, intramolecular singlet energy transfer from the anthracene chromophore to the cyclopentenone in **24** is energetically feasible because of the favourable electron spectral overlap of the anthracene absorption around 380 nm, and the absorption due to the cyclopentenone $n \longrightarrow \pi^*$ transition. The subsequent intersystem-crossing step is assumed to be an efficient process, as may be deduced from the relatively low fluorescence quantum yield of **24**.[78]
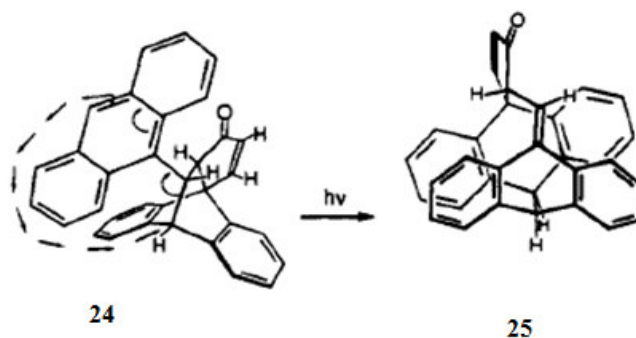
Scheme 1.8

1.8.1.4. Dehydrocyclizations

Intramolecular photochemical dehydrocyclizations of anthracene-related compounds are well known for bianthrone and similar stilbene-like anthrone derivatives. Several examples of styryl-substituted anthracenes undergoing photochemical dehydrocyclization have been reported. The conversion l-(9'-anthryl)-4-phenyl-l,3-butadiene **26** leading to the dibenzopyrene **27** by way of two consecutive cyclization and dehydrogenation steps is an example. The reaction is represented in Scheme 1.9 below.[79]
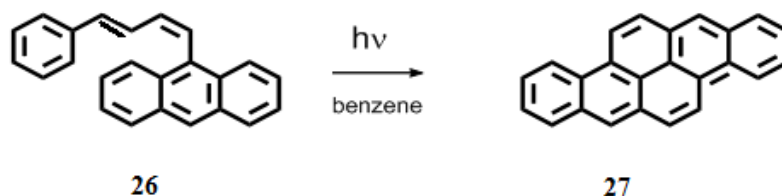
Scheme 1.9

1.9. Applications of above Systems

A-B substituted systems also have a number of potential applications. These bischromophoric arrays serve as prototypical light-harvesting devices, molecular photonic wires and optoelectronic gates by combining these systems with various other systems. Concentrated assemblies of chromophore centres in macromolecular superstructures offer ideal media for the absorption of light - a principle that applies to both solar and laser radiation. The development of molecular photonic devices requires the creation of molecular arrays that absorb light of specific wavelengths and undergo excited-state energy and/or charge transfer reactions.

Also the excitation of the above systems is usually associated with an increase in dipole moment. The properties of such systems depend on solvent polarity, and these can be exploited to determine the polarity of unknown solvent mixtures. The emission characteristics of the CT fluorescence bands are sensitive to the environment. Parameters such as fluorescence emission maximum, intensity, lifetime, polarization, and excitation spectrum can act as potential indicators of the features of probe surroundings. Molecules exhibiting ICT fluorescence have been used as fluorescent probes for probing the polarity of various micro heterogeneous systems and also as sensors.

In short, the substrates reviewed in this thesis serve to illustrate the difficulties facing a photochemist who attempts to predict the excited-state properties of multifunctional molecules using only a background of monochromophoric chemistry. Conversely, the diversity of photophysical and photochemical phenomena evident in even the small number of molecules discussed confirms that multichromophoric compounds will provide a fruitful area of investigation for photochemists, spectroscopists, and theoreticians for some time to come.

1.10. Objectives of the Present Work

The primary goal of the research presented in this thesis is to investigate the photophysical and photochemical properties of the bischromophoric arrays in relation to their structure and to determine a systematic change in intermolecular orientation or conformation of these influences their properties. Furthermore, it is aimed, based on the knowledge gathered by studying these arrays, at the design, synthesis and characterization of new multichromophoric structures, with anticipated properties and /or combination of properties which might be useful in future functional materials or molecular devices.

For this purpose several structurally and geometrically different arrays have been synthesized, their conformational changes have been studied in detail both experimentally and theoretically. The spatial arrangement of chromophores is varied by changes in the connecting linkers, thus varying e.g. the angle and/or distance between the chromophoric units. A systematic change in the chromophoric unit, furthermore led to series of compounds from which structure-properties relationships were derived.

Based on these considerations, we propose to develop efficient synthetic procedures for the preparations of suitable bischromophoric arrays in which the following constraints are built in: *i*) the two chromophores are separated through a suitable linker that shuts electronic communication between the two, *ii*) the procedure should provide the flexibility to tune the geometry of resultant arrays and *iii*) the procedure should be scaleable.

The chromophores used in these studies consist of aromatic system of varying sizes, which makes them, in principle, suitable for nonlinear optical measurements.

1.11. References

1.   Lehn, J. M. *Angew. Chem. Int. Ed. Engl.* **1988**, *27*, 89.

2.   Lehn, J. M. *Supramolecular Chemistry: Concepts and Perspectives*, VCH Verlag, Weinheim, **1995.**

3.   Nicolaou, K. C.; Sorensen, E. J. *Classics in Total Synthesis: Targets, Strategies, Methods*, VCH, Verlag, Weinheim, **1995.**

4.   McGimpsey, W. G.; Samaniego, W. N.; Chen, L.; Wang, Z. *J. Phys. Chem. A.* **1998**, *102*, 8679.

5.   (a) Hisda, K.; Tsuchida, A.; Ito, S.; Yamamoto, M. *J. Phys. Chem. A.* **1998**, *102*, 2640.

6.   Levine, B. F.; Bethea, C. G. *J. Chem. Phys.* **1975,** *63*, 2666.

7.   Singer, K. D.; Garito, A. F. *J. Chem. Phys.* **1981,** *75*, 3572.

8.   Meredith, G. R. *Rev. Sci. Instrum.* **1982,** *53*, 48.

9.   Clays, K.; Persoons, A. *Phys. Rev. Lett.* **1991**, *66*, 2980.

10.   Clays, K.; Persoons, A.; Maeyer, L. De*. Adv. Chem. Phys*, **1994***, 85(II),* 45.

11.   Clays, K.; Persoons, A. *Rev. Sci. Instrum.* **1992,** *63*, 3285.

12.   de Haas, M. P.; Warman, J. M. *Chem. Phys.* **1982**, *73*, 35.

13.   Warman, J. M.; de Hass, M. P. *Pulse Radiolysis*, Y Tabata Ed, CRC Press, Boca Raton, **1991**, ch.6.

14.   (a) Closs, G. L.; Miller, J. R. *Science.* **1988**, *240*, 440. (b) Marcus, R. A. *Angew. Chem. Int. Ed. Engl.* **1993**, *32*, 1111. (c) Marcus, R. A.; Sutin, N. *Biochim. Biophys. Acta.* **1985**, *811*, 265.

15.   Weller, A. Z. *Phys. Chem. Neue Folge.* **1982**, *133*, 93.

16.   Marcus, R. A. *J. Chem. Phys.* **1965**, *43*, 679.

17.   Ying, L.; Xie, X. S. *J. Phys. Chem. B.* **1998**, *102*, 10399.

18.   Garcia-Parajo, M. F.; Koopman, M.; van Dijk, E. M. H. P.; Subramaniam, V.; van Hulst, N. F. *Proc. Natl. Acad. Sci. USA* **2001**, *98*, 14392.

19.   (a) Wu, M.; Goodwin, P. M.; Ambrose, W. P.; Keller, R. A. *J. Phys. Chem.* **1996,** *100,* 17406. (b) Bopp, M. A.; Jia, Y.; Li, L.; Cogdell, R. J.; Hochstrasser, R. M. *Proc. Natl. Acad. Sci.* USA. **1997**, *94,* 10630. (c) van Oijen, A. M.; Ketelaars, M.; Kçhler, J.; Aartsma, T. J.; Schmidt, J. *Science.* **1999,** *285,* 400.

20.   (a) Bout, D. A.; Yip, W.; Hu, D.; Fu, D.; Swager, T. M.; Barbara, P. F. *Science.* **1977,** *277,* 1074. (b) Hu, D.; Yu, J.; Barbara, P. F. *J. Am. Chem. Soc.* **1999**, *121*, 6936. (c) Huser, T.; Yan, M.; Rotherberg, L. J. *Proc. Natl. Acad. Sci.* USA. **2000**, *97*, 11187. (d) Muller, J. G.; Lemmer, U.; Raschke, D.; Anni, A.; Scherf, U.; Lupton, J. M.; Feldmann, J. *Phys. Rev. Lett*. **2003,** *91,* 267.

21.   (a) Kasha, M.; Rawls, H. R.; Ashaf El-Bayoumi, M. *Pure Appl. Chem.* **1965**, *11*, 371.

22.   Forster, T.   in *Modern Quantum Chemistry* (Ed.: O. Sinanoglu), Academic Press, New York, **1965.**

23.   Merrigan, J. A. *Prospects for Solar Energy Conversion by Photovoltaics*, MIT Press, Cambridge, **1975.**

24.   Lehninger, A. L.; Nelson, D. L.; Cox, M. M. *Principles of Biochemistry*, Worth Publishers Inc., New York, **1993.**

25.   X. Hu, X.; Damjanovic, A.; Ritz, T.; Schulten, K. *Proc. Natl. Acad. Sci.*   U.S.A. **1998**, *95*, 5935.

26.   McDermott, G.; Prince, S. M.; Freer, A. A.; Hawthornthwaite-Lawless, A. M.; Papiz, M. Z.; Cogdell, R. J.; Isaacs, N. W. *Nature.* **1995,** *374,* 517.

27.   (a) Huber, R. *Angew. Chem. Int. Ed.* **1989**, *28*, 848. (b) Moser, C. C.; Keske, J. M.; Warncke, K.; Farid, R. S.; Dutton, P. L. *Nature.* **1992**, *355*, 796.

28.   (a) Jortner, J. *J. Chem. Phys.* **1976**, *64*, 4860. (b) Jortner, J. *J. Am. Chem. Soc.* **1980**, *102*, 6676. (c) Franzen, S.; Goldstein, R. F.; Boxer,

S. G. *J. Phys. Chem.* **1993**, *97*, 3040. (d) Page, C. C.; Moser, C. C.; Chen, X.; Dutton, P. L. *Nature.* **1999**, *402*, 47.

29.   (a) Wasielewski, M. R. *Chem. Rev.* **1992**, *92*, 435. (b) Gust, D.; Moore, T. A.; Moore, A. L. *Acc. Chem. Res.* **1993**, *26*, 198. (c) Gray, H. B.; Winkler, J. R. *Ann. Rev. Biochem.* **1996**, *65*, 537. (d) Gust, D.; Moore, T. A.; Moore, A. L. *Acc. Chem. Res.* **2001**, *34*, 40.

30.   (a) Holten, D.; Bocian, D. F.; Lindsey, J. S. *Acc. Chem. Res.* **2002**, *35*, 57. (b) Lindsey, J. S.; Wagner, R. W. *J. Org. Chem.* **1989**, *54,* 828. (c) Wagner, R.W.; Johnson, T.E.; Lindsey, J. S. *J. Am. Chem. Soc.* **1996**, *118*, 11166.

31.   Ambroise, A.; Li, J.; Yu**,** L**.;** Lindsey**,** J. S. *Org. Lett*. **2000**, 2, 2563.

32.   (a) Milgrom, L. R. *J. Chem. Soc., Perkin Trans. 1.* **1983**, 2535. (b) Davila, J.; Harriman, A.; Milgrom, L. R. *Chem. Phys. Lett.* **1987**, *136*, 427. (c) Wennerstrom, 0*.;* Ericsson, H.; Raston, I.; Svensson, S.; Pimlott, W. *Tetrahedron Lett.* **1989**, *30*, 1129. (d) Nagata, T.; Osuka, A.; Maruyama, K. *J. Am. Chem. SOC.* **1990**, *112,* 3054. (e) Anderson, S.; Anderson, H. L.; Sanders, J. K. M. *Angew. Chem. Inr. Ed. Engl.* **1992**, *31*, 907. (f) Dubowchik, G. M.; Hamilton, A. D. *J. Chem. Soc. Chem. Commun.* **1987**, 293.

33.   Prathapan, S.; Johnson, T. E.; Lindsey, J. S. *J. Am. Chem. Soc.* **1993***, 115,* 7519.

34.   Van der Boom, T; Hayes, R. T.; Zhao, Y.; Bushard, P. J.; Weiss, E. A.; Wasielewski, M. R. *J. Am. Chem. Soc.* **2002**, *124*, 9582.

35.   (a) Williams, R. M.; Zwier, J. M.; Verhoeven, J. W. *J. Am. Chem. Soc.* **1995**, *117*, 4093. (b) Guldi, D. M. *Chem. Soc. Rev.* **2002**, *31*, 22. (c) Fukuzumi, S. *Org. Biomol. Chem.* **2003**, *1*, 609.

36.   (a) Wasielewski, M. R.; Niemczyk, M. P. *J. Am. Chem. Soc.* **1984**, *106*, 5043, (b) Paddon-Row, M. N. *Acc. Chem. Res.* **1994**, *27*, 18.

37. (a) Guldi, D. M. *Chem. Soc. Rev.* **2002**, *31*, 22. (b) Imahori, H.; Mori, Y.; Matano, *J. Photochem. Photobiol. C.* **2003**, *4*, 51.

38. (a) Kuciauskas, D.; Liddell, P. A.; Lin, S.; Johnson, T. E.; Weghorn, S. J.; Lindsey, J. S.; Moore, A. L.; Moore, T. A.; Gust, D. *J. Am. Chem. Soc.* **1999**, *121*, 8604. (b) Andersson, M.; Sinks, L. E.; Hayes, R. T.; Zhao, Y.; Wasielewski, M. R. *Angew. Chem. Int. Ed.* **2003**, *42*, 3139.

39. (a) Chambron, J.-C.; Chardon-Noblat, S.; Harriman, A.; Heitz, V.; Sauvage, J.-P. *Pure Appl. Chem.* **1993**, *65*, 2343. (b) Harriman, A.; Sauvage, J.-P. *Chem. Soc. ReV.* **1996**, *26*, 41. (c) Blanco, M.-J.; Jimenez, M. C.; Chambron, J.-C.; Heitz, V.; Linke, M.; Sauvage, J.-P. *Chem. Soc. Rev.* **1999**, *28*, 293. (d) Kurreck, H.; Huber, M. *Angew. Chem. Int. Ed. Engl.* **1995**, *34*, 849. (e) Balzani, V.; Juris, A.; Venturi, M.; Campagna, S.; Serroni, S. *Chem. Rev.* **1996**, *96*, 759. (f) Amabilino, D. B.; Stoddart, J. F. *Chem. Rev.* **1995**, *95*, 2725.

40. (a) Boyd, P. D. W.; Hodgson, M. C.; Rickard, C. E. F.; Oliver, A. G.; Chaker, L.; Brothers, P. J.; Bolskar, R. D.; Tham, F. S.; Reed, C. A. *J. Am. Chem. Soc.* **1999**, *121*, 10487. (b) Wang, Y.-B.; Lin, Z. *J. Am. Chem. Soc.* **2003**, *125*, 6072. (c) Shirakawa, M.; Fujita, N.; Shinkai, S. *J. Am. Chem. Soc.* **2003**, *125*, 9902. (d) Shoji, Y.; Tashiro, K.; Aida, T. *J. Am. Chem. Soc.* **2004**, *126*, 6570. (e) Guldi, D. M.; Gouloumis, A.; Vazquez, P.; Torres, T.; Georgakilas, V.; Prato, M. *J. Am. Chem. Soc.* **2005**, *127*, 5811.

41. (a) Yamaguchi, T.; Ishii, N.; Tashiro, K.; Aida, T. *J. Am. Chem. Soc.* **2003**, *125*, 13934. (b) D'Souza, F.; Smith, P. M.; Zandler, M. E.; McCarty, A. L.; Itou, M.; Araki, Y.; Ito, O. *J. Am. Chem. Soc.* **2004**, *126*, 7898. (c) Hasobe, T.; Kamat, P. V.; Troiani, V.; Solladie, N.; Ahn, T. K.; Kim, S. K.; Kim, D.; Kongkanand, A.; Kuwabata, S.; Fukuzumi, S. *J. Phys. Chem. B.* **2005**, *109*, 19.

42.   Zhang, X.; Xiao, Y.; Qian, X. *Org. Lett*. **2008**, *10*, 29.

43.   Coskun, A.; Akkaya, E. U. *J. Am. Chem. Soc*. **2005**, *127*, 10464.

44.   Hargland, R. P. *Handbook of Fluorescent Probes and Research Products*, 9th ed.; Molecular Probes: Carlsbad, CA, **2002**, Chapter 1.

45.   Ziessel, R.; Ulrich, G.; Harriman, A. *New J. Chem*. **2007**, *31*, 496.

46.   Li, F.; Yang, S.; Ciringh, Y.; Seth, J.; Martin, C.; Singh, D.; Kim, D.; Birge, R.; Bocian, D. F.; Holten, D.; Lindsey, J. S. *J. Am. Chem. Soc*. **1998**, *120*, 10001.

47.   O'Neil, M. P.; Niemczyk, M. P.; Svec, W. A.; Gosztola, D.; Gaines, G. L.; Wasielewski, M. R. *Science*. **1992**, *257*, 63.

48.   (a) Gvishi, R.; Reisfeld, R.; Burshtein, Z. *Chem. Phys. Lett*. **1993**, *213*, 338. (b) Langhals, H. *Heterocycles*. **1995**, *40*, 477. (c) Würthner, F. *Chem. Commun*. **2004**, 1564.

49.   (a) De Schryver, F. C.; Vosch, T.; Cotlet, M.; Van der Auweraer, M.; Müllen, K.; Hofkens, J. *Acc. Chem. Res*. **2005**, *38*, 514. (b) Gronheid, R.; Stefan, A.; Cotlet, M.; Hofkens, J.; Qu, J.; Mullen, K.; Van der Auweraer, M.; Verhoeven, J. W.; De Schryver, F. C. *Angew. Chem. Int. Ed. Engl*. **2003**, *42*, 4209.

50**.**   Adronov**,** A.**;** Frechet, J. M. J. *Chem. Commun*. **2000,** 1701**.**

51.   Freeman, A. W.; Frechet, J. M. J.; Koene, S. C.; Thompson, M. E. *Polym. Prepr.* **1999,** *40,* 1246.

52.   Odobel, F.; Zabri, H. *Inorg. Chem*. **2005**, *44*, 5600.

53.   Wenz, G. *Angew. Chem. Int. Ed. Engl.* **1994***, 33,* 803.

54.   Jullien, L.; Canceill, J.; Valeur, B.; Bardez, E.; Lefevre,J.-P.; Lehn,J.-M.; Marchi-Artzner, V.; Pansu, R. *J. Am. Chem. Soc*. **1996**, *118*, 5432.

55.   Berberan-Santos, M. N.; Canceill, J.; Brochon, J. C.; Jullien, L.; Lehn, J. M.; Pouget, J.; Tauc, P.; Valeur, B. *J. Am. Chem. Soc*. **1992**, *114*, 6427.

56.   Vincent Souchon, V.; Maisonneuve, S.; David, O.; Leray, I.; Xie, J. ;
       Valeur, B. *Photochem. Photobiol. Sci.* **2008**, *7,* 1323.

57.   Valeur, B.; Leray, I. *Inorg. Chim. Acta.* **2007**, *360*, 765.

58.   Van Wageningen, A. M. A.; Timmerman, P.; van Duynhoven, J. P.
       M.; Verboom, W.; van Veggel, F. C. J. M.; Reinhoudt, D. N. *Chem.
       Eur. J.* **1997**, *3*, 639.

59.   Chattopadhyay, N.; Haldar, B.; Mallick, A.; Sengupta, S. *Tetrahedron
       Lett.* **2005**, *46*, 3089.

60.   Brasseur, N.; Ali, H.; Langlois, R.; van Lier, J. E. *Photochem.
       Photobiol.* **1988***, 47,* 705.

61.   Garcia-Parajo, M. F.; Hernando, J.; Mosteiro, G. S.; Hoogenboom, J.
       P.; van Dijk, E. M. H. P.; van Hulst, N. F. *Chem. Phys. Chem.* **2005,**
       6, 819.

62 .   Forster, Th.; *Angew. Chem.* **1969**, *81*, 364. (b) Birks, J. B.;
       Photophysics of Aromatic Molecules, Wiley-Interscience, London,
       1970, chap. 7.

63.   Lin, Z.; Priyadarshy, S.; Bartko, A.; Waldeck, D. H. *Photochem.
       Photobiol.* **1997***, 110,* 131.

64.   Hochstrasser, R. M. *Can. J. Chem.* **1961**, *39,* 459.

65.   Friedel, R. A.; Orchin, M.; Reggel, L. *J. Am. Chem. Soc*. **1948**, *70,*
       199.

66.   Greenfield, N.; Fasman, G. D. *J. Am. Chem.Soc.* **1970**, *92*, 177.

67.   Williams, D. H.; Fleming, I.; *Spectroscopic Methods in Organic
       Chemistry*, Fourth edition, **1986**, p.8.

68.   (a) Fromm, R.; Ahmed, S. A.; Hartmann, T.; Huch, V.; Abdel-
       Wahab, A. A.; Durr, H. *Eur. J. Org. Chem.* **2001,** *21*, 4077. (b)
       Weber, C.; Rustemeyer, F.; Durr, H. *Adv. Mater.* **1998**, *10*, 1348. (c)
       Andreis, C.; Durr, H.; Wintgens, V.; Valat, P.; Kossanyi, J. *Chem.
       Eur. J.* **1997**, *3*, 509.

69.   (a) Ahmed, S. A.; Abdel-Wahab, A. A.; Durr, H.; *CRC Handbook of Organic Photochemistry and Photobiology* (2nd edn). Horspool WM, Lenci F (eds). CRC press: New York, **2004**, Chapter 96, 1. (b) Seto, J. *In Infrared Absorbing Dyes*, Matsuoka M (ed). Plenum Press: New York, **1990**, 71.

70.   (a) Leonhardt, H.; Weller, A. *Ber. Bunsenges. Phys. Chem.* **1963**, *67*, 791. (b) Mataga, N.; Okada, T.; Ezumi, K. *Mol. Phys.* **1966**, *10*, 203. (c) Beens, H.; Weller, A. *Acta Phys. Pol.* **1968**, *34*, 593. (d) Weller, A. in *The Exciplex;* Gordon, M., Ware, W. R., Eds.; Academic: New York, **1976**, p 23.

71.   Dyer, J. R.; *Applications of Absorption Spectroscopy of Organic Compounds,* (Ninth ed), Prentice-Hall of India Private Limited, New Delhi, **1994**, p-8.

72.   Suppan, P.; *Chemistry and Light;* The Royal Society of Chemistry, Thomas Graham House, The Science Park, Cambridge, **1994,** p-92.

73.   Becker, H.-D.; Andersson, K. *J. Org. Chem.* **1983,** *48*, 4542.

74.   (a) Becker, H.-D.; Hansen, L.; Andersson, K. *J. Org. Chem.* **1981**, *46*, 5419. (b) Becker, H.-D.; Sandros, K.; Andersson, K. *Angew. Chem. Int. Ed. Engl.* **1983**, *22*, 495.

75.   Becker, H.-D.; Becker, H.-C.; Sandros, K.; Andersson, K. *Tetrahedron Lett.* **1985,** *26*, 1589.

76.   Bouas-Laurent, H.; Castellan, A.; Desvergne, J-P. *Pure and Appl. Chem.* **1980**, *52*, 2633.

77.   Daney, M.; Vanucci, C.; Desvergne, J-P.; Castellan, A.; Bouas-Laurent, H. *Tetrahedron Lett.* **1985**, *26,* 1505.

78.   Becker, H.-D.; Skelton, B. W.; White, A. H. *Aust. J. Chem.* **1986**, *38,* 1471.

79.   Hayward, R. J.; Leznoff, C. C. *Tetrahedron.* **1971**, *27*, 2085.

SYNTHESIS AND PHOTOCHEMICAL STUDIES OF A FEW BISAROMATIC SYSTEMS: STRUCTURE - ACTIVITY RELATIONSHIPS

2.1. Abstract

Intramolecular energy transfer is reviewed from several perspectives, such as the generally accepted mechanism and molecular structure dependence. Some unique molecules such as bischromophores linked by rigid bridges were designed to serve as models for studying excited state interaction between constituent chromophore residues. Bischromophoric molecules containing benzene, naphthalene, anthracene and pyrene as donor and acceptor linked by a unique rigid 1,4-dien-3-one linker were synthesized.

2.2. Introduction

In this chapter we describe the effect of structure on photochemical and photophysical properties in a series of conformationally rigid bischromophoric molecules. Our results are discussed *vis-à-vis* the properties of a flexible bischromophoric molecule reported in literature. Becker and co-workers have shown that irradiation of dianthrylalkenones[1] gave *cis-trans* isomerization for enone linkage in dianthrylpentenone. In this context, we examined several bischromophoric compounds containing different π-aromatic systems as chromophores connected through cyclopentanone spacer. Dramatic structure-activity relationship could be observed with these molecules. Some of our compounds underwent *cis-trans* isomerization, while

some others remained inactive. The most probable reasons can be: (a) Insufficient energy for reaction, (b) Exciton coupling and further excited state interaction like excimer formation and (c) Restricted rotation around alkenyl bond. A detailed overview on exciton coupling of bisaromatic systems and the photochemistry of bisanthrylalkenone reported in literature is explained in the following paragraphs.

2.2.1. An Overview on the Photochemistry of Bisarylalkenones

Earlier studies by Becker *et al.* have shown that upon direct irradiation, *trans,trans*-1,5-bis(9-anthryl)pentadienone **1** is smoothly converted into the *trans,cis* isomer **2**. In oxygen saturated solution of dichloromethane with conventional fluorescent "warm white" light tubes, the above *cis,trans* isomer **2** gets converted to *cis,cis* isomer **3**[1] (Scheme 2.1). This result clearly indicates that 1,5-bis(9-anthryl)pentadienones undergo facile photochemical *cis-trans* isomerization. Similar *cis-trans* isomerization reactions can, in principle, be expected in the case of other pentadienones as well.
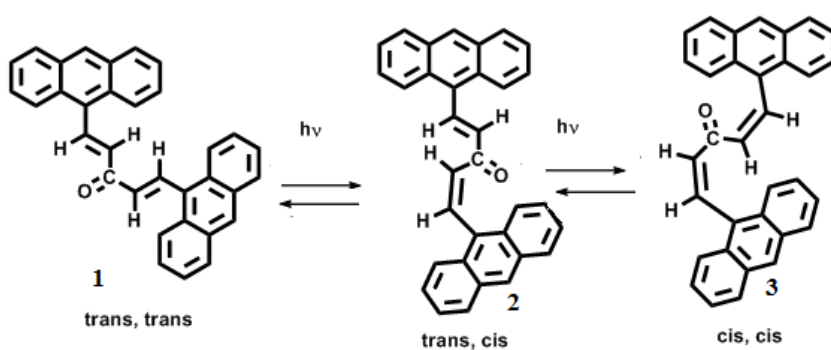
Scheme 2.1

2.2.2. Interaction between Chromophores in Bisaromatic Systems - Exciton Coupling

Depending upon the orientation of chromophores along molecular axis, interaction takes between chromophore components in these molecules.[2] The exciton chirality rule advanced by Harada and Nakanishi[3,4,5] is a powerful method for predicting such interactions. Interactions of conjugated systems have often been discussed in the frame work of molecular exciton theories[6] based on dipole-dipole interaction models.[7] Absorption of UV-Vis light causes changes in the distribution of electron density in a molecule (or in a chromophore in the molecule). The movement of electron density due to promoting the molecule from its electronic ground state to an excited state creates momentary dipole, called electronic transition dipole (μ). Consequently, with each electronic transition there is a polarization (electric transition dipole) that has both direction and intensity that vary according to the chromophores and particular excitation. The transition moments of the $\pi-\pi*$ band of conjugated dienes, enones, etc., are almost parallel to the long axis of chromophores.[8]
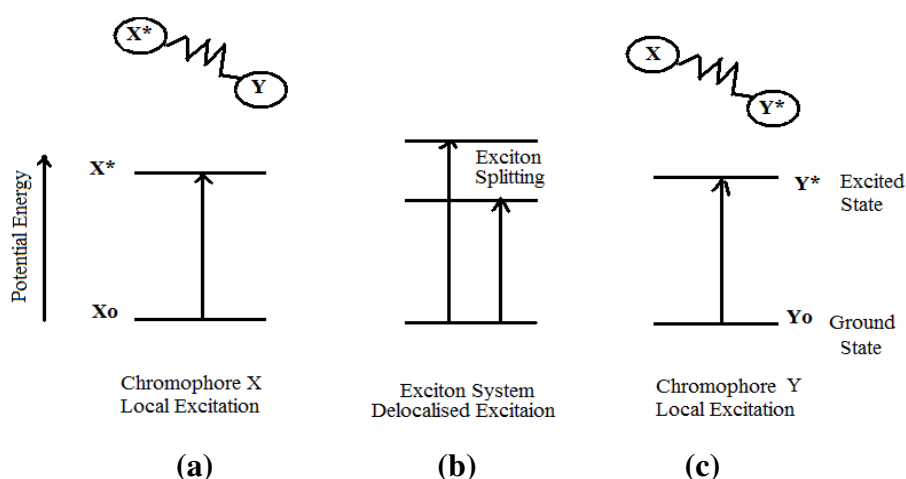
Figure 2.1: *Diagrammatic representation for a system with two chromophores (X and Y) held together through covalent bonding[7].*

Suppose two chromophores (represented by X and Y in Figure 2.1) are brought into close proximity, but orbital overlap and electron exchange are negligible. The chromophores may interact through dipole-dipole coupling of their locally excited state to produce a delocalized excitation (called an exciton) and a splitting called exciton coupling of the locally excited states (Figure 2.1).[7]

Orientation-dependence of the exciton coupling forms the basis for the exciton chirality rule. The UV-Vis spectra of the composite system originate not only from the electronic excitation spectral properties of the component chromophores, but they also depend on interchromophoric distance, mutual orientation, and geometry. The spectral shifts and splitting magnitudes can be correlated with the intensity and relative orientation of the electric transition dipole moments associated with the particular UV-Vis absorption band of each chromophore (Figure 2.2).
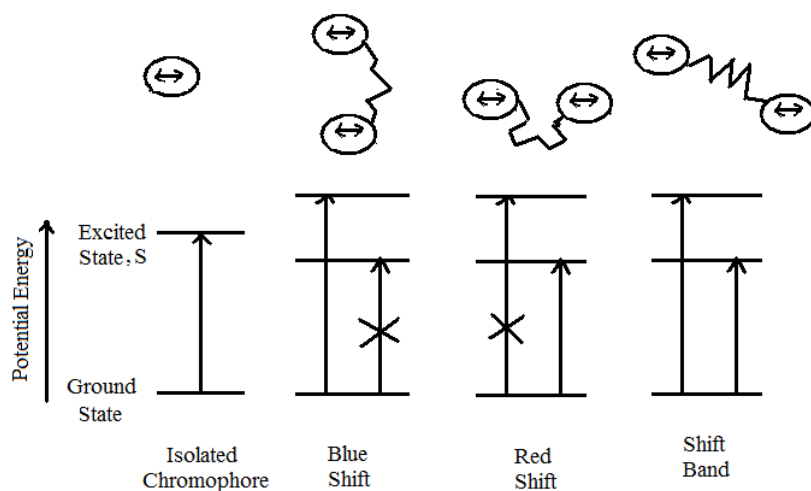
Figure 2.2: *Diagram for the origin of UV-Vis spectral shifts and splitting due to exciton interaction of two chromophores. Chromophores are represented by ellipses and electric transition dipoles by (↔).[7]*

In Figure 2.2, for two limiting orientations (a) only excitation into the higher lying exciton state is allowed for the parallel orientation (resulting in a

blue shift), and (b) only excitation into the lower lying exciton state is allowed for the in-line orientation (resulting in a red shift) relative to the isolated chromophore. For orientations lying in between these two limiting cases, (c) a split or broadened band is typically observed. This result arises since dipole-dipole interaction falls off with inverse cube of the separation distance. Consequently, the most useful chromophores for examining exciton coupling phenomena over short and especially over long distances are those with accessible, electric dipole allowed UV-Vis transitions, typically $\pi-\pi*$, such as aromatic chromophores and polyenes.

The exciton splitting energy for a molecular dimer,[9,10,11] or a double molecule,[12] with oblique transition dipoles corresponding to the separation, "ΔE" is given by (Eqn 2.1)[13]

$$\Delta E = 2 \ |\mathbf{M}|^2 /r^3 \ (Cos \ \alpha + 3 \ Cos^2 \ \Theta) \qquad \text{(Equation 2.1)}$$

where $\mathbf{M}$ is the transition moment for the singlet-singlet transition in the monomer, r is the centre to centre distance between the chromophores, α is the angle between polarization axes for the component absorbing units and Θ is the angle made by the polarization axes of the unit molecule with the line of molecular centres.

Anthracene is a good example of a chromophore useful for exciton coupling. It exhibits several $\pi \rightarrow \pi*$ transitions, including ^1L_a, short-axis polarized UV absorption near 360 nm (E ~ 7,500) and ^1B_b, a very intense long–axis polarized intense UV absorption near 250 nm (E ~ 2,00,000) (Figure 2.3).

In a composite system, where two anthracenes are fused to bicyclo[2.2.2]octane (Figure 2.3), the intense long axis-polarized transition dipoles are oriented neither parallel nor in-line, but intersect at an obtuse angle and lie one in each of the two intersecting planes (dihedral angle of ~120°). Then the two overlapping exciton transitions interact. The result of exciton splitting of excited states in the composite molecule may be the appearance of

strong spectral shifts or splittings (which may be of the order of 2000 cm^{-1}) of the absorption bands for the component molecules.[14]
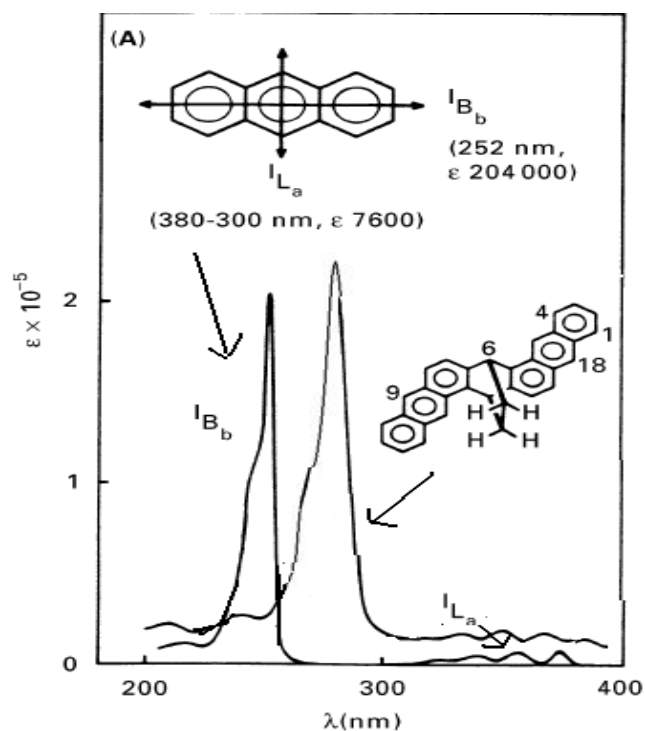
Figure 2.3: *UV spectra of anthracene and ring fused bisanthracene.*

At the same time, as a consequence of the exciton splitting of the excited state manifold, an enhancement of triplet state excitation may result. Toluene, diphenylmethane,[15] and triphenylmethane[16] offer definite example of the triplet state enhancement through exciton splitting. The experimental results for these shows that the phosphorescence-fluorescence ratio (intersystem crossing ratio) increases conspicuously in this series, while at the same time the phosphorescence mean lifetime remains relatively constant.

To conclude, in bischromophoric molecules the triplet state excitation enhancement depends on the exciton interaction among excited states of the component molecules,[17] which in turn depends on the alignment of the

bischromophoric system. This is how geometry influences the photochemistry of such systems.

2.2.3. Application of Photochemical *cis-trans* Isomerization of Organic molecule – Optical Molecular Switch

The basic requirement for a molecular switch is bistability, i.e. the occurrence of two stable forms A and B which can be interconverted by external stimuli, S_1 and S_2. For an optical molecular switch optical molecular interconversion is effected by means of light. Also the molecular forms must be identified by an external detection method.

Organic compounds can be used for optical information storage.[18] In those systems switching process occurs through photochemically induced *cis-trans* isomerization or electrocyclization. For example, in the case of azobenzene, *cis-trans* isomerization readily occurs photochemically.[19] Here the isomers have clearly different UV absorption spectra. Absence of side reactions as well as high energy barrier for thermal *cis-trans* isomerization makes it a good optical molecular switch. From these considerations it is clear that bisaromatic systems with alkene linkage capable of *cis-trans isomerization* can be used as molecular switch.

We synthesized several such systems by employing Claisen-Schmidt reaction.[20,21] The condensation of aromatic aldehydes (or between ketones and aldehydes lacking α-hydrogen) with aliphatic or mixed alkyl aryl ketones in the presence of a relatively strong base to form α,β-unsaturated ketones is termed as the Claisen-Schmidt reaction. This reaction is of tremendous value in synthetic organic chemistry[22,23] and is frequently encountered as a key step in several elegant total synthesis protocols. Claisen-Schmidt condensation can also be catalysed by acid.[24]

The first step is a condensation of aldol type, enols or enolates are involved as intermediates in this reaction. This reaction involves the nucleophilic addition of enol or enolate ion derived from methyl ketone to the carbonyl-carbon of the aromatic aldehyde. Dehydration of the hydroxylketone to form the conjugated unsaturated carbonyl compound occurs spontaneously (Scheme 2.3).[25] There exists a pronounced preference for the formation of a *trans* double bond in the Claisen-Schmidt condensation of methyl ketones.[26]
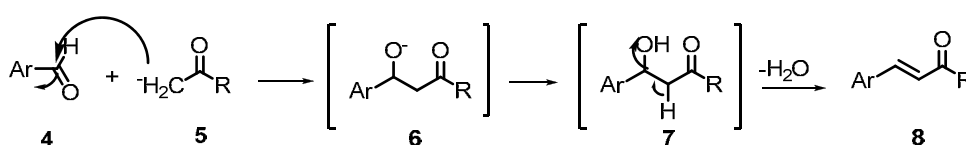
Scheme 2.3

Cycloalkanones such as cyclopentanone and cyclohexanone readily participate in Claisen-Schmidt reaction.[27] The crossed aldol condensation of cyclopentanone with aldehydes is faster than that of cyclohexanone. This may be due to the removal of the eclipsing effect of the adjacent hydrogen atom in cyclopentanone after the formation of the arylmethylidene derivative.[28]

2.3. Results and Discussion

To investigate the hypothesis concerning structural control on chromophore-chromophore interaction, we have prepared a set of dimeric arrays (Chart 2.1). The target compounds proposed by us are good models for studying intramolecular chromophore interactions. The common feature of these bisaromatic compounds is that they all contain rigid 2,5-dialkylidene-cyclopentanone spacer. Compound **12e** is an exception and was synthesized to execute a comparative study of bischromophoric systems having flexible linkages vis-à-vis those having rigid linkages.
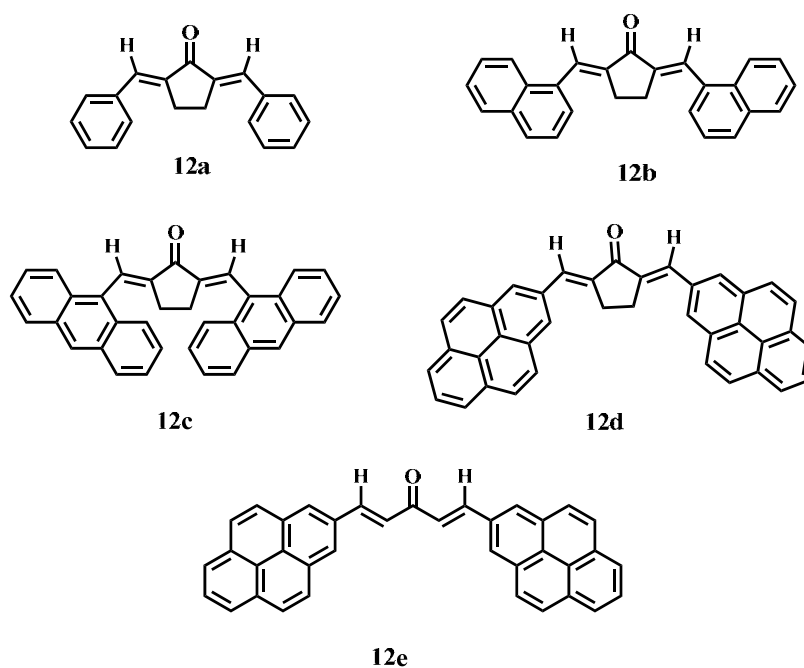
Chart 2.1

2.3.1. Synthesis and Characterization

Cyclopentanone (1 equiv.) on reaction with (2 equiv.) of benzene-carboxaldehyde, 1-naphthalenecarboxaldehyde, 9-anthracenecarboxaldehyde, 1-pyrenecarboxaldehyde in the presence of either acid or base catalyst (2 equiv.) and methanol (10 mL) give the corresponding diarylidene-cyclopentanones **12a-d** in very good yield (Scheme 2. 4). We selected the base catalyzed Claisen-Schmidt condensation in methanol to prepare desired compounds.[29] The advantages of base catalyzed reaction include simple reaction and work up procedures and relatively mild reaction conditions.

Acid-catalyzed Claisen-Schmidt condensation was utilized for the synthesis of the bispyrene compound **12e.** A solution of 1-pyrene-carboxaldehyde **10d** and acetone **14** (1:10) in ethyl acetate was saturated with hydrogen chloride gas and stirred for 24 h at room temperature (Scheme 2.5). Bispyrene **12e** precipitated from the reaction mixture was purified by soxhlet extraction.
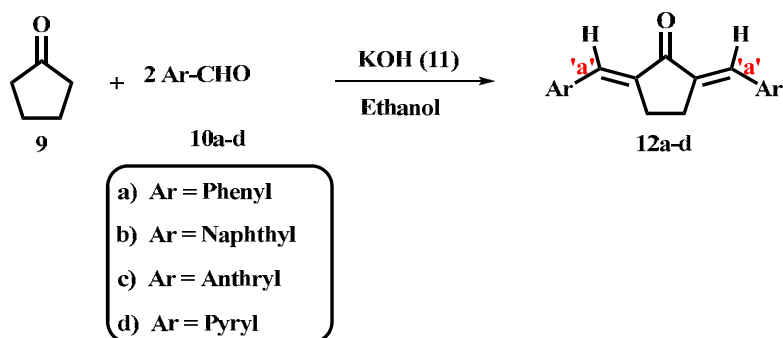
Scheme 2.4
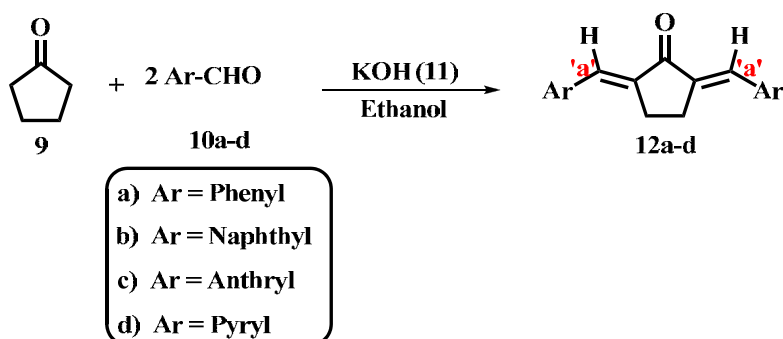
Scheme 2.5

The structures of the bisaromatic compounds **12a-e** were established on the basis of analytical results and spectral data. The UV absorption spectra of **12a** indicated the presence of extended conjugation in benzene residues. The physical data obtained for **12a** was identical to those reported in literature. The α,β-unsaturated keto group in **12a** is indicated in the IR spectrum, by the strong peak at 1690 cm^{-1} and the peak at 1664 cm^{-1} is indicative of conjugated olefinic bond. The ^{1}H NMR shows a singlet at δ 2.95 denoting aliphatic proton of cyclopentanone moiety, further proving that **12a** is a symmetric molecule. The multiplets appeared from δ 6.99 to δ 7.54 established the aromatic protons of **12a.** The proposed structure was further supported by ^{13}C NMR spectrum showing a single carbonyl peak positioned at δ 195.0. The aliphatic carbon of the cyclopentenone part appeared at δ 23.9. Based on

NMR data, we have established that the molecule has a rigid structure with extended conjugation between aryl and dienone components. In the ^{13}C NMR spectrum of *2E,5E*-dibenzylidene-cyclopentanone, six signals coresponding to aromatic carbons were observed. This suggests partial double bond character and restricted rotation around the bond '*a*' as a direct consequence of efficient extended π-orbital overlap. The molecular ion peak at *m/z* 261.39 (M^++1) in the FAB mass spectrum, ascertains the structural identity of bisbenzylidene **12a**. Satisfactory elemental analysis data also supported the formation of the adduct.

Absorption spectrum of **12b** indicated the presence of extended conjugation in naphthalene residues. In the IR spectrum of **12b**, the peak at 1662 cm^{-1} is due to the keto group of the dienone functionality. The ^{1}H NMR spectrum showed a singlet at δ 3.00 denoting aliphatic proton of cyclopentanone moiety, further proving that **12b** is a symmetric molecule. The appearance of multiplets from δ 7.47 to δ 8.37 established the aromatic protons of **12b**. The proposed structure was further supported by ^{13}C NMR spectrum showing a single carbonyl peak positioned at δ 195.4. The aliphatic carbon of the cyclopentanone part appeared at δ 27.1. The molecular ion peak at *m/z* 361.16 (M^++1) in the FAB mass spectrum, ascertains the structural identity of bisnaphthalene **12b**. Satisfactory elemental analysis data also supported the formation of the adduct.

Absorption spectrum of **12c** indicated the presence of extended conjugation in the anthracene residues. In the IR spectrum of **12c**, the peak at 1634 cm^{-1} symbolizes the keto group of the dienone functionality. The ^{1}H NMR spectrum showed a singlet at δ 2.31 denoting aliphatic proton of cyclopentanone moiety, further proving that **12c** is a symmetric molecule. The multiplets at δ 7.46 to δ 8.57 establish the aromatic protons of **12c.** The proposed structure was further supported by ^{13}C NMR spectrum showing a single carbonyl peak positioned at δ 194.1. The aliphatic carbon atom of

cyclopentanone part appeared at δ 25.7. Furthermore, fourteen signals attributable to the anthracene moiety were observable in the ^{13}C NMR spectrum. This clearly indicated extended conjugation and concomitant restriction rotation around bond '*a*' in the case of **12c.** The molecular ion peak at *m/z* 461.20 ($M^+ + 1$) in the FAB mass spectrum, ascertains the structural identity of bisanthracene **12c.** Satisfactory elemental analysis data also supported the formation of the adduct.

Indisputable evidence for the structure and stereochemistry of the adduct was provided by single crystal X-ray analysis (Figure 2.4).
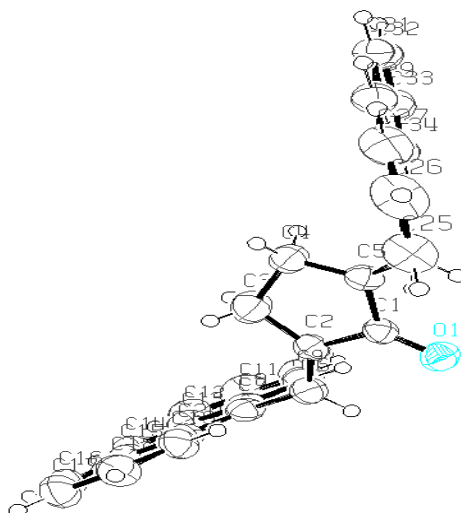
Figure 2.4: ORTEP diagram of **12c.**

Crystallographic data authenticated the roof-like geometry of the compound **12c.** In this geometry, both long-axes polarized (^1B_b) and short-axis polarized (^1L_a) transitions are expected to undergo weak exciton coupling. While red shift is expected in the case of ^1B_b band, blue shift is expected in the case of (^1L_a) band. However, extended conjugation and concomitant red shift in anthracene absorption is expected in this case. Structural rigidity imposed by the cyclopentanone spacer is expected to augment the red shift in absorption

maximum of **12c** with respect to both an isolated anthracene and conjugated systems such as **1**. Comparison of peak position of (^1L_a) band in **12c** with that of an isolated anthracene should be quite revealing. If a blue shift is observed, exciton coupling is significant; if a red shift is observed, extended conjugation is more significant. It should be interesting to examine the absorption characteristics and correlate them with the photochemistry and photophysics of compounds such as **12c**. Subtle changes in absorption characteristics can have far reaching consequences on the photochemistry and photophysics of bisanthracenes such as **12c**.

A strong peak at 1628 cm^{-1} in the IR spectrum of **12d** depicts the presence of $\alpha,\beta-$unsaturated keto group. The UV absorption spectra of **12d** indicated the presence of extended conjugation in the pyrene residues. Due to the poor solubility of the compound **12d** in deuterated CHCl$_3$, DMSO and in acetone reliable solution phase NMR spectral data could not be collected. So, we recorded its ^{13}C solid state NMR (Figure 2.5a-b) spectrum.
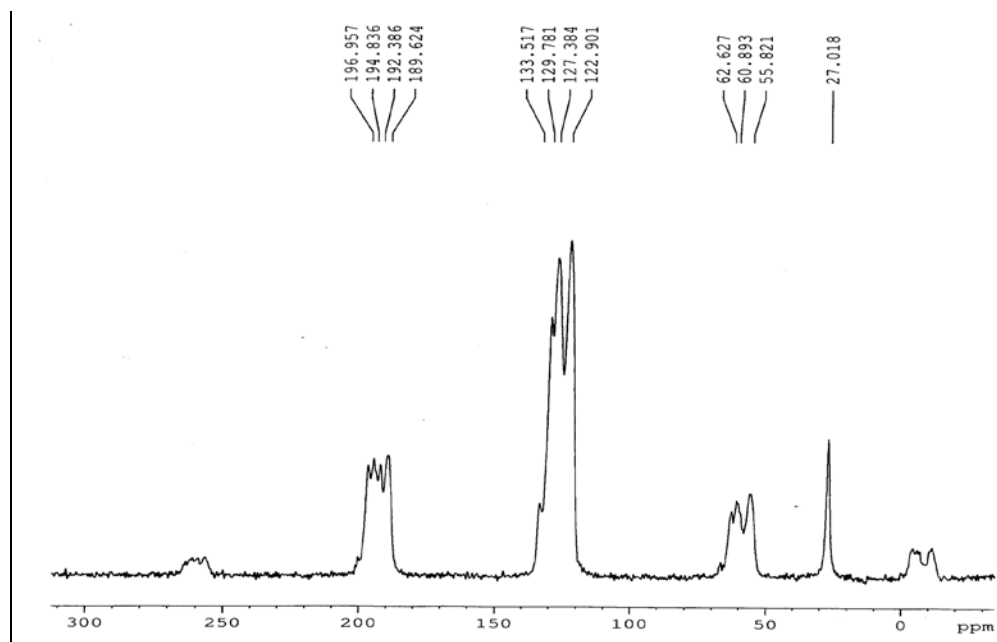
Figure 2.5a: Solid-state NMR of the prepared bispyrene compound **12d** (5 KHz)
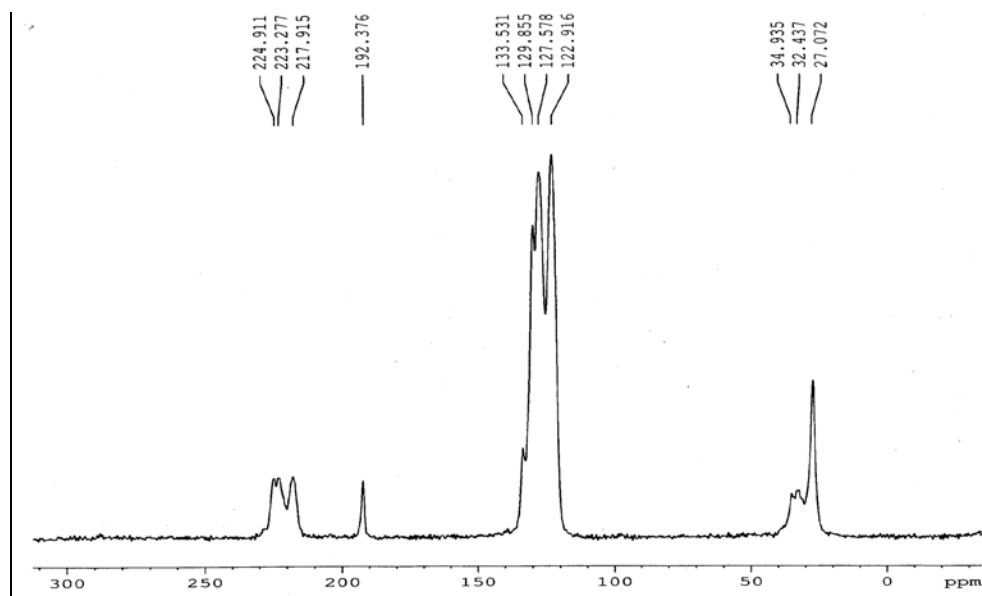
Figure 2.5b: Solid-state NMR of the prepared bispyrene compound **12d** (7.2 KHz)

The ^{13}C solid state NMR is usually collected by means of a technique called CP/MAS (Cross-polarization, magic angle spinning). Unlike solution phase spectrum, the solid state spectrum consists of two types of signals. The isotropic peaks (the actual peaks from the sample) and the spinning side bands, which are equally spaced on either side of the main isotropic bands are observable here. The spinning side bands originate from the Chemical Shift Anisotropy (CSA) of the system, which is a molecular property.

We have taken the spectrum at two different spinning speeds, *i.e.* at 5 KHz and 7.2 KHz, the spinning side bands moved apart with the spinning speed while the isotropic peak remained at the same position. Hence, **12d** sample shows isotropic peaks at 192.4, 133.5, 129.9, 127.6, 122.9 and 27.1. All the other signals are due to spinning side bands. So the data confirmed the presence on one aliphatic carbon with other aromatic carbons, suggesting the identity of compound **12d**.

2.3.2. Photochemical Properties

The photochemistry and photophysics of the above compounds could unravel interesting aspects. We carried out all irradiation experiments with very dilute solutions of **12a-d** at 350 nm using a Rayonet Photochemical Reactor. The criterion for the selection of 350 nm lamps for irradiation was based on a simple Beer-Lambert calculation which revealed that for bulk reactivity, photolysis wavelength near the absorption tail should be used or else the incident radiation will be absorbed near the surface. Diarylidene-cyclopentanones **12a-d** absorb strongly in the 300-400 nm region. Due to the solubility of the diarylidenecyclopentanones in benzene, and its transparency in the 350 nm region, we selected benzene as a suitable solvent for photochemical studies. Extra precaution was taken while handling benzene. All manipulations involving this solvent was carried out in a fume hood provided with powerful exhaust fan.

2.3.2.1. Photochemistry of Compounds 12a-e

Benzene solutions of dibenzylidenecyclopentanones 12a-d were degassed by bubbling nitrogen through it and irradiated with UV light of 350 nm wavelength for 10 h. In the irradiation, for the compounds 12a and 12b, new products were formed. Based on prior reports on enone photochemistry, we conclude that *cis-trans* isomerization is taking place in the case of both 12a and 12b (Scheme 2.7).

12a-b   **13a-b**
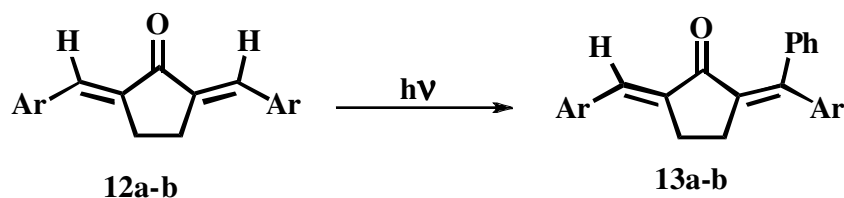
a) **Ar = Phenyl**

b) **Ar = Naphthyl**

Scheme: 2.7.

The spectral and analysis data indicated that the products formed were isomers of the starting materials **12a,b**. In the IR spectrum of **12a**, the α,β−unsaturated carbonyl stretching peak appears at 1663 cm^{-1}. ^{1}H NMR spectrum of the photoproduct showed that the CH$_2$ groups in the cyclopentanone unit are not chemical shift equivalent. This is a clear indication that the symmetry available in **12a** is lifted in the photoproduct. ^{13}C NMR analysis also confirmed unsymmetrical nature of the molecule. The molecular ion peak at 261.5 (M^++1) in the mass spectrum also supported the structure. All the above observations confirmed *cis-trans* isomerization around of the double bond in the molecule.

Similarly, in the IR spectrum of **12b**, the α,β−unsaturated carbonyl stretching peak appears at 1643 cm^{-1}. ^{1}H NMR spectrum of the photoproduct showed that the CH$_2$ groups in the cyclopentanone unit are not chemical shift equivalent. ^{13}C NMR analysis also confirmed unsymmetrical nature of the molecule. The molecular ion peak at 361.1 (M^++1) in the mass spectrum also supported isomerisation upon photolysis. All the above observations confirmed *cis-trans* isomerization around of the double bond in the molecule. However, **12c,d** remained unchanged even after prolonged irradiation. This result deserves special attention. Becker *et al*[1] have reported that compounds such as **1** undergo facile photochemical *cis-trans* isomerization. Though not reported in literature, based on Becker's findings, **12d** also may be expected to undergo *cis-trans* isomerization. The absorption spectra of **12c** and **12d** are not very different from those of **1** and **12e** respectively. In fact, with respect to **12c**, bisanthracene **1** exhibits a more red-shifted absorption maximum. Interestingly, irradiation of **12e** resulted in the formation of new product/s as evidenced by absorption and emission spectral changes with irradiation. We attribute the observable spectral changes here to photochemical *cis-trans* isomerization reactions. Our attempts to isolate the photoproduct generated

from **12e** were not successful and hence our conclusions on the photochemistry of **12e** are somewhat speculative in nature.

2.4. Conclusions and Pointers

We have examined the photochemistry of various diarylidene-cycloalkanones. Photochemical studies have shown that *cis-trans* isomerization takes place in **12a** and **12b**, while **12c** and **12d** were unresponsive towards photolysis. These results deserve close scrutiny. Though one can argue that excitation energy is concentrated in anthracene and pyrene components in **12c** and **12d**, literature survey regarding the photochemistry of dianthrylpentenones such as **1** revealed that *cis-trans* isomerization is possible for these enones.

Absorption spectra of **12c,d** should hold the key to their odd photochemical behavior. The posers here include: a) why photochemistry of **12a** and **12b** differs from that of **12c** and **12d,** and b) why photochemistry of **12c** differs from that of dianthrylpentenone **1**? It may be noted that, thanks to potential exciton coupling in the ground state, roof-like geometry of **12c** should result in a slight blue shift in the absorption maximum of the ^1L_a band. However, in reality, while the absorption maximum of compound **1** is located at 410 nm (~69 kcalmole^{-1}), compound **12c** and **12d** showed absorption maxima at 428 (~66 kcalmole^{-1}) nm and 447 nm (~64 kcalmole^{-1}) respectively. Red-shifted UV spectra of **12c** and **12d** support efficient conjugation between anthracene and enone components. However, such slight change (~5 kcalmole^{-1}) in excitation energy is unlikely to shut a possible photochemical reaction pathway totally. This points to the effect of other contributing features. A roof-like geometry can also facilitate excimer formation in the excited state for those compounds. This might facilitate an energy wastage pathway and thereby preventing bisaromatic systems from undergoing photochemical reactions. Excimer formation anyway is inefficient with compounds **12a** and **12b** and hence they are more likely to undergo *cis-*

trans isomerization. Alternatively, the restricted rotation around vinylic bond or due to adverse steric interaction with cyclopentane methylene hydrogen might have prevented isomerization reaction of **12c** and **12d**.

Based on the limited substrate set examined in this chapter, we cannot pick the exact reason behind the reluctance of certain compounds to undergo photochemical transformation. At this juncture, excimer formation remains purely speculative. Detailed photophysical investigation including examination of emission spectra and determination of emission life time and fluorescent quantum yield (ϕ_F) are required to establish the role of excimer formation. All these factors are systematically examined and analyzed in the next chapter.

Coming to potential application of bischromophoric systems **12a-d**: some of them might find application as optical molecular switch. The starting material and isomeric photoproduct are thermally stable and are interconvertable by a photochemical forward/thermal backward reaction sequence without degradation (side products).

2.5. Experimental Section

2.5.1. General Techniques

All reactions were conducted in oven-dried glasswares under an atmosphere of nitrogen with magnetic stirring unless otherwise noted. The reagents used were purchased from Aldrich Chemical Co. and were used without further purification. Solvents used for experiments were distilled and dried according to procedures given in standard manuals. All reactions were monitored by thin layer chromatography (TLC). Analytical thin layer chromatography was performed on glass plates coated with silica gel containing calcium sulphate as the binder or aluminium sheets coated with silica gel (Merck); visualization was achieved by exposure to iodine vapors or

UV radiation. Solvent removal was done on an IKA-WERKE rotary evaporator. Gravity column was performed using 60-120 mesh silica gel (Qualigens) and mixtures of hexane-dichloromethane were used for elution. Melting points were recorded on a POLMON melting point apparatus and are uncorrected. Infrared spectra were recorded using JASCO 4100 series, FTIR spectrometer. NMR spectra were recorded at 300 (^{1}H) and 75 (^{13}C) MHz respectively on a Bruker Avance DPX-300 MHz NMR spectrometer. Chemical shifts are reported in δ (ppm) relative to TMS (^{1}H) and CDCl$_3$ (^{13}C) as the internal standards. Coupling constants (*J*) are reported in Hertz (Hz). Mass spectra were recorded under FAB/LRMS at 5000 resolution using JEOL JMS 600H mass spectrometer. Elemental analyses were performed on Elementar Vario ELIII at Sophisticated Test and Instrumentation Centre (STIC), Kochi. Recrystallization was done by slow evaporation method from chloroform-methanol mixture at room temperature. Photochemical reactions were carried out in a Rayonet reactor fitted with sixteen lamps.

2.5.2. Materials

Cyclopentanone, benzenecarboxaldehyde, 1-naphthalenecarboxaldehyde, 9-anthracenecarboxaldehyde, 1-pyrenecarboxaldehyde were purchased from Sigma-Aldrich and used as received. Solvents were distilled and used in the reaction. Benzene used for photochemical reaction was dried using calcium chloride and distilled over sodium wire.

2.5.3. Preparation of 2,5-Diarylidenecyclopentanones, 12a-d

2.5.3.1. Synthesis of (2*E*,5*E*)-2,5-dibenzylidenecyclopentanone (12a)

To a mixture of cyclopentanone (2.10 g, 25 mmol) and benzenecarboxaldehyde (5.31 g, 50 mmol) in methanol (25 mL) taken in a 100 mL conical flask, potassium hydroxide pellets (2.80 g, 50 mmol) was added and

the reaction mixture was stirred at room temperature for 15 min whilst a yellow product precipitated out. The mixture was heated in a hot water bath at 60 °C for 6 h, until an appreciable amount of solid formed. The flask was then cooled in an ice chest and the precipitate that separated out was collected by vacuum filtration. The crude product was washed several times with ice-cold 1 mL portions of ethanol. The product was further purified by recrystallization from a mixture (1:2) of methanol and chloroform to give **12a.** The product separated was collected by vacuum filtration and air-dried to yield material of good quality.

Yellow Powder. Yield 90%;

mp = 186-188 °C

UV λ_{max} (CH$_2$Cl$_2$) 300 (ε 2,700), 350 (ε 10,600), 400 (ε 450); **IR** (KBr) ν_{max} : 1690, 1664, 1626, 1610, 1441, 1180, 726 cm^{-1};

^{1}H NMR (300 MHz, CDCl$_3$) : δ 7.54-7.53 (m, 2H), 7.41-7.38 (m, 4H), 7.35-7.32 (m, 2H), 7.29-7.27 (m,2H), 7.01-6.99 (m, 2H), 2.95 (s, 4H);
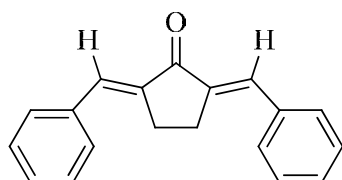
^{13}C NMR (75 MHz, CDCl$_3$) : δ 195.0, 141.3, 139.8, 136.6, 132.7, 129.0, 128.8, 23.9;

MS (FAB, [M$^+$+1]): Calcd for C$_{19}$H$_{16}$O: 260.40. Found: 261.39;

Elemental analysis calculated for C$_{19}$H$_{16}$O: C, 87.66; H, 6.19; O, 6.15. Found: C, 87.67; H, 6.17; O, 6.16.

2.5.3.2. Synthesis of (2*E*,5*E*)-2,5-bis(naphthalen-1-ylmethylene)cyclopentanone (12b)

To a mixture of cyclopentanone (1.08 g, 12.8 mmol) and 1-naphthalene-carboxaldehyde (4.01 g, 25.6 mmol) in methanol (25 mL) taken in a 100 mL conical flask, potassium hydroxide pellets (1.40 g, 25.6 mmol) was added and the reaction mixture was stirred at room temperature for 15 min whilst a yellow product precipitated out. The mixture was heated in a hot water bath at 60 °C for 6 h, until an appreciable amount of solid formed. The flask was then cooled in an ice chest and the precipitate that separated out was collected by vacuum filtration. The crude product was washed several times with ice-cold 1 mL portions of ethanol. The product was further purified by recrystallization from a mixture (1:2) of methanol and chloroform to give **12b.** The product separated was collected by vacuum filtration and air-dried to yield material of good quality.

Yield 87%; mp = 183-185 °C

UV λ_{max} (CH$_2$Cl$_2$) 260 (ϵ 14,900), 350 (ϵ 15,600), 400 (ϵ 31,800); **IR** (KBr) ν_{max} : 1662, 1630, 1530, 726 cm^{-1};

^{1}H NMR (300 MHz, CDCl$_3$) : δ 8.37 (s, 2H), 8.25-8.22 (m, 2H), 7.88-7.85 (m, 4H), 7.65-7.60 (m, 2H), 7.57-7.47 (m, 6H), 3.00 (s, 4H);

^{13}C NMR (75 MHz, CDCl$_3$) : δ 195.4, 139.8, 133.7, 132.5, 132.4, 130.5, 129.8, 128.7, 127.1, 126.8, 126.3, 125.1, 124.1, 27.1;

MS (FAB, [M$^+$+1]): Calcd for C$_{27}$H$_{20}$O: 360.15. Found: 361.16;

Elemental analysis calculated for C$_{27}$H$_{20}$O: C, 89.97; H, 5.59; O, 4.44. Found: C, 89.87; H, 5.55; O, 4.54.
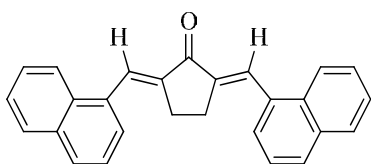
2.5.3.3. Synthesis of (2*E*,5*E*)-2,5-bis(anthracen-9-yl-methylene)cyclopentanone (12c)

To a mixture of cyclopentanone (0.81 g, 9.6 mmol) and 9-anthracene-carboxaldehyde (3.97 g, 19.2 mmol) in methanol (25 mL) taken in a 100 mL conical flask, potassium hydroxide pellets (1.08 g, 19.2 mmol) was added and the reaction mixture was stirred at room temperature for 15 min whilst a yellow product precipitated out. The mixture was heated in a hot water bath at 60 $^{\circ}$C for 6 h, until an appreciable amount of solid formed. The flask was then cooled in an ice chest and the precipitate that separated out was collected by vacuum filtration. The crude product was washed several times with ice-cold 1 mL portions of ethanol.   The product was further purified by recrystallization from a mixture (1:2) of methanol and chloroform to give **12c**. The product separated was collected by vacuum filtration and air-dried to yield material of good quality.

Yield 88%; mp > 300 °C

UV λ_{max} (CH$_2$Cl$_2$) 260 (ϵ 65,900), 350 (ϵ 14,900), 420 (ϵ 31,600); **IR** (KBr) ν_{max} : 1634, 1624, 1207, 745 cm^{-1};

^{1}H NMR (300 MHz, CDCl$_3$) : δ 8.57 (s, 2H), 8.46 (s, 2H), 8.08-8.01 (m, 8H), 7.54-7.46 (m, 8H), 2.31 (s, 4H); **^{13}C NMR** (75 MHz, CDCl$_3$) : δ 194.1, 144.0, 141.2, 137.1, 132.1, 131.3, 130.0, 129.1, 129.0, 127.9, 126.2, 126.0, 125.8, 125.7, 125.4, 25.7;

MS (FAB, [M$^+$+1]): Calcd for C$_{35}$H$_{24}$O: 460.18. Found: 461.20;

Elemental analysis calculated for C$_{35}$H$_{24}$O: C, 91.27; H, 5.25; O, 3.47.   Found: C, 91.25; H, 5.27; O, 3.48.
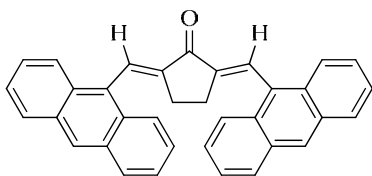
2.5.3.4. Synthesis of (2*E*,5*E*)-2,5-bis(pyren-2-ylmethylene)-cyclopentanone (12d)

To a mixture of cyclopentanone (0.36 g, 4.3 mmol) and 1-pyrene carboxaldehyde (2.01 g, 8.6 mmol) in methanol (25 mL) taken in a 100 mL conical flask, potassium hydroxide pellets (0.49 g, 8.6 mmol) was added and the reaction mixture was stirred at room temperature for 15 min whilst a yellow product precipitated out. The mixture was heated in a hot water bath at 60 °C for 6 h, until an appreciable amount of solid formed. The flask was then cooled in an ice chest and the precipitate that separated out was collected by vacuum filtration. The crude product was washed several times with ice-cold 1 mL portions of ethanol. The product was further purified by recrystallization from a mixture (1:2) of methanol and chloroform to give **12d**. The product separated was collected by vacuum filtration and air-dried to yield material of good quality.


Yield 89%; mp > 300 °C

UV λ_{max} (CH$_2$Cl$_2$) 260 (ε 66,900), 350 (ε 13,900), 380 (ε 25,900), 447 (ε 34,600);

IR (KBr) ν_{max} : 1628, 1594, 1349, 1214, 726 cm^{-1};

NMR: Used solid state NMR for analysis (explained earlier).

Elemental analysis calculated for C$_{39}$H$_{24}$O: C, 92.10; H, 4.76; O, 3.15. Found: C, 92.30; H, 4.75; O, 3.25.
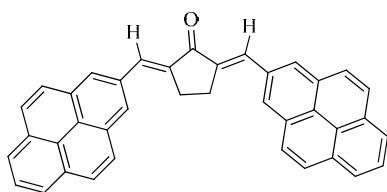
2.5.3.5. Synthesis of (1*E*,4*E*)-1,5-di(pyren-2-yl)penta-1,4-dien-3-one (12e)

A solution of 1-pyrenecarboxaldehyde **11d** (2.01 g, 8.6 mmol) and acetone **14** (1.5 mL) in ethylacetate (50 mL) was saturated with hydrogen

chloride gas and stirred for 24h at room temperature. Bispyrene **12e** precipitated from the reaction mixture was purified by soxhlet extraction with dichloromethane.
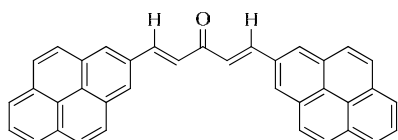
Yield 46%; mp 224-226 °C

IR (KBr) ν_{max} : 1700, 1210, 789 cm^{-1};

^{1}H NMR: 8.52-8.41 (m, 7H), 8.18-7.91 (m, 4H), 7.87-7.64 (m, 2H), 7.65-7.63 (m, 2H), 7.57-7.42 (m, 5H), 6.78-6.62 (m, 2H);

MS (FAB, [M$^+$+1]): Calcd for C$_{37}$H$_{22}$O: 482.16; Found: 483.20.

2.5.4. Photochemical Transformations of Diarylidene Compounds 12a-e

2.5.4.1. Procedure for the Photolysis of 12a

A sample of **12a** (0.17 g, 0.7 mmol) was dissolved in a small volume of dry benzene and then made up to 130 mL. The solution was degassed by bubbling dry nitrogen through it and then irradiated at 350 nm. Progress of the reaction was followed by TLC analysis. Starting material was almost completely consumed in 10 h. Solvent was removed under reduced pressure and the residue was chromatographed over silica gel. Elution of the column with a mixture (2:3) of hexane and dichloromethane gave a new product tentatively identified as the *E,Z*-isomer **13a**.
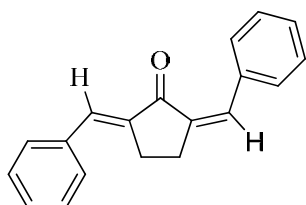
Greenish Yellow crystals. Yield 48%; mp = 216-218 °C

IR (KBr) ν_{max} : 1663, 1627, 1324, 1107, 722 cm^{-1};

^{1}H NMR (300 MHz, CDCl$_3$) : δ 7.99-7.98 (m, 2H),

7.59-7.58 (m, 2H), 7.52-7.51 (m, 2H), 7.47-7.29 (m, 4H), 6.92 (s, 2H), 3.10-3.07 (m, 2H), 2.99-2.96 (m, 2H);

^{13}**C NMR** (75 MHz, CDCl$_3$) : δ 194.0, 139.8, 137.8, 137.5, 135.8, 135.0, 133.5, 130.8, 130.7, 130.6, 129.4, 129.3, 129.2, 128.8, 128.7, 128.5, 127.9, 30.8, 26.6;

MS (FAB, [M$^+$+1]): Calcd for C$_{19}$H$_{16}$O: 260.4. Found: 261.2;

Elemental analysis calculated for C$_{19}$H$_{16}$O: C, 87.66; H, 6.19; O, 6.15. Found: C, 87.77; H, 6.18; O, 6.14.

2.5.4.2. Procedure for the Photolysis of 12b

A sample of **12b** (0.17 g, 0.5 mmol) was dissolved in a small volume of dry benzene and then made up to 130 mL. The solution was degassed by bubbling dry nitrogen through it and then irradiated at 350 nm. Progress of the reaction was followed by TLC analysis. Starting material was almost completely consumed in 10 h. Solvent was removed under reduced pressure and the residue was chromatographed over silica gel. Elution of the column with a mixture (2:3) of hexane and dichloromethane gave a new product tentatively identified as the *E,Z*-isomer **13b**.
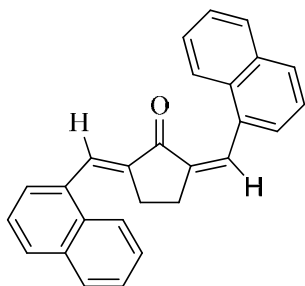
Yield 48%; mp = 216-218 °C

IR (KBr) ν$_{max}$: 1650, 1623, 1450, 728 cm^{-1};

^{1}**H NMR** (300 MHz, CDCl$_3$) : δ 8.03-7.99 (m, 2H), 7.87-7.84 (m, 2H), 7.74-7.70 (m, 4H), 7.49-7.43 (m, 2H), 7.40-7.31 (m, 6H), 2.86 (s, 2H), 2.82 (s, 2H);

^{13}**C NMR** (75 MHz, CDCl$_3$) : δ 193.4, 141.3, 139.8, 139.1, 134.7, 133.7, 133.5, 132.5, 132.4, 131.7, 131.6, 130.5, 130.2, 129.9, 129.7, 129.3, 128.8, 128.7, 128.4, 127.0, 126.8, 126.7, 126.2, 125.7, 125.1, 124.3, 124.1, 30.1, 26.8;

MS (FAB, [M$^+$+1]): Calcd for C$_{27}$H$_{20}$O: 360.2. Found: 361.3;

Elemental analysis calculated for C$_{27}$H$_{20}$O: C, 89.97; H, 5.59; O, 4.44. Found: C, 89.86; H, 5.58; O, 4.46.

2.5.4.3. Procedure for the Photolysis of 12c

A sample of **12c** (0.17 g, 0.6 mmol) was dissolved in a small volume of dry benzene and then made up to 130 mL. The solution was degassed by bubbling dry nitrogen through it and then irradiated at 350 nm. Progress of the reaction was monitored by TLC analysis. Even after 12 hours no new products were observed and starting compound was recovered unchanged.

2.5.4.4. Procedure for the Photolysis of 12d

A sample of **12d** (0.17 g, 0.4 mmol) was dissolved in a small volume of dry benzene and then made up to 130 mL. The solution was degassed by bubbling dry nitrogen through it and then irradiated at 350 nm. Progress of the reaction was monitored by TLC analysis. Even after 12 hours no new products were observed and starting compound was recovered unchanged**.**

2.5.4.5. Procedure for the Photolysis of 12e

A sample of **12e** (0.17 g, 0.3 mmol) was dissolved in a small volume of dry benzene and then made up to 130 mL. The solution was degassed by bubbling dry nitrogen through it and then irradiated at 350 nm. Progress of the reaction was monitored by TLC analysis. During the course of irradiation

yellow fluorescent solution was changed to blue fluorescent solution with concomitant change in absorption spectrum. Due to poor solubility of the materials, purification and spectral analyses were not feasible.

2.6. References

1. Becker, H.-D.; Anderseon, K. *J. Org. Chem.* **1983**, *48*, 4542.

2. Davydov, A. S. *Theory of Molecular Exciton*, translated by Kasha, M.; Oppenheimer, M. Jr. New York: McGraw-Hill, **1962**.

3. Harada, N.; Nakanishi, K. *Circular Dichroic Spectroscopy – Exciton Coupling in Organic Stereochemistry*. Mill Valley, CA: University Science Books, **1983**.

4. Harada, N.; Chen, S. L.; Nakanishi, K. *J. Am. Chem. Soc.* **1974***, 97,* 5345.

5. Harada, N.; Nakanishi, K. *Acc. Chem. Res.* **1972**, *5*, 257.

6. Nakanishi, K.; Berova, N.; Woody, R. *Circular Dichroism – Principles and Applications*, New York: VCH, **1994**, 361.

7. Lambert, J. B.; Shurvell, H. F.; Lightner, D. A.; Cooks, R. G. *Organic Structural Spectroscopy*, prentice Hall, Inc. Simon & Schuster / A Viacom Company, New Jersey, **1998,** 312.

8. Berova, N.; Harada, N.; Nakanishi, K. *Electronic Spectroscopy, Theory & Applications***,** Academic Press, New York. **1999**.

9. McRae, E, G.; Kasha, M. *J. Chem. Phys.* **1958**, *28,* 721.

10. McRae, E, G.; Kasha, M. *In Physical Processes in Radiation Biology.* **1964,** Academic Press, New York, p. 23.

11. Kasha, M.; E1-Bayoumi, M. A.; Rhodes, W. *J. Chim. Phys*. **1961,** *58,* 916.

12. McClure, D. S. *Can. J. Chem.* **1958***, 36,* 59.

13. Kasha, M.; Rawls, H. R.; El-Bayoumi, M. A. *Pure Appl. Chem.* **1965,** *11*, 371.

14. Berova, N.; Gargiulo, D.; Derguini, F.; Nakanishi, K.; Harada, N. *J. Am. Chem. Soc.* **1993***, 115,* 4769.

15. Ramart-Lucas, P.; *In Traite de Chimie Organique* (Ed. V. Grignard), Massonet Cie, Paris, **1936***, 2*, 72.

16. KortUm, G.; Dreesen, G. *Chem. Ber.* **1951**, *84,* 182.

17. Lewis, G. N.; M. Kasha, M. *J. Am. Chem. Soc.* **1944,** *66,* 2100.

18. Feringa, B. L.; Jager, W. F.; Lange**,** B. de**.** *Tetrahedron.* **1993,** *49,* 8267.

19. Saltiel, J.; Sun, Y. P in *Photochromism, Molecules and Systems in Organic   Chemistry*, Vol 40; Durr, H.; Bouas Laurent, H. Eds.; Elsevier: Amsterdam. **1990,** Chapter 3.

20. Claisen, L.; Claparede, A. *Ber.* **1881**, *14,* 2460.

21. Schmidt, J. G. *Ber.* **1881**, *14,* 1459.

22. Wayne, W.; Adkins, H. *J. Am. Chem. Soc.* **1940,** *62,* 3401.

23. Marvel, C. C.; King, W. B. *Org. Syn.* **1944**, *1*, 252.

24. Stiles, M.; Wolf, D.; Hudson, G. V. *J. Am. Chem. Soc*. **1959**, *81*, 628.

25. Vogel, A. I. *Practical Organic Chemistry*, English Language Book Society and Longman group Ltd: London; **1996**, p 1032.

26. House, H. O. *Modern Synthetic Reactions,* 2nd ed.; Benjamin: Menlo Park, California; **1972**.

27. Bhagat, S.; Sharma, R.; Chakrabarti, A. K. *J. Mol. Catal. A.* **2006***, 260*, 235.

28. Wang, M.; Chang, K. R. *Ind. Eng. Chem. Res.* **1990***, 29,* 40.

29. Russel, A.; Happoldt, W. B. Jr. *J. Am. Chem. Soc*. **1942**, *64*, 1101.

SYNTHESIS, PHOTOCHEMICAL AND PHOTOPHYSICAL STUDIES OF BISANTHRACENES - GEOMETRY EFFECTS

3.1. Abstract

In order to identify structural constraints that prevented photoreactions of bisanthracenylidenecyclopentanones described in Chapter 2, we synthesized a series of bisanthracene compounds of varying cycloalkanone ring size and examined their geometry and photophysical properties. Slight variations in the nature of spacers have brought drastic changes in the orientation of the anthracene subunits and it was reflected in their reactivity. This chapter is also an attempt to understand the effect of geometry and nature of chromophores in determining photochemical and photophysical properties of engineered arrays. We investigated the effects of geometry in a more systematic way.

3.2. Introduction

Bisanthracenes are interesting compounds with varying photochemistry. They are broadly classified on the basis of derivative group on the anthracene units and also on the basis of connectors joining the two anthracene units. The connectors can either be non-rigid (flexible) groups like straight aliphatic chain, polyether chain etc. or rigid entities like ring spacers. Bisanthracenes with flexible connectors display interesting excimer fluorescence emission and photocyclomerization.[1] In those systems where the anthracene chromophores are linked together by flexible chain, conformational mobility allows the terminal groups to interact.[2] On the other hand, relative

orientation of chromophore subunits in multichromophoric arrays is of cardinal importance in deciding the overall properties of rigid systems. More convenient and specific methods are still required to arrange the chromophores in various well-defined geometries in order to regulate the orientation of chromophores by means of both covalent and non-covalent approaches. From mechanistic studies of intramolecular energy transfer process, it has been clearly demonstrated that factors at the molecular level, such as, (a) the nature of the chromophores, (b) the interchromophoric distance and orientation, and (c) the nature of the linker dictate overall photophysical and photochemical properties of the constructed arrays. So, better models for quantitative study of energy transfer are provided by rigid covalently linked donor-bridge-acceptor systems in which the chromophores are held at well-defined distances and orientation.

We have constructed several bischromophoric systems by covalently linking simple molecular building blocks. Preliminary investigations indicated that the photochemistry of such dimeric arrays is chromophore controlled. Relative orientation of the chromophores and efficacy of through bond interactions in such systems appear to have definite control over the differential photochemistry exhibited by arrays. In this chapter, we discuss a series of bisanthracene compounds with cycloalkanones of increasing ring size (Chart 3.2). The idea behind the selection of substrates is simple, and is taken from well-documented spectral characteristics of 1,2-dialkylidene-cycloalkanones.
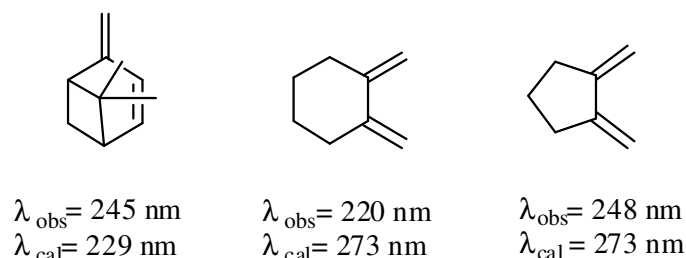

λ_{obs}= 245 nm λ_{obs}= 220 nm λ_{obs}= 248 nm
λ_{cal}= 229 nm λ_{cal}= 273 nm λ_{cal}= 273 nm

Figure 3.1: *Conjugated dienes with different constraints*

The λ_{max} values for the following series of dienes (Figure 3.1) reveal the tenacity of cycloalkanes of varying ring sizes in maintaining orientation of 1,2-dialkylidine components. Conformational preferences and relief of Pitzer strain may be responsible for such dramatic variation in λ_{max} for these compounds. While planarity is nearly maintained in the cyclopentyl case, planarity and accompanying extended conjugation are severely compromised for six-membered rings.

Possible interactions in α, α'-dialkylidenecycloalkanones also deserve special mention. With five and six membered ring compounds, carbons 1 and 3 can lie in the same plane – a feature that will initiate transannular interactions and concomitant red-shifted absorption maxima. Thus it is conceivable that even slight variations in the nature of spacers induce drastic changes in the orientation of exocyclic double bonds in dialkylidenecycloalkanones.

In this investigation, we propose to synthesize and examine the photochemistry and photophysics of several bisanthracenylidinecyclo-alkanones of different ring sizes. We foresee subtle variation in the relative orientation of anthracene (and/or other chromophore) components present in these systems. Depending on ring size, extended conjugation and possible transannular interactions will vary and reflect in the photophysical and photochemical behaviour of individual arrays. Our investigation should provide definite answer on the effect of relative orientation of chromophore subunits on the photochemistry and photophysics of these dimeric arrays that may be applicable to larger arrays as well. In other words, we propose to establish yet another edict on designing multichromophoric arrays.

3.2.1. An Overview on the Photochemistry and Photophysics of Bisanthracene Compounds

The essentials of anthracene photochemistry[3] as seen by 1963/1964 were the subject of a contribution to the first volume of the *Advances in Photochemistry* and were discussed in a review of photochemical reactions of organic molecules. Also bischromophoric compounds[4] in which the anthracene chromophore was one of the two interacting π-systems or both were anthracene systems also gained interest due to their intramolecular energy transfer processes.

Reports on the photochemical and photophysical properties of a few bisanthracene derivatives similar to those we propose to synthesize have appeared in literature and are summarized below. Becker *et al.*[4] have studied the *E,Z* isomers of 1,3-bis(9-anthryl)propenone **1**, 1,3-bis(9-anthryl)propene **2** and 1,5-bis(9-anthryl)pentadienone **3** (Chart 3.1).
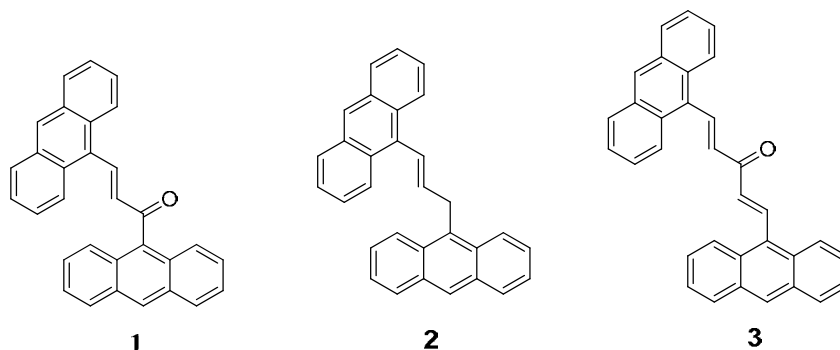
Chart 3.1

Irradiation of *trans*-1,3-bis(9-anthryl)propenone **1** resulted in geometrical isomerization followed by a more efficient intramolecular $[4\pi+4\pi]$ cycloaddition[4] described in Scheme 3.1.
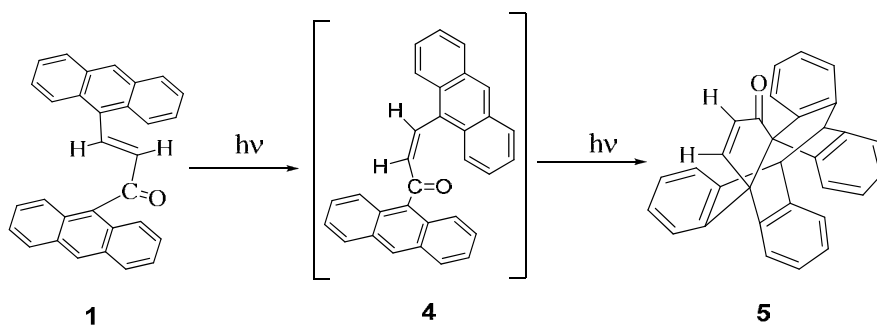
Scheme 3.1

The photochemical isomerization[4] of *trans*-1,3-bis(9-anthry1)propene **2** to give the intramolecular [4π+4π] cycloaddition product **7** is given in Scheme 3.2.
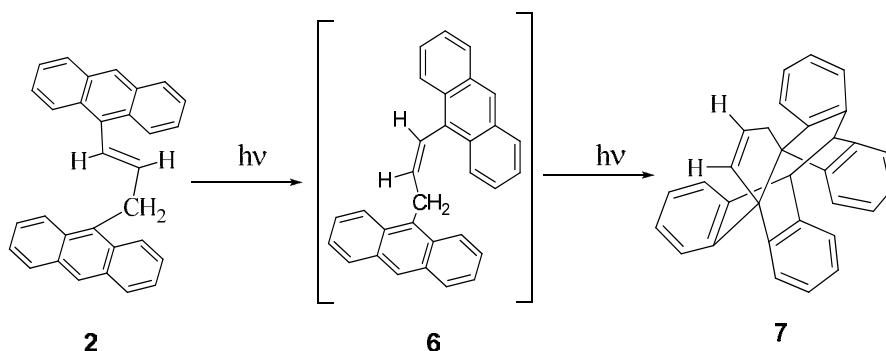
Scheme 3.2

Interesting results were obtained when investigation was extended to *trans,trans*-1,5-bis(9-anthryl)pentadienone **3**. Upon irradiation in methylene chloride solution, with light of λ > 360 nm, **3** smoothly isomerized to the *cis,trans*-isomer which subsequently underwent intramolecular [4π+2π] Diels-Alder addition to give **10**.[4] The reaction is represented in Scheme 3.3. It may be noted that the key common step in the phototransformation of bisanthracenes **1**-**3** is an initial *cis-trans* isomerization reaction.
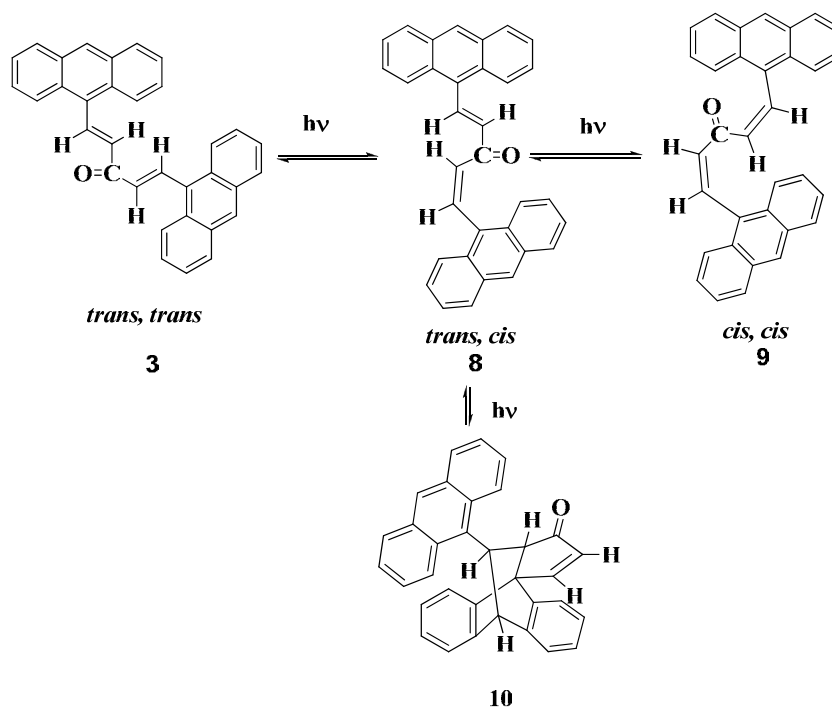
Scheme 3.3

Electronic absorption and emission spectra of bisanthracenes are described in detail in most textbooks and monographs on photochemistry and spectroscopy.   For anthracene, the electronic absorption spectrum is characterized by a series of vibrationally spaced bands around 350 nm. Absorption spectrum of *trans*-1,3-bis(9-anthryl)propenone **1**,[4] on the other hand, revealed bischromophoric nature of this compound: superimposed are a structureless absorption due to one anthracene unit in conjugation with the enone component and a structured absorption, characteristic of isolated anthracene chromophores.   Comparison with the electronic absorption spectrum of dianthrylpropanone proved that the carbonyl group and the anthracene moiety are in the same plane to extend its conjugation over the two groups.   The electronic absorption spectra of both *cis* and *trans*-1,3-bis(9-anthryl)propene are structured and are strikingly similar suggesting absence of conjugation.   Again the absorption spectrum of *trans,trans*-isomer of 1,5-

bis(9-anthryl) pentadienone **3**[4] was red-shifted with loss of fine structure of the anthracene chromophore. All these revealed the effect of geometry and nature of substituent on alkenylanthracene in determining the properties of bisanthracenes.

In Chapter **2** of this thesis, we had reported the reluctance of 2,5-dianthrylidenecyclopentanone to undergo light-induced *cis-trans* isomerization reaction. In order to unravel the exact reason behind the photoinertness of this bisanthracene compound, we synthesized a series of structurally related bisanthracenes (Chart 3.2) with cycloalkanone spacer of varying ring size and examined their geometry and photophysical properties.
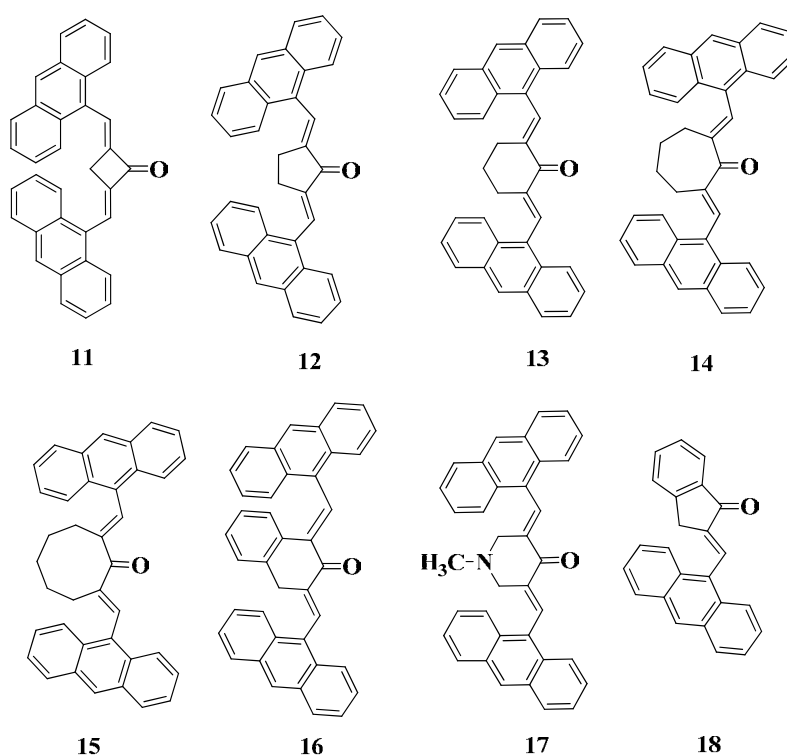

Chart 3.2

We observed that even slight variations in the nature of spacers brought drastic changes in the orientations of the bischromophoric systems in space. These geometry variations were confirmed through single crystal X-ray

analysis of these molecules. The rigid cycloalkanone spacer was a suitable linker due to the following reasons; the spatial arrangement of chromophores is varied by changing the cycloalkanone ring size, thus varying geometrical parameters such as the angle and/or distance between the chromophoric units. It also effectively shuts electronic communication between the two chromophores upon increasing ring size (by compromising the degree of conjugation between anthracene components). So they can show relatively large variation in photochemical and photophysical properties with almost identical structures.

3.3. Results and Discussion

3.3.1. Synthesis and Characterization

We employed Claisen-Schimdt condensation[5] for the preparation of the desired   (*E,E*)-bis(anthracen-9-yl-methylene)cycloalkanones   **11-17**. Condensation of 1-anthracenecarboxaldehyde **19** and various cyclic ketones **20a-g** of varying ring size in the presence of potassium hydroxide afforded novel (*E,E*)-bis(anthracen-9-yl-methylene)cycloalkanones **11-17** in good yields (60-90%) (Scheme 3.4). Cyclic ketones of our choice were cyclobutanone **20a**, cyclopentanone **20b**, cyclohexanone **20c**, cycloheptanone **20d**, cyclooctanone **20e**, β-tetralone **20f**, and *N*-methylpiperidone **20g**. We have also prepared a monoanthracene compound **18** from 1-anthracenecarboxaldehyde **19** and 1-indanone **20h**.

Refluxing a mixture of 1-anthracenecarboxaldehyde **19** and cyclic ketone **20a-g** (taken in a 2:1 ratio) in methanol with potassium hydroxide for 6 h gave bisanthracenes **11-17** as yellow precipitates which were filtered and further purified by recrystallization from chloroform-methanol mixture.
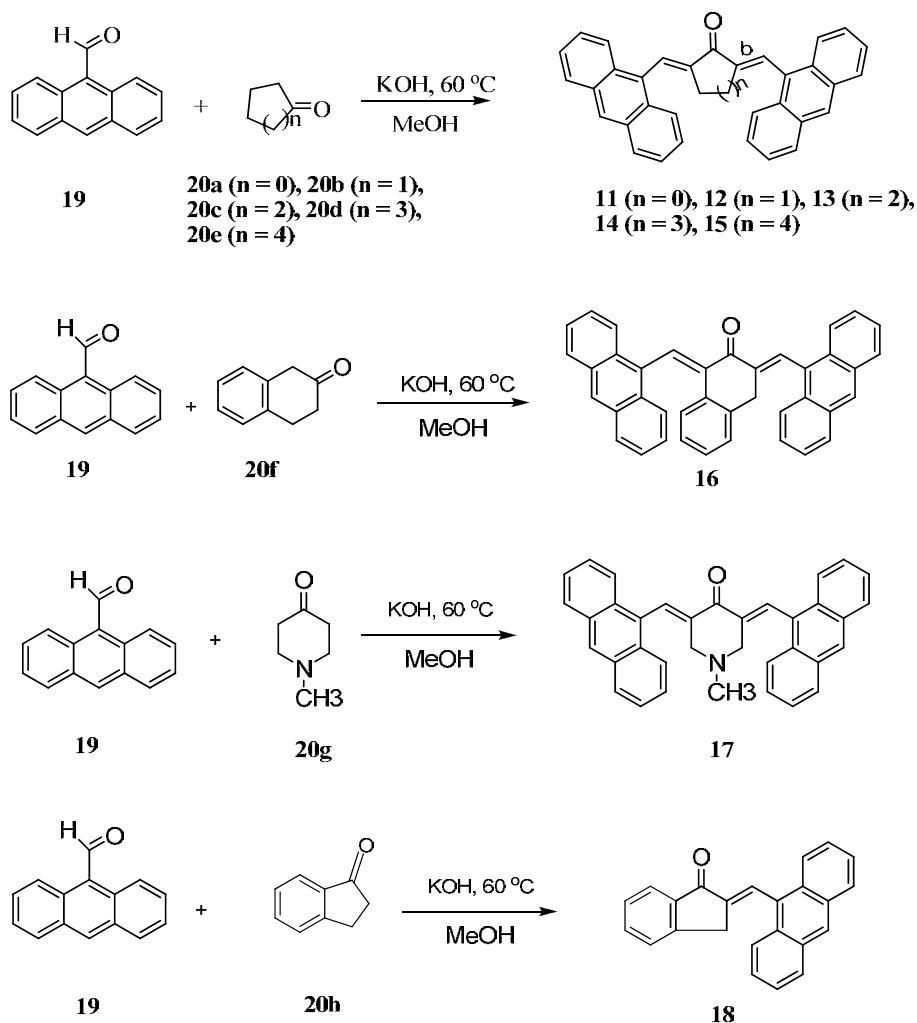
Scheme 3.4

Compounds **12** and **13** exhibited poor solubility in common solvents suggesting aggregation. Motivation behind the synthesis of **16-18** will be discussed subsequently.

The molecular structures of **11-18** were established on the basis of spectral and analytical data. Detailed description of structure of the compound **12** is given in Chapter **2**. The UV absorption spectrum of **11** indicated the presence of extended conjugation to anthracene residues in the bisanthracene sample. The α,β-unsaturated keto group in **11** is indicated in the IR spectrum

by the strong peak at 1633 cm^{-1} and the shoulder peak at 1593 cm^{-1} are indicative of conjugated olefinic bond. The ^{1}H NMR spectrum showed a singlet at δ 2.87, denoting the aliphatic hydrogen of cyclobutanone moiety. The multiplets from δ 7.46 to 8.44 establish aromatic and vinylic protons of **11**. In the ^{13}C NMR spectrum, the carbonyl signal is positioned at δ 189.9 ppm. ^{13}C NMR spectrum shows 14 aromatic carbon signals, which points to absence of rotation around bond '*a*'. If there is rotation around bond '*a'*, there will be only eight carbon signals. Restricted rotation around bond '*a'* lifted the chemical shift equivalence of aromatic carbon pairs (such as 1 and 8, 2 and 7 etc.). Partial double bond character of bond '*a*' may be responsible for the restricted rotation around this bond. The molecular ion peak at *m/z* 447.36 (M^{+}+1) in the FAB mass spectrum ascertains the structural identity of bisanthracene **11.** Satisfactory elemental analysis data also supported the formation of the adduct.

Similarly, the structures of bisanthracene compounds **12-17** and monoanthracene **18** were established through spectral data, which are given in detail in experimental section. ^{13}C NMR spectra of **12-18** exhibited interesting features that deserve special mention. In the case of compounds **12**, **13**, **16**, **17**, and **18** none of the anthracene carbons are chemical shift equivalent while for **14** and **15** chemical shift equivalency between sets of carbon (1 and 8 for example) is evident. These results denote remarkable difference in the structure of bisanthracenes. Rotation around bond '*a*' is restricted in the case of compounds **11**, **12**, **13**, **16**, **17**, and **18** while free rotation is apparent in the case of **14** and **15**. Based on this, we conclude that bisanthracenes can be separated into two groups. Compounds **11**, **12**, **13**, **16**, **17**, and **18** where free rotation around bond '*a*' is restricted falls in one group whereas compounds **14** and **15** where free rotation around bond '*a'* is possible may be included in another group. Thus, NMR data suggest dramatic variation in the structure of bisanthracene compounds synthesized by us.

3.3.2. Photophysical Studies:

3.3.2.1. Absorption and Fluorescence Studies

We examined the absorption and emission characteristics of compounds **12**-**15** in some detail. Compound **11** was not included in this comparative study. The absorption and fluorescence emission spectra[4] of bisanthracenes **12**-**15** were recorded in various solvents of increasing solvent polarity. Figure 3.2 shows the absorption spectra of compounds **12**-**15** in toluene. The absorption spectrum of compounds **12** and **13** suggested bischromophoric nature for these compounds. Anthracene-like vibrationally resolved absorption is evident below 400 nm whereas broad structureless absorption is evident above 400 nm. This is taken to mean that the compounds absorb both as an anthracene and another chromophore that exhibits a bathochromically shifted absorption band extending up to 480 nm indicating extensive conjugation. Interestingly, compounds **14** and **15** showed exclusively anthracene-like absorption. This observation suggests that electronic interaction[6] occurs between anthracene rings and enone components in the ground state for **12** and **13**. Such interaction is not observed for compounds **14** and **15** due to their peculiar geometry. This observation is consistent with the NMR spectral evidence on structural diversity.

However, no solvent dependence is evident for the absorption spectra of **12** and **13**. Hence, intramolecular charge transfer (ICT)[7] arising from two anthracene rings to the central carbonyl group is not prominent for any of thee molecules. If this is true, the anthracene unit is not in conjugation with the carbonyl chromophore. It may be mentioned here that *K*-band of enones exhibit substantial solvent shift. Another exciting possibility here is exciton coupling between anthracene components. Bischromophoric compounds where chromophore components are aligned in a roof-like geometry can undergo exciton coupling and exhibit red-shifted absorption bands akin to the

observed absorption spectral characteristics of bisanthracenes **12** and **13**. Position of the bands arising through exciton coupling will not be seriously affected by solvent polarity. An attractive conclusion here is that exciton coupling is possible for **12** and **13** while no such effect is observable for **14** and **15**.
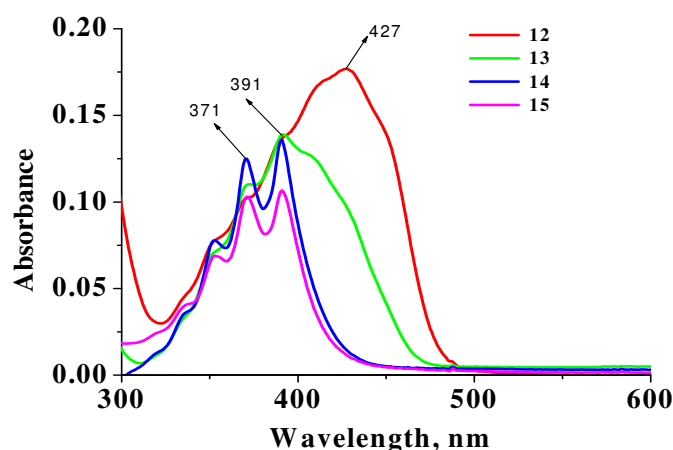
Figure 3.2. *Absorption spectra of compounds **12-15** in toluene.*

Unlike simple anthracenes, bisanthracenes **12-15** exhibited weak emission. Figure 3.3 shows the fluorescence emission spectra of **12-15** in toluene. Interestingly, compounds **12** and **13** showed static excimer type emission as they appear to be associated in the ground state (as evidenced by their poor solubility in common organic solvents). In order to gain further insight on possible excited state interactions, solvent dependence in the emission spectra[8] of **12-15** was also examined. The peak observed at 490 nm in the fluorescence emission spectrum of compound **12** showed a red shift of 100 nm with increasing solvent polarity from toluene to DMSO. Similar observation was made with compound **13** where with increasing solvent polarity from toluene to DMSO, the peak observed at 418 nm in the fluorescence emission spectrum showed a red shift of 142 nm. Fluorescence

spectrum of **12** and **13** is characterized by large Stokes shift indicating formation of excited state complexes.[9]   As these compounds are found associated in the ground state, these excimers can be called as static excimers. Interestingly, emission maxima of **12, 13** exhibited significant solvent dependence (100-140 nm).   The observed red shift in emission maximum correlates well with the polarity of the solvents employed suggesting CT character of the excited state.   On the other hand, no solvent dependence is observed in the emission spectra of **14, 15**.   These observations are also in agreement with the structural variation exhibited by **12-15**.   These results deserve special scrutiny.   Mapping of electron distribution and orbital coefficients on various significant atoms in both HOMO and LUMO of bisanthracenes **12-17** by theoretical calculations will provide better insight into this anomaly.
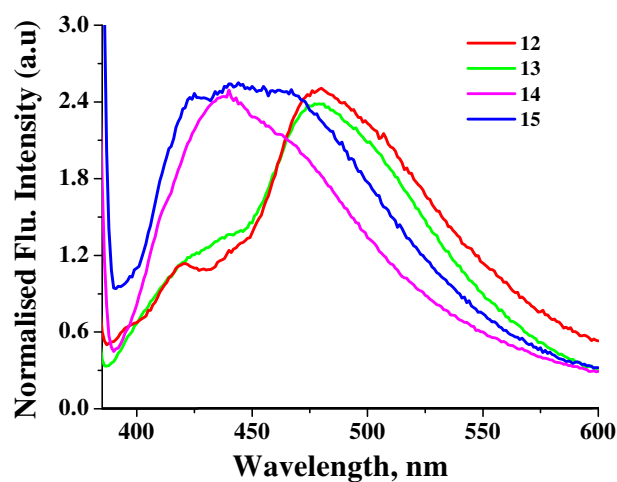
Figure 3.3. *Fluorescence emission spectra of compounds **12-15** in toluene.*

To understand the observation of peaks in the emission spectra in detail, solvent dependent changes in absorption and emission have been examined for compounds **12-15** in solvents of varying polarity such as toluene, CHCl$_3$ and DMSO (Figures 3.4 to 3.7).
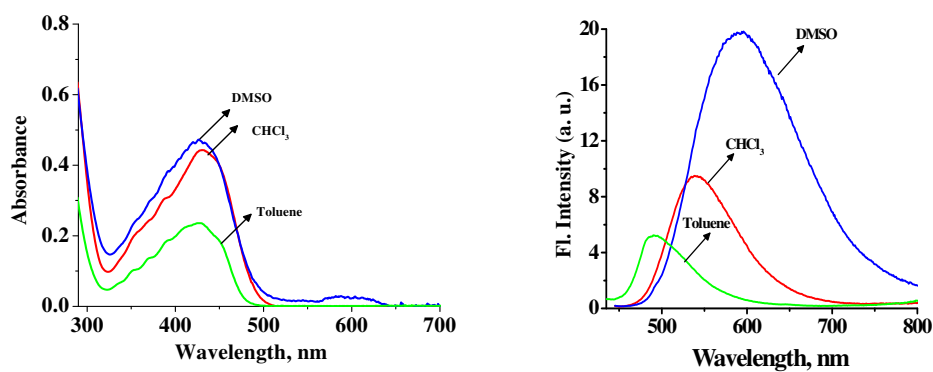
Figure 3.4. *Absorption and fluorescence emission spectra of compound **12** in various solvents.*
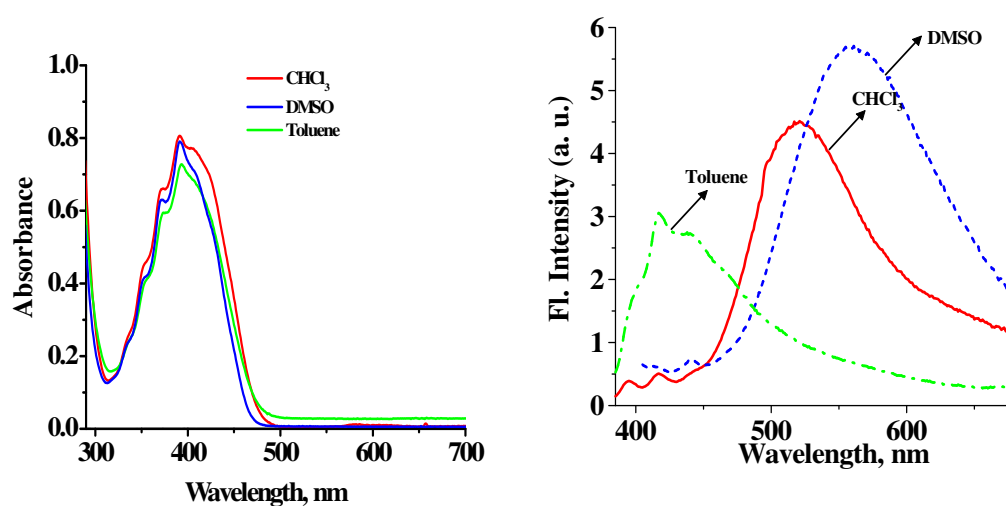
Figure 3.5. *Absorption and fluorescence emission spectra of compound **13** in various solvents*
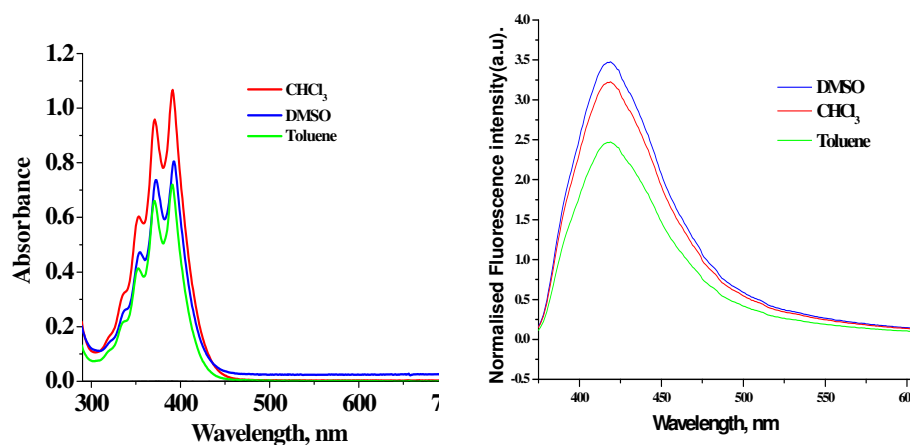
Figure 3.6. *Absorption and fluorescence emission spectra of compound **14** in various solvents.*
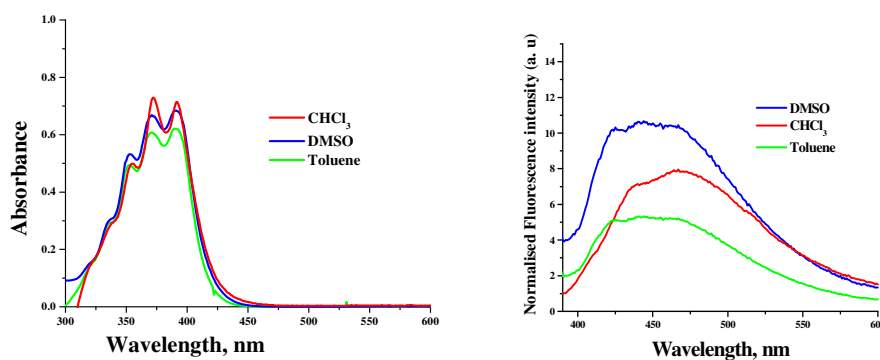
Figure 3.7. *Absorption and fluorescence emission spectra of compound **15** in various solvents.*

As evident from data presented in Figures 3.4 to 3.7, absorption spectrum of **12**-**15** exhibit negligible solvent dependence. However, emission characteristics are more complex in nature. In the case of **12** and **13**, substantial solvent dependence is evident while no solvent dependence is observed for **14** and **15**.

3.3.2.2. Fluorescence Quantum Yield of Bisanthracenes 12-15

The fluorescence emission quantum yields[10] of compounds **12-15** were measured in toluene and CHCl$_3$. It has been observed that as the solvent polarity increases, the quantum yield also increases for compounds **12** and **13** while a decrease in emission quantum yield was observed for compounds **14** and **15**. Further, the quantum yield was found to decrease on moving from compounds **12** to **15** and is negligible for compounds **14** and **15**.

Compound	Φ	
	Chloroform	Toluene
12	0.006	0.005
13	0.001	0.0004
14	0.0001	0.0003
15	0.00006	0.0002

The data are the average of more than two independent experiments and the error is *ca.* ±5%. Fluorescence quantum yields were calculated using quinine sulphate as the standard ; (Φ = 0.54)

Table 3.1. *Fluorescence quantum yield of the bisanthracenes 12-15*

The above observation of quantum yield suggests significant CT in the excited states of **12** and **13**. The CT excited states are more stabilized in polar solvents leading to an increase in life time. These results in a decrease in the non-radiative states and an increase in fluorescence quantum yields of the respective compounds.

In summary, emission spectral characteristics of **12**-**15** are also indicative of control exerted by ring size of cycloalkanone spacer on the excited state geometry and electron distribution of these bisanthracenes.

3.3.2.3. Structural Studies

To understand the observation of intramolecular charge transfer interactions (ICT) for the compounds **12** and **13** and absence thereof for **14** and **15**, structural studies were performed on bisanthracenes **12-15**. Preliminary molecular modeling of **12**-**15** indicated that the two anthracene units are aligned cofacial to each other in **12** and **13**, while it is not the situation for **14** and **15**. X-ray single crystal analyses were also performed for **12**, **14**, **15** and the obtained structures are given below. Interestingly, energy minimization and crystallographic studies revealed almost identical structural feature for **12**, **14**, and **15**.

Several interesting structural features were observed with **12**-**15**. Most remarkable feature here is that in none of these compounds, the anthracene unit is in conjugation with the carbonyl group due to different structural constraints. In the case of **12** and **13**, van der Waals interaction with the methylene hydrogens present on the cycloalkanone residue will force the anthracene ring out of planarity and induce accompanying loss of conjugation. The anthracene residues are constrained to lie at an angle to the cycloalkanone component. This explains the roof-like geometry of these molecules. Thus, free rotation around bond '***a***' is not prevented due to partial double bond character (induced by conjugation) of this bond, but due to restriction to rotation induced by steric factors.

With **14** and **15**, the story is completely different. Here the medium rings are more flexible. In the minimum energy configuration, carbonyl group is almost orthogonal to the anthracene ring. Puckering of the ring relieves steric interaction between methylene group of cycloalkanone and anthracene components. Hence, free rotation around bond '***a***' is permissible. This will induce chemical shift equivalence between anthracene carbon pairs and reduction in the number of ^{13}C NMR signals. Needless to mention, anthracene component in this molecule will act, at best, as a vinylanthracene-type

chromophore. More interestingly, HOMO and LUMO mapping indicated that carbonyl group is not involved in the first excited state of these bisanthracenes. Consequently, absorption and emission spectra of these compounds should be anthracene like with respect to position of absorption band and solvent effects. However, emission quantum yield will be lower here thanks to vibrational relaxation induced by fast conformational flipping of medium ring residues present in these molecules. The interesting observation here is that results obtained from spectral, structural and theoretical studies on these bisanthracenes converge impressively to provide unique yet unambiguous conclusions on the structure-activity relationships in these molecules.
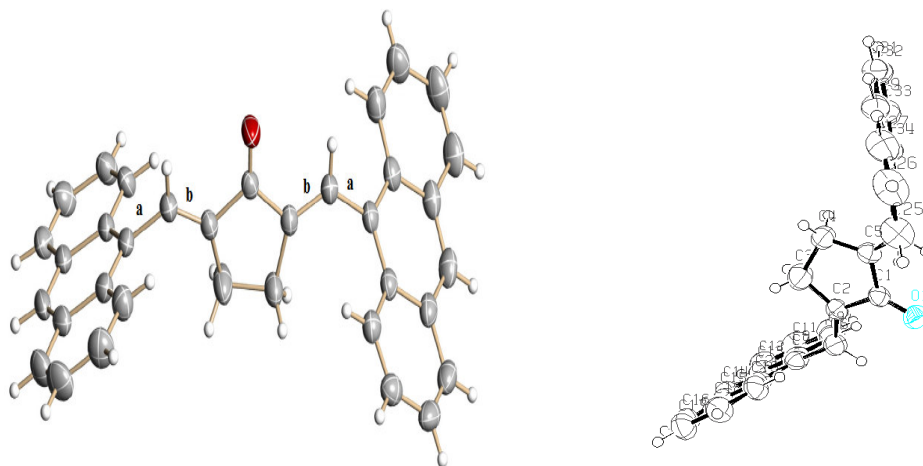
Figure 3.8. *ORTEP diagram of* **12**.
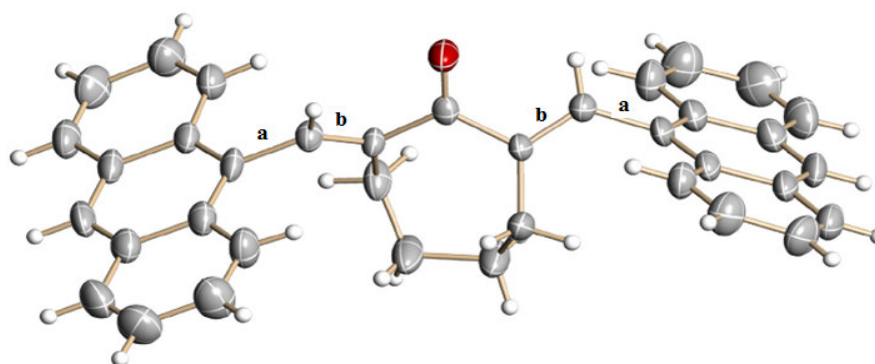
Figure 3.9. *ORTEP diagram of* **14**.
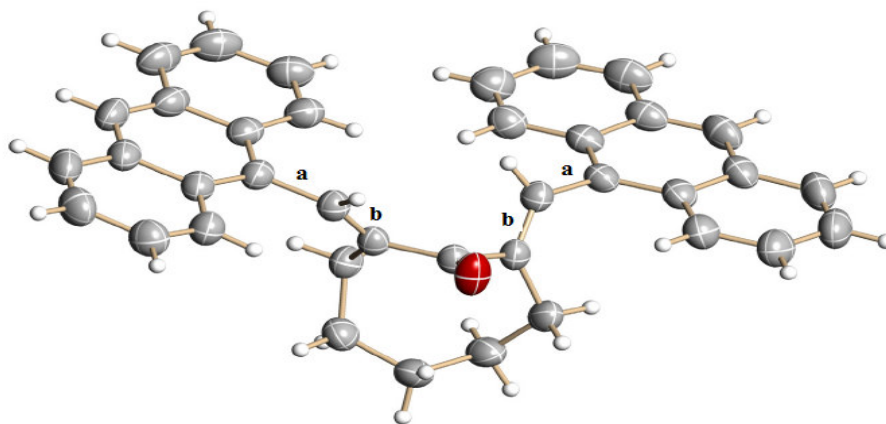
Figure 3.10. *ORTEP diagram of 15.*

ORTEP diagram of compound **12** shows that the two anthracenes are cofacial to each other with the carbonyl group and the π-bond in the same plane. The presence of 14 aromatic signals in ^{13}C NMR spectrum points to restricted rotation around the bond '*a*'. But for compounds **14** and **15**, the cycloalkanone ring systems are in more puckered form and here enone systems are not in same plane. The carbonyl group is more or less perpendicular to aromatic ring system. So, there will not be any extended conjugation from aromatic rings to the enone component as with earlier cases. The presence of fewer aromatic carbon signals in the ^{13}C NMR spectrum of **14** and **15** supports above structure with free rotation around bond '*a*'.

To understand the geometry controlled behaviour of bisanthracenes in detail, we did the HOMO-LUMO mapping for the bisanthracenes **12-15**. Semiemperical AM1 calculations were performed for the geometry optimization and mapping of the highest occupied molecular orbital (HOMO) and the lowest unoccupied molecular orbital (LUMO). The representations are given below (Figure 3.11 - 3.14).
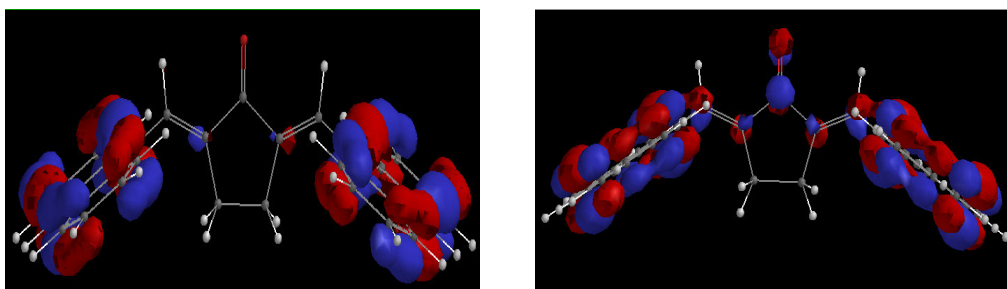
Figure 3.11. *HOMO and LUMO of **12** generated after geometry optimization.*
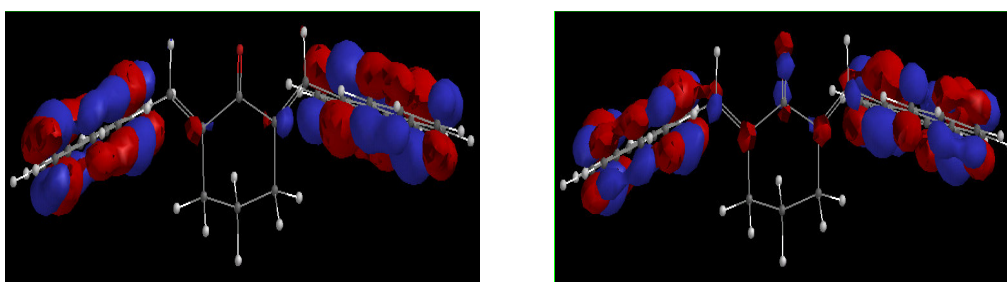
Figure 3.12. *HOMO and LUMO **13** generated after geometry optimization.*
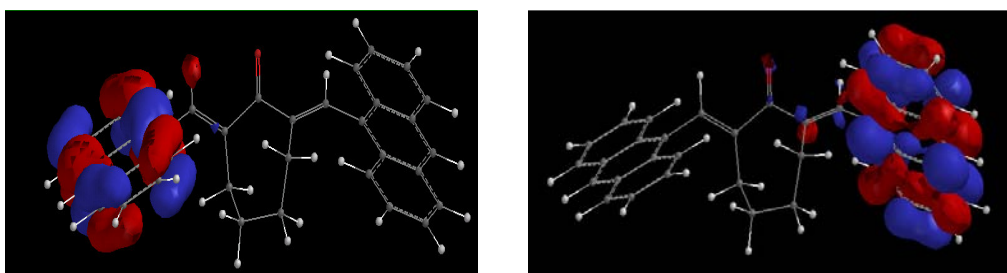
Figure 3.13. *HOMO and LUMO of **14** generated after geometry optimization.*
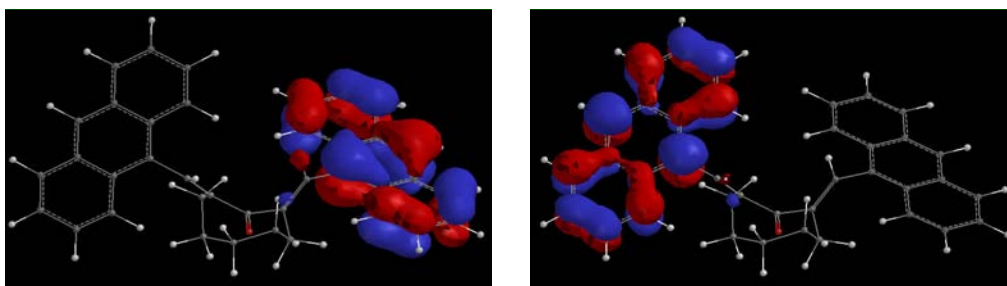
Figure 3.14. *HOMO and LUMO of **15** generated after geometry optimization.*

Analysis of highest occupied molecular orbital (HOMO) and lowest unoccupied molecular orbital (LUMO) reveals that, for compounds **12** and **13**, the central cyclic ketone permits a more or less parallel superposition of the two anthracene rings, while such geometry is not possible for **14** and **15** due to the constrained geometry of the seven and eight membered central cyclic ketone. So for compounds **12** and **13**, the less constrained geometry of the central cyclic ketone with the two anthracene rings permit the mixing of orbitals. Hence the HOMO and LUMO shows extended delocalization over the two anthracene rings while such a delocalization is absent for **14** and **15** due to the more constrained geometry. For compounds **12** and **13**, the HOMO is mainly localized on the two anthracenes and to a less extent on the central carbonyl group while, the LUMO shows significant contribution of the carbonyl group which supports the charge transfer interaction. Hence, the theoretical calculations clearly support the intramolecular charge transfer interaction (ICT) observed for compounds **12** and **13** and in turn confirms the experimental results.

3.3.2.4. Photochemical Studies

The photochemistry of anthracene chromophore with straight aliphatic chain in between is characterized by cycloadditions[11] in which the central ring represents a 4π electron system or, more rarely, one of the lateral ring acts as diene or dienophile. 9-Anthrylalkenes upon photoexcitation may undergo geometrical isomerization of the alkene moiety, but quantum yields of the *cis-trans* isomerization vary greatly. α,ά-Diarylidenecycloalkanones (Scheme 3.5) upon photoexcitation behave in a different manner to undergo a skeletal transformation into furano-annelated dibenzocyloheptenes.

Irradiation of **11-15** in benzene under nitrogen atmosphere in a Rayonet photochemical reactor at 350 nm for 3 h gave exciting results. During the course of 3 h the original yellow solution of **14** and **15** gradually turned light yellow, while the yellow colour of solution was retained for

compounds **11**, **12**, and **13** even after prolonged irradiation. Work-up of light yellow fluorescent solutions obtained upon irradiation of **14** and **15** by vacuum evaporation of solvent followed by column chromatography on silica gel gave yellow fluorescent product **22** and **27** respectively. The products formed were characterized using IR, NMR and mass spectrometry. Mass spectrum confirmed the product formed was an isomer of the starting material. ^{1}H NMR spectrum (Figure 3.15) suggested that product formation has involved an unusual reaction of the anthracene chromophore. The aromatic signal appearing remarkably upfield (at δ 4.86) provided valuable information on the 3-D structure of the photoproduct. It is clear that one of the aromatic protons is lying in the region that falls in the shielding cone of anthracene ring residue.
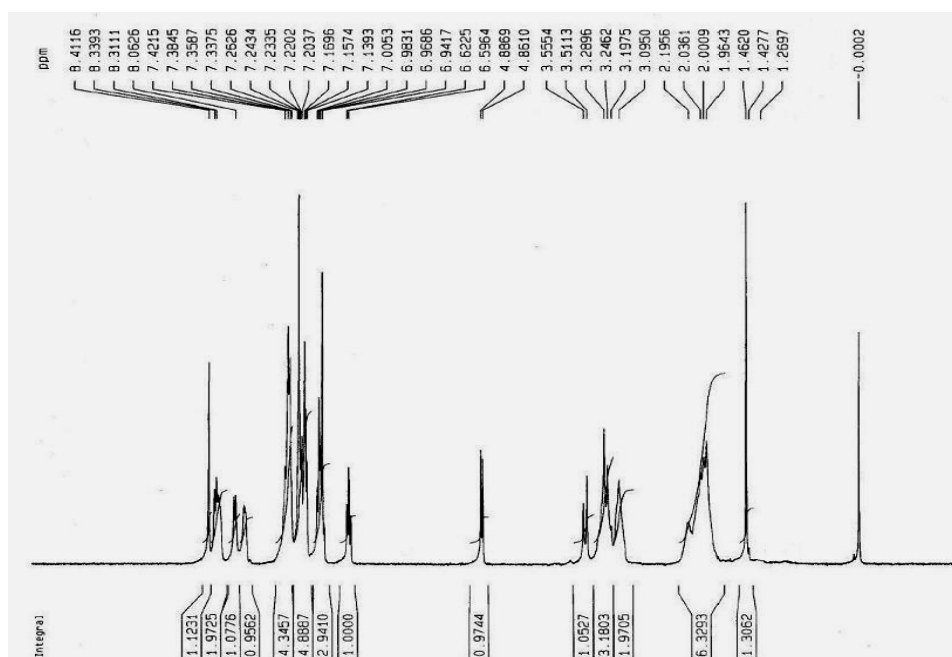
Figure 3.15. [1]*H NMR spectra of 27.*

Though the structure could be deduced on the basis spectral data alone, the proposed structure **27** was confirmed unambiguously by single crystal X-

ray analysis (Figure 3.16). Single crystals of suitable quality were obtained by slow evaporation of hexane-ethyl acetate solution of **27.**
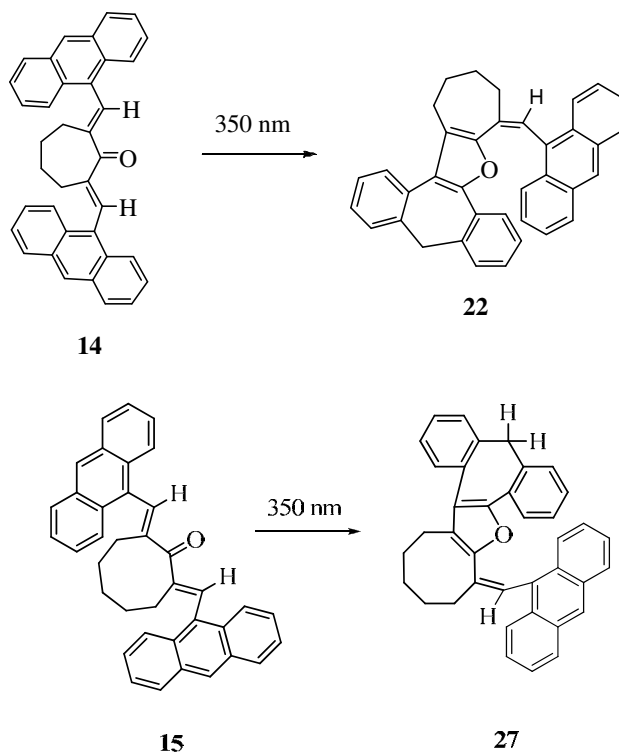
Scheme 3.5. *Photochemical products of 14 and 15.*
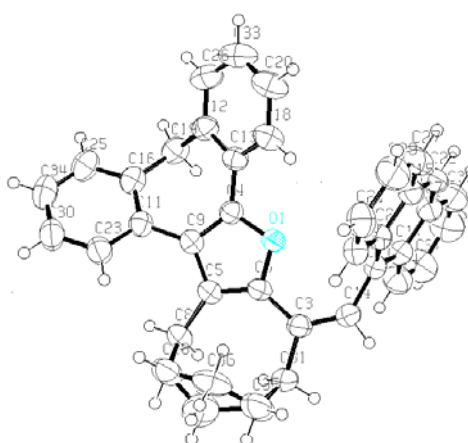
Figure 3.16. *ORTEP diagram of the crystal 27.*

The possible mechanism[12] for the formation of photoproducts begins with double *cis-trans* isomerization[13] of the *trans* compound. The *cis,cis-* isomer then undergoes [4+2] cycloaddition to give a strained tricyclic system. A [4+2] electrocyclic ring opening and eventual 1,5-prototropic shift completes the reaction sequence (Scheme 3.6).
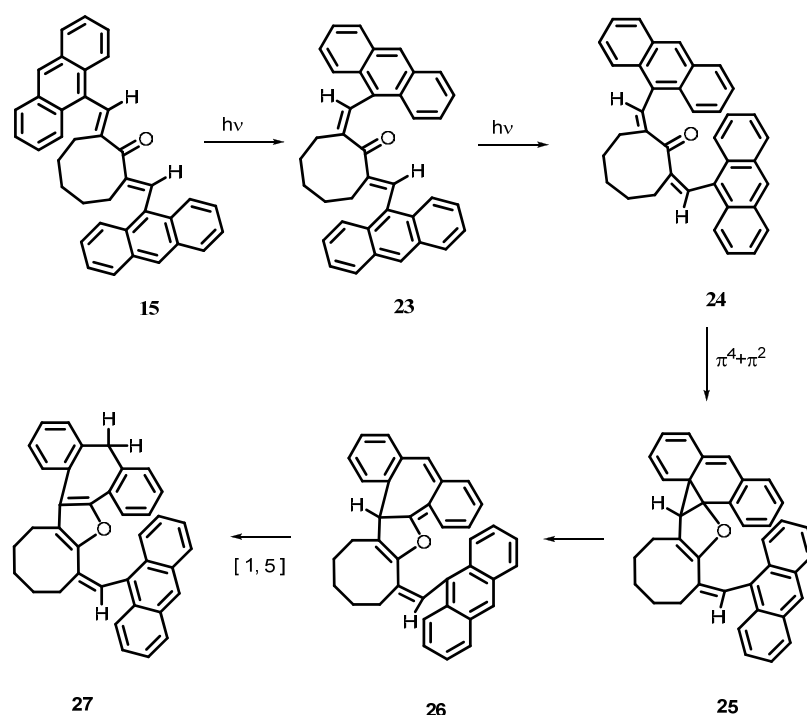
Scheme 3.6. *Possible mechanism of photoreaction for the compound 15.*

From the above reaction, it is clear that *cis-trans* isomerization is the key step in determining the reaction. Subsequent steps should be "dark reactions". The possible explanation for the photoinertness of **12** and **13** can be given as follows. X-ray analysis and preliminary modeling have shown that compounds **12** and **13** possess cofacial geometry and extended conjugation between anthracene-ene-one-ene-anthracene pentad preset in these molecules. Both extended conjugation and exciton coupling can create

substantial red shift in the absorption maxima in compounds such as **12** and **13**. This implies a crippling reduction in excited state energy. Cofacial geometry can also lead to excimer formation that in turn will sap the molecule of excited state energy or channel it into unproductive pathways. Thus both cofacial geometry and possibility of extended conjugation would leave the molecule energy deficient to undergo useful photochemical reactions. Charge transfer interaction between anthracene and carbonyl group components may also be invoked as another energy wasting interaction. Since all these factors can operate either in tandem or independently for **12** and **13**, identifying the actual reason behind observed photoinertness needs closer scrutiny.

The absorption maxima of the bisanthracenes **12** and **13** were found considerably red-shifted with respect to Becker's compound, 1,5-bis(9-anthryl)pentadienone **3** and with other bisanthracenes such as **14** and **15** that undergo facile photoreaction. Thus a reduction in excited state energy may be considered as a possible reason for lack of photoactivity of **12** and **13**. Based on their absorption spectra, we can peg the excited state energy of **12** and **13** below 66 kcal mole^{-1}. However, compounds such as rhodopsin[14] that absorb at 500 nm undergo facile *cis-trans* isomerization reaction. So, excited state energy of bisanthracenes **12** and **13** also should be enough to initiate *cis-trans* isomerization. Consequently, reasons other than insufficient excited state energy should be invoked to account for their photoinertness. An alluring explanation for the lack of photoreactivity in the case of **12** and **13** is energy wastage by excimer formation.

In order to confirm the role of exciton coupling and excimer formation on the photochemistry of bisanthracenes, we prepared a monoanthracene derivative such as **18**. With **18**, co-planarity and hence extended conjugation is not compromised. In fact, absorption spectrum of **18** is similar to that of **3** that undergoes facile photoreaction. We found that **18** is also reluctant to undergo *cis-trans* isomerization. This result is significant: excimer formation is not possible with **18**. Based on this result, we concluded that excimer

formation and resultant energy wastage is not responsible for the photoinertness of **12** and **13**. We extended our investigation to other compounds such as **16** and **17** to establish the generality of our observation. It may be noted that both **16** and **17** contain cyclohexanone-type linkers as with **13**. In the case of **16**, intramolecular charge transfer from nitrogen to oxygen is possible[15]. This will compete with and probably minimize charge transfer from anthracene donor to the carbonyl acceptor. Compound **17** may be regarded as an unsymmetrical analogue of **13**. Absorption spectra of both **16** and **17** were similar to that of **13**. These compounds also were reluctant to undergo light-induced *cis-trans* isomerization reactions.

　　We have thus established that compounds such as **12**, **13, 16, 17**, and **18** are incapable of undergoing *cis-trans* isomerization. Neither exciton coupling nor excimer formation alone or taken together can explain the lack of photoreactivity with these molecules. Charge transfer interactions are also unlikely to contribute to the observed lack of photochemistry. We concluded that other damaging structural features should be present in these molecules. So, we decided to have a closer look at the structure of **12** and **13** as revealed by energy minimization and X-ray crystallographic analysis. A remarkable structural feature observable for **12** and **13** is the cofacial orientation of the two anthracene components. As explained earlier, adverse van der Waals interaction with the cycloalkanone component is responsible for maintaining cofacial orientation and resultant roof like geometry of these molecules. Furthermore rotation around bond '*a*' is restricted and the structures of these compounds are static in nature. In order for the crucial double *cis-trans* isomerization reaction to manifest, both anthracene components will have to cross over to the opposite side of the enone double bond while maintaining their orientation due to restrictions imposed by adverse steric interaction with ring methylenes. This process will involve "cutting through" the carbonyl group that is physically impossible. Hence compounds such as **12**, **13**, **16**, **17**, and **18** cannot undergo photoreactions due to their restricted geometry. With

14 and **15**, the situation is quite different. Here, the flexibility of the central medium ring permits free rotation around bond '*a*'. Thus a variety of conformations are possible here. Hence, rotation around bond '*b*' does not invoke "cutting through' the carbonyl group. Consequently, **14** and **15** are free to undergo *cis-trans* isomerization and subsequent dark reactions.

In continuation, we examined the photochemistry of a cyclobutanone bridged bisanthracene such as **11**. This molecule possesses interesting structural features. Most significant among these is the absence of ring methylene that will generate adverse steric interaction with the anthracene units. Consequently, the two anthracene components can lie in the same plane whereby conjugation in **11** is maximized. Support for this assumption comes from the NMR spectral data of **11** that indicated restricted rotation around bond '*a*'. If this is true, *cis-trans* isomerization will involve impossible "cutting through" the carbonyl component. Consequently, **11** also should not undergo *cis-trans* isomerization. In fact, **11** were isolated unchanged even after prolonged irradiation at 350 nm. This result is consistent with our prediction on structural constraints of photoreactivity.

3.4. Conclusions

The photophysical and photochemical properties of bisanthracenes linked through strained cyclic ketones of varying ring size have been evaluated under different conditions. The photochemical and photophysical properties of these bisanthracenes exhibited dramatic variation that is attributable to the relative geometry of the significant components: two anthracene and the cycloalkanone building blocks. The constrained geometry of the central ring was found to have pertinent effects on the ground as well as excited state properties of the bisanthracenes. Five and six-membered cyclic structures permits a charge transfer interaction from the two anthracene rings to the

central carbonyl group while seven and eight-membered cyclic structures does not permit such an interaction due to their constrained geometry.

Geometry of **12**, **14**, and **15** were established on the basis of single crystal X-ray analysis and molecular modeling studies. In **12** and **13**, the two anthracene components maintain cofacial orientation while the anthracene units are perpendicular to the enone component and free to rotate around bond '*a*' in **14** and **15**. While significant ground state as well as excited state interactions between components were apparent for **12** and **13**, negligible interactions were observed for **14** and **15**. So the bisanthracenes with five and six membered cyclic structures showed fluorescence emission from an intramolecular charge transfer (ICT) state. Molecular modeling studies and HOMO-LUMO mapping confirms the ICT interaction observed for bisanthracenes with five and six membered cyclic structures. Interestingly, while **12** and **13** did not undergo any change upon irradiation, **14** and **15** underwent interesting rearrangement to give ring-expanded products.

We conclude that, *cis-trans* isomerization is the key step in determining photoreaction of these types of compounds. Constrained geometry prevented **12** and **13** from undergoing photochemical rearrangement involving rotation around bond '*b*' while such constraints are absent for **14** and **15**. Our investigations on suitable model compounds ruled out the role of exciton coupling and consequent lowering of excited state energy, adverse interaction between methylene group and aromatic residues, and possibility of excimer formation in controlling the photochemistry of these bisanthracenes. Our results emphatically proclaim the role of geometry in controlling photophysics and photochemistry of multichromophoric systems. Along with other constraints, relative geometry and orientation of non-interacting chromophore components also should be properly fixed for obtaining desired photophysical and photochemical properties of engineered arrays. Thus, we add one more constraint to the paradigm of array assemblage.

3.5. Experimental Section

3.5.1. General Techniques

General information about the experiments is given in section **2.5.1** of Chapter **2**. Recrystallization was done by slow evaporation method from a 2:1 mixture of chloroform-methanol at room temperature. Absorption and emission spectra were recorded at 25 ^{o}C in a 1 cm quartz cuvette. Absorption spectra were measured using Shimadzu-3101PC UV/Vis/NIR scanning spectrophotometer. Emission spectra were recorded on a SPEX Fluorolog F112X Spectrofluorimeter. HPLC grade solvents were used for all photophysical experiments. All fluorescence spectra were corrected for detector response.

3.5.2. Materials

Cyclobutanone, cyclopentanone, cyclohexanone, cycloheptanone, cyclooctanone, tetralone, *N*-methylpiperidone, and indanone were purchased from Sigma-Aldrich and used as received. Solvents were purchased from S. D. Fine Chem. Ltd. and were purified by distillation as per required.

3.5.3. General Procedure for the Synthesis of α,α'-diarylidene cycloalkanones, 11-17

9-Anthracenecarboxaldehyde (2 equiv.), cyclic ketones (1 equiv.) and KOH (2 equiv.) and methanol (10 mL) were taken in round bottom flask and refluxed with stirring at 60 ^{o}C for 5-6 h to get the product. The reaction mixture was concentrated in vacuum and the crude product was purified by column chromatography. The yellow powder obtained was subjected to recrystallization from a chloroform-methanol mixture.

3.5.3.1. Synthesis of (2*E*,4*E*)-2,4-bis(anthracen-9-ylmethylene)cyclobutanone (11)

The synthesis procedure as above, using compound **19** (4.00 g, 19.4 mmol) and compound **20a** (0.68 g, 9.7 mmol) with KOH (1.09 g, 19.4 mmol) afforded 3.72 g (86%) of **11**. Recrystallization gave yellow powder. (mp > 300 ^{o}C).
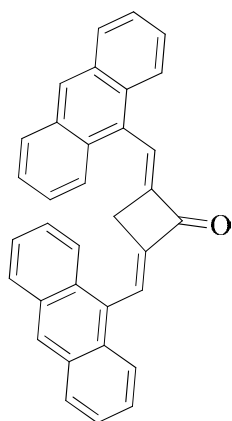
IR (KBr) ν_{max} : 1633, 1593, 1093, 727 cm^{-1};

^{1}H NMR (300 MHz, CDCl$_3$) : δ 8.44-8.42 (m, 4H), 8.16-8.14 (m, 4H), 8.01-8.00 (m, 4H), 7.54-7.46 (m, 8H), 2.87 (s, 2H);

^{13}C NMR (75 MHz, CDCl$_3$) : δ 189.9, 151.2, 157.2, 148.9, 131.2, 127.9, 129.4, 129.0, 128.6, 127.9, 126.5, 125.8, 125.7, 125.5, 125.4, 36.3;

MS (FAB, [M$^+$+1]): Calcd for C$_{34}$H$_{22}$O: 446.16; Found: 447.36;

Elemental analysis calculated for C$_{34}$H$_{22}$O: C, 91.45; H, 4.97; O, 3.58. Found: C, 91.46; H, 4.95; O, 3.48.

3.5.3.2. Synthesis of (2*E*,5*E*)-2,5-bis(anthracen-9-ylmethylene)cyclopentanone (12)

The synthesis procedure as above, using compound **19** (4.00 g, 19.4 mmol) and compound **20b** (0.82 g, 9.7 mmol) with KOH (1.09 g, 19.4 mmol) afforded 4.01 g (90%) of **12**. Recrystallization gave yellow crystals. (mp > 300 ^{o}C).
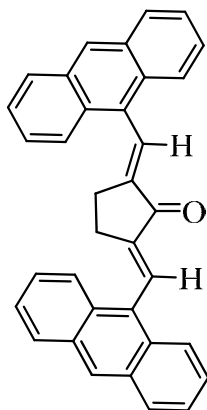
IR (KBr) ν_{max} : 1697, 1634, 1624, 1207, 987, 745 cm^{-1};

^{1}H NMR (300 MHz, CDCl$_3$) : δ 8.57 (s, 2H), 8.46 (s, 2H), 8.08-8.01 (m, 8H), 7.54-7.46 (m, 8H), 2.31 (s, 4H);

^{13}C NMR (75 MHz, CDCl$_3$) : δ 194.1, 144.0, 141.2, 137.1, 132.1, 131.3, 130.0, 129.1, 129.0, 127.9, 126.2, 126.0, 125.8, 125.7, 125.4, 25.7;

MS (FAB, [M$^+$+1]): Calcd for C$_{35}$H$_{24}$O: 460.18; Found: 461.34;

Elemental analysis calculated for C$_{35}$H$_{24}$O: C, 91.27; H, 5.25; O, 3.47. Found: C, 91.25; H, 5.27; O, 3.48.

3.5.3.3. Synthesis of (2*E*,6*E*)-2,6-bis(anthracen-9-ylmethylene)cyclohexanone (13)

The synthesis procedure as above, using compound **19** (4.00 g, 19.4 mmol) and compound **20c** (0.95 g, 9.7 mmol) with KOH (1.09 g, 19.4 mmol) afforded the formation of **13.** Recrystallization gave 4.09 g (89%) of yellow powder (mp > 300 ^{o}C).
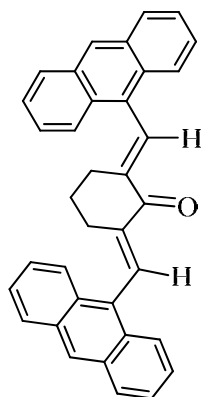
IR (KBr) ν_{max} : 1662, 1625, 1604, 1221, 725 cm^{-1};

^{1}H NMR (300 MHz, CDCl$_3$) : δ 8.67 (s, 2H), 8.46 (s, 2H), 8.09-8.02 (m, 8H), 7.55-7.47 (m, 8H), 2.31-2.27 (m, 6H);

^{13}C NMR (75 MHz, CDCl$_3$) : δ 188.3, 140.9, 135.9, 131.4, 130.6, 129.2, 128.9, 127.4, 126.1,

125.9, 125.4, 125.1, 123.4, 122.8, 29.8, 28.7;

MS (FAB, [M^++1]): Calcd for $C_{36}H_{26}O$: 474.19; Found: 475.33;

Elemental analysis calculated for $C_{36}H_{26}O$: C, 91.11; H, 5.52; O, 3.37.   Found: C, 91.13; H, 5.54; O, 3.35.

3.5.3.4. Synthesis of (2*E*,7*E*)-2,7-bis(anthracen-9-ylmethylene)cycloheptanone (14)

The synthesis procedure as above, using compound **19** (4.00 g, 19.4 mmol) and compound **20d** (1.09 g, 9.7 mmol) with KOH (1.09 g, 19.4 mmol) afforded the formation of **14**. Recrystallization gave 3.17 g (67%) of yellow crystals (mp > 300 ^{o}C).
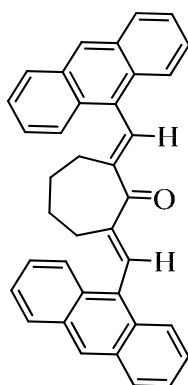
IR (KBr) ν_{max} : 1670, 1648, 1610, 1408, 1168, 718 cm^{-1};

^{1}H NMR (300 MHz, CDCl$_3$) : δ 8.45 (s, 2H), 8.16-8.12 (m, 6H), 8.05-8.01 (m, 4H), 7.51-7.48 (m, 8H), 1.84-1.82 (m, 4H), 1.37-1.34 (m, 4H);

^{13}C NMR (75 MHz, CDCl$_3$) : δ 197.7, 146.6, 134.7, 131.5, 130.7, 129.2, 128.9, 126.9, 125.9, 28.6, 28.0;

MS (FAB, [M^++1]): Calcd for $C_{37}H_{28}O$: 488.21; Found: 489.41;

Elemental analysis calculated for $C_{37}H_{28}O$: C, 91.03; H, 5.65; O, 3.32. Found: C, 91.05; H, 5.63; O, 3.33.

3.5.3.5. Synthesis of (2*E*,8*E*)-2,8-bis(anthracen-9-ylmethylene)cyclooctanone (15)

The synthesis procedure as above, using **c**ompound **19** (4.00 g, 19.4 mmol) and compound **20e** (1.23 g, 9.7 mmol) with KOH (1.09 g, 19.4 mmol) afforded 3.12 g (64%) of **15**. Recrystallization gave yellow crystals (mp > 300 ^{o}C).
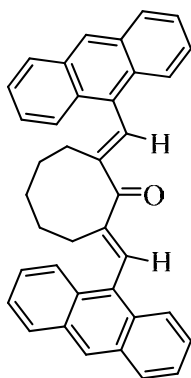
IR (KBr) ν_{max} : 1673, 1612, 1156, 1162, 722 cm^{-1};

^{1}**H NMR** (300 MHz, CDCl$_3$) : δ 8.45 (s, 2H), 8.21-8.18 (m, 4H), 8.05-8.02 (m, 4H), 7.85 (s, 2H), 7.54-7.47 (m, 8H), 2.50-2.48 (m 4H), 1.40-1.38 (m, 6H);

^{13}**C NMR** (75 MHz, CDCl$_3$) : δ 202.9, 147.5, 133.1, 131.5, 130.1, 129.6, 128.9, 127.1, 125.9, 30.3, 27.4, 26.4;

MS (FAB, [M^{+}+1]): Calcd for C$_{38}$H$_{30}$O: 502.22; Found: 503.39;

Elemental analysis calculated for C$_{38}$H$_{30}$O: C, 90.80; H, 6.02; O, 3.18. Found: C, 90.82; H, 6.03; O, 3.20.

3.5.3.6. Synthesis of (1*E*,3*E*)-1,3-bis(anthracen-9-ylmethylene)-3,4-dihydronaphthalen-2(1H)-one (16)

The synthesis procedure as above, using **c**ompound **19** (4.00 g, 19.4 mmol) and compound **20f** (1.42 g, 9.7 mmol) with KOH (1.09 g, 19.4 mmol) afforded 4.01 g (79%) of **17**. Recrystallization gave yellow crystals (mp > 300 ^{o}C).
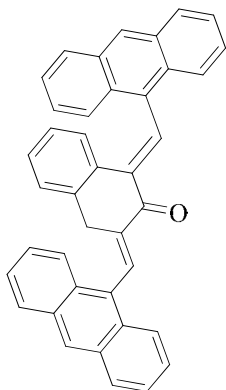
IR (KBr) ν$_{max}$: 1668, 1632, 1608, 1223, 898, 725, cm^{-1};

^{1}H NMR (300 MHz, CDCl$_3$) : δ 8.68-8.64 (m, 2H), 8.52-8.45 (m 2H), 8.09-7.99 (m, 6H), 7.52-7.36 (m, 10H), 6.80-6.72 (m, 2H), 6.43-6.42 (m, 2H), 3.63 (s, 2H);

^{13}C NMR (75 MHz, CDCl$_3$) : δ 190.1, 139.4, 136.2, 134.7, 134.2, 144.0, 132.4, 131.5, 131.3, 130.2, 129.5, 129.4, 128.9, 128.6, 127.9, 127.8, 127.5, 126.4, 126.2, 126.1, 125.9, 125.6, 125.5, 33.2;

MS (FAB, [M$^+$+1]): Calcd for C$_{40}$H$_{26}$O: 522.19; Found: 523.39;

Elemental analysis calculated for C$_{40}$H$_{26}$O: C, 91.92; H, 5.01; O, 3.06. Found: C, 91.82; H, 5.03; O, 3.07.

3.5.3.7. Synthesis of (3*E*,5*E*)-3,5-bis(anthracen-9-ylmethylene)-1-methylpiperidin-4-one (17)

The synthesis procedure as above, using **c**ompound **19** (4.00 g, 19.4 mmol) and compound **20g** (1.11 g, 9.7 mmol) with KOH (1.09 g, 19.4 mmol) afforded 3.79 g (80%) of **3d**. Recrystallization gave yellow crystals (mp > 300 °C).

IR (KBr) ν$_{max}$: 1660, 1628, 1604, 1218, 722 cm^{-1};

^{1}H NMR (300 MHz, CDCl$_3$): δ 8.70 (s, 2H), 8.48 (s, 2H), 8.09-8.03 (m, 8H), 7.56-7.48 (m, 8H), 3.10-3.08 (m, 4H), 1.89 (s, 3H);
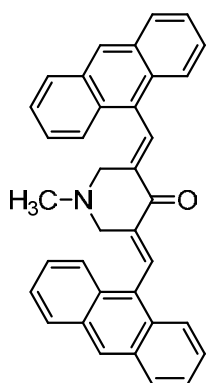
13C NMR (75 MHz, CDCl$_3$) : δ 185.3, 137.5, 135.6, 131.2, 129.4, 129.3, 129.1, 128.9, 127.7, 126.3, 125.7, 125.5, 123.6, 122.0, 121.2, 45.3, 28.7;

MS (FAB, [M$^+$+1]): Calcd for C$_{36}$H$_{27}$NO: 489.20; Found: 490.39;

Elemental analysis calculated for C$_{36}$H$_{27}$NO: C, 88.31; H, 5.56; N, 2.86; O, 3.27. Found: C, 88.32; H, 5.58; N, 2.76; O, 3.20.

3.5.3.8. Synthesis of (*E*)-2-(anthracen-9-ylmethylene)-2,3-dihydro-1H-inden-1-one (18)

9-Anthracenecarboxaldehyde **19** (4.00 g, 19.4 mmol), 1-indanone **20h** (1.42 g, 19.4 mmol) and KOH (1.09 g, 19.4 mmol) and methanol (10 mL) were taken in round bottom flask and refluxed with stirring at 60 ^{o}C for 5-6 h gave yellow precipitate. The reaction mixture was concentrated in vacuum and the crude product was purified by recrystallization in CHCl$_3$-methanol (2:1) mixture gave yellow powder of **18** (mp > 300 ^{o}C).
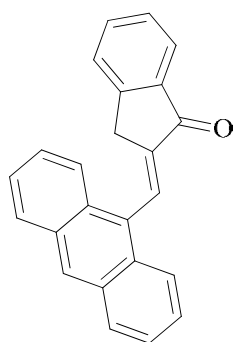
IR (KBr) ν$_{max}$: 1668, 1642, 1250, 1156, 732 cm^{-1}

1H NMR (300 MHz, CDCl$_3$) : δ 8.54-8.46 (m, 2H), 8.05-7.97 (m, 4H), 7.56-7.39 (m, 4H), 7.28-7.25 (m, 4H), 3.38 (s, 2H);

13C NMR (75 MHz, CDCl$_3$) : δ 192.8, 149.8, 141.5, 138.5, 134.8, 132.0, 131.3, 130.0, 129.0, 128.9, 127.7, 127.6, 126.2, 126.1, 125.7, 125.4, 124.7, 31.3;

MS (FAB, [M$^+$+1]): Calcd for C$_{24}$H$_{16}$O: 320.12; Found: 321.32;

Elemental analysis calculated for C$_{24}$H$_{16}$O: C, 89.97; H, 5.03; O, 4.99.   Found: C, 89.82; H, 5.03; O, 4.89.

3.5.4. Photochemical Transformations of α,ά-diarylidene Compounds

3.5.4.1. Procedure for the Photolysis of 11

A solution of **11** (150 mg, 0.34 mmol) in dry, distilled benzene (130 mL) was taken in a 250 mL two necked photochemical reaction vessel fitted with rubber septum and gas inlet tube. The vessel was flushed with nitrogen for 30 min. The sample was irradiated in a photochemical reactor for 3 h**.** The solution obtained was concentrated and analyzed**.** Most of **11** were recovered unchanged even after prolonged irradiation.

3.5.4.2. Procedure for the Photolysis of 12

A solution of **12** (150 mg, 0.33 mmol) in dry, distilled benzene (130 mL) was taken in a 250 mL two necked photochemical reaction vessel fitted with rubber septum and gas inlet tube. The vessel was flushed with nitrogen for 30 min. The sample was irradiated in a photochemical reactor for 3 h**.** The solution obtained was concentrated and analyzed**.** Here the starting material remained as such.

3.5.4.3. Procedure for the Photolysis of 13

A solution of **13** (150 mg, 0.32 mmol) in dry, distilled benzene (130 mL) was taken in a 250 mL two necked photochemical reaction vessel fitted with rubber septum and gas inlet tube. The vessel was flushed with nitrogen for 30 min. The sample was irradiated in a photochemical reactor for 3 h**.** The

solution obtained was concentrated and analyzed. Here the starting material remained as such.

3.5.4.4. Procedure for the Photolysis of 14

A solution of **14** (150 mg, 0.31 mmol) in dry, distilled benzene (130 mL) was taken in a 250 mL two necked photochemical reaction vessel fitted with rubber septum and gas inlet tube. The vessel was flushed with nitrogen for 30 min. Irradiation of the sample in a photochemical reactor for 3 h resulted in the subsequent disappearance of **14.** Work-up of yellow fluorescent solution by vacuum evaporation of solvent followed by column chromatography on silica gel/ethyl acetate gave 75 mg (50%) of yellow fluorescent product **22** along with some polymerized and unreacted starting material. mp 160-162 $^{\circ}$C.

22
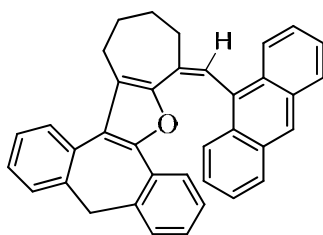
IR (KBr) ν_{max} : 1435, 1210, 1068, 744, 726 cm^{-1};

^{1}H NMR (300 MHz, CDCl$_3$) : δ 8.40 (s, 1H), 8.33-8.27 (m, 2H), 7.96-7.94 (m, 2H), 7.39-7.36 (m, 2H), 7.28-7.18 (m, 4H), 7.15-7.12 (m, 2H), 7.06 (s,1H), 7.01-6.94 (m, 2H), 6.61 (t, 1H, J = 7.35 Hz), 6.15 (d, 1H, J = 7.7 Hz), 3.49-4.00 (m, 4H), 2.95-2.91 (m, 2H), 2.26-1.65 (m, 4H);

^{13}C NMR (75 MHz, CDCl$_3$) : δ 150.2, 149.2, 137.6, 136.9, 136.2, 131.6, 129.9, 128.5, 128.4, 127.8, 127.5, 127.2, 127.1, 125.9, 125.8, 125.6, 125.0, 124.9, 124.8, 122.5, 41.4, 36.5, 29.8, 28.3, 24.7;

MS (FAB, [M$^+$+1]): Calcd for C$_{37}$H$_{28}$O: 488.21; Found: 489.40;

Elemental analysis calculated for C$_{37}$H$_{28}$O: C, 90.95; H, 5.78; O, 3.27. Found: C, 90.97; H, 5.76; O, 3.30.

3.5.4.5. Procedure for the Photolysis of 15

A solution of **15** (150 mg, 0.30 mmol) in dry, distilled benzene (130 mL) was taken in a 250 mL two necked photochemical reaction vessel fitted with rubber septum and gas inlet tube. The vessel was flushed with nitrogen for 30 min. Irradiation of the sample in a photochemical reactor for 3 h resulted in the subsequent disappearance of **15.** Work-up of yellow fluorescent solution by vacuum evaporation of solvent followed by column chromatography on silica gel/ethyl acetate gave yellow fluorescent product **27** (80 mg, 53.3%) along with some polymerized and unreacted starting material. Recrystallization with hexane-ethyl acetate gave yellow crystals.   (mp 156-158 $^{\mathrm{o}}$C).

27
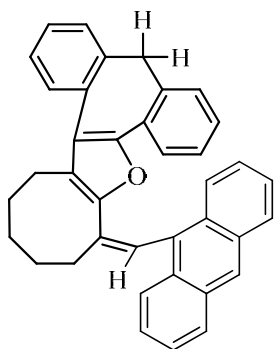
IR (KBr) ν_{max} : 1437, 1209, 1102, 740 cm^{-1};

^{1}**H NMR** (300 MHz, CDCl$_3$) : δ 8.41 (s, 1H), 8.34-8.29 (m, 2H), 8.09-8.06 (m, 2H), 7.42-7.34 (m, 4H), 7.26-7.14 (m, 5H), 7.01-6.92 (m, 2H), 6.59 (t, 1H, J = 7.84 Hz), 4.89-4.86 (d, 1H, J = 7.78 Hz), 3.55-3.51 (m, 2H), 3.29-3.09 (m, 4H), 2.20-1.96 (m, 6H);

^{13}**C NMR** (75 MHz, CDCl$_3$) : δ 150.9, 149.6, 137.9, 137.2, 135.0, 134.5, 131.7, 130.4, 129.7, 128.5, 128.4, 128.2, 127.9, 127.5, 127.1, 127.0, 126.8, 126.4, 126.0, 125.5,

125.3, 125.2, 125.0, 124.1, 122.9, 121.3, 41.2, 34.8, 29.9, 27.0, 23.1, 22.7;

MS (FAB, [M$^+$+1]): Calcd for $C_{38}H_{30}O$: 502.22; Found: 503.23;

Elemental analysis calculated for $C_{38}H_{30}O$: C, 90.80; H, 6.02; O, 3.18. Found: C, 90.81; H, 6.03; O, 3.16.

3.5.4.6. Procedure for the Photolysis of 16

A solution of **16** (150 mg, 0.29 mmol) in dry, distilled benzene (130 mL) was taken in a 250 mL two necked photochemical reaction vessel fitted with rubber septum and gas inlet tube. The vessel was flushed with nitrogen for 30 min. The sample was irradiated in a photochemical reactor for 3 h. The solution obtained was concentrated and analyzed. Here the starting material remained as such.

3.5.4.7. Procedure for the Photolysis of 17

A solution of **17** (150 mg, 0.31 mmol) in dry, distilled benzene (130 mL) was taken in a 250 mL two necked photochemical reaction vessel fitted with rubber septum and gas inlet tube. The vessel was flushed with nitrogen for 30 min. The sample was irradiated in a photochemical reactor for 3 h. The solution obtained was concentrated and analyzed. Here the starting material remained as such.

3.5.4.8. Procedure for the Photolysis of 18

A solution of **18** (150 mg, 0.47 mmol) in dry, distilled benzene (130 mL) was taken in a 250 mL two necked photochemical reaction vessel fitted with rubber septum and gas inlet tube. The vessel was flushed with nitrogen for 30 min. The sample was irradiated in a photochemical reactor for 3 h. The

solution obtained was concentrated and analyzed**.** Here the starting material remained as such.

3.6. References

1.   von Bunau, G.; Wolff, T. *Advances in Photochemistry*; Volman, D. H., Hammond, *G.* S., Gollnick, K., Eds.; Interscience Publishers: New York, **1988**, *14*, 273

2.   Desvergne, J-P.; Bitit, N.; Castellan, A.; Laurent, H. B. *J. Chem. Soc. Perkin Trans II.* **1983**, 109. (b) Laurent, H. B.; Desvergne, J-P.; Castellan, A.; Lapouyade, R. *Chem. Rev.* **2000**, *29*, 43. (c) Becker, H. D.; *Pure and Appl. Chem.* **1982**, *54*, 1589. (d) Lin, Z.; Priyadarshy, S.; Bartko, A.; Waldeck, D. H. *Photochem. Photobiol.* **1997**, *110, 131*.

3.   (a) Bouas-Laurent, H.; Castellan, A.; Daney, M.; Desvergne, J.-P.; Guinand, G.; Marsau, P.; Riffaud, M.-H. *J. Am. Chem. Soc.* **1986**, *108*, 315. (b) Becker, H.-D.; Patrick, V. A.; White, A. H. *Aust. J. Chem.* **1964**, *37*, 2215. (c) Becker, H.-D.; Engelhardt, L.M.; Hansen, L.; Patrick, V. A.; White, A. H. *Aust. J. Chem.* **1964**, *37*, 1329. (d) Becker, H.-D.; Hansen, L.; Skelton, B. W.; White, A. H. *Aust. J. Chem.* **1985**, *38*, 809. (e) Castel, N.; Fiacher, E.; Bartocci, G.; Maeetti, F.; Mazzucato, U. *J. Chem. Soc., Perkin Trans. 2.* **1986**, 1969. (f) Bhattacharyya, K.; Chattopadhyay, **S.** K.; Bard-Tosh, S.; Das, P. K. *J. Phys. Chem.* **1986**, *90*, 2646. (g) Becker, H.-D.; Anderaeon, K. *J. Org. Chem.* **1987**, *52*, 6205. (h) Becker, H.-D.; Hansen, L.; Skelton, B. W.; White, A. H. *Aust. J. Chem.* **1988**, *41*, 1557. (i) Becker, H.-D.; Sandros, K. *Chem. Phys. Lett.* **1978***, 53*, 228. (j) Becker, H.-D.; Sandros, K. Chem. *Phys. Lett.* **1978**, *55,* 498. (k) Becker, H.-D.; Andemon, K.; Sandros, K. *J. Org. Chem.* **1980**, *45*,

4549. (l) Becker, H.-D.; Sandros, K.; Andemon, K. *Chem. Phys. Lett.* **1981**, *77*, 246.

4.   Becker, H.-D.; Anderseon, K. *J. Org. Chem.* **1983**, *48*, 4542.

5.   (a) Nielsen, A. T.; Houlihan, W. J. *Organic Reactions.* **1968**, *16*, 1. (b) Mukaiyama, T. *Organic Reactions*; Dauben, W. G.,et al.,Eds.; Wiley: New York, NY, **1982**; Vol. *28*, p 203. (c) Heathcock, C. H. *Comprehensive Organic Synthesis;* Trost, B. M., Flemming, I., Eds.; Pergamon: Oxford, **1991**; Vol. *2*, p 133. (d) e Gennari, C. *Comprehensive Organic Synthesis;* Trost, B. M., Flemming, I., Eds.; Pergamon: Oxford, **1991**; Vol *2*, p 629. (e) Mahrwald, R. *Modern Aldol Reactions;* Wiley-VCH: Weinheim, Germany, **2004**; Vols. *1* and *2*. (f) Reeves, R. L. *Chemistry of Carbonyl Group;* Patai, S., Ed.; Wiley Intersciences: New York, NY, **1966**; p 580. (g) Russel, A.; Happoldt, W. B.; Jr. *J. Am. Chem. Soc*. **1942**, *64*, 1101. (h) Deli, J.; Lorand, T.;Szabo, D.; Foldesi, A. *Pharmacie.* **1984**, *39*, 539. (i) Claisen, L.; Claparede, A. *Ber.* **1881**, *14,* 2460. (j) Perkin, W. *Ber.* **1882,** *15,* 2802. (k) Claisen, L.; Claparede, A. *Ber.* **1881**, *14,* 2460. (l) Schmidt, J. G. *Ber.* **1881**, *14,* 1459. (m) Bhagat, S.; Sharma, R.; Chakrabarti, A. K. *J. Mol. Catal. A*. **2006**, *260*, 235.

6.   Klonkowski, A. M.; Kledzik, K.; Ostaszewski, R.;Widernik, *T. Colloids and Surfaces A.* **2002**, *208*, 115. (b) Castellan, A.; Desvergne, J-P.; Lesclaux, R. *Chem. Phy. Lett.* **1984**, *106,*117. (c) Grabowski, Z. R.; Rotkiewicz, K. *Chem. Rev*. **2003**, *103*, 3899.

7.   (a)Lamola, A. A.; Turro, N. J. *Energy Transfer and Organic Photochemistry*, Interscience Publishers, New York, **1969,** *16*. (b) Manoj, N.; Gopidas, K. R. *Chem. Phy. Lett*., **1997**, *267*, 567.

8.   Hayashi, T.; Suzuki, T.; Mataga, N. *J. Phys. Chem.* **1977**, *81,* 420.

9.   Chandross, E. A.; Dempster, C-J. *J. Am. Chem. Soc.* **1970**, *92,* 3586.

10.   Sumalekshmy, S.; Gopidas, K. R. *J. Phys. Chem. B.* **2004**, 108, 3705.

11.   Daney, M.; Vanucci, C.; Desvergne, J-P. *Tetrahedron Lett.* **1985**, *26,* 1505.

12.   Becker, H. D.; Becker, H. C.; Sandros, K. *Tetrahedron Lett.* **1985**, *26,* 1589.

13.   Becker, H. D. *Chem. Rev.* **1993**, *93,* 145.

14.   Hubbard, R. *Nature* **1969**, *221*, 435.

15.   Jacob, J. P.; Mallia, R. R.; Unnikrishnan, P. A.; Prathapan, S. unpublished results from this laboratory.

INVESTIGATIONS ON PHOTOPHYSICAL PROPERTIES OF A FEW BISPYRENE SYSTEMS

4.1. Abstract

As an extension to our studies on effects of geometry on photochemical and photophysical behaviour of bisanthracenes, we synthesized a few bispyrene systems and examined their photochemical and photophysical behaviour. We present here an overview of these interesting properties and a detailed analysis of the results obtained.

4.2. Introduction

In continuation of our previous work dealing with the synthesis of bisanthracenes, we wish to report the synthesis of novel highly conjugated bispyrenes that exhibit interesting photophysical properties including solvatochromism. These bispyrenes were synthesized and examined to generalize our results on the effect of geometry on the photophysics and photochemistry of various bisanthracenes achieved by connecting anthracene units through cycloalkanones of varying ring size. We examined the excited state behaviour of bispyrene systems **4a-d** in some detail. Fluorescence life-time measurements were done by time-correlated single photon counting technique (TCSPC). We noted excellent solvatochromic behavior in the case of bispyrene system with cyclopentanone spacer. Pyrene is one of the most widely used neutral fluorescence probes. Its solvatochromic property seemed

to be enhanced in the typical bispyrene system.   A brief overview on solvatochromism is presented in the following paragraphs.

4.2.1. An Overview on the Solvatochromic Behaviour of Organic Compounds

The chromic behavior of compounds may be due to photochromism (light), thermochromism (heat), electrochromism (electricity), solvatochromism (solvent), ionochromism(ions), halochromism (pH), tribochromism (friction), and piezochromism (pressure).

The term solvatochromism is used to describe changes in UV visible absorption band following a change in the polarity of the medium.   When absorption spectra are measured in solvents of different polarity it is found that not only the position but also the intensity and shape of the absorption band can vary, depending on the nature of the solvent.[1]   The influence of solvents on the course of chemical reactions has been studied for a long time, and efforts have been made to correlate equilibrium constants, reaction rate constants, or positions of ultraviolet absorption bands with ''polarity'' of the solvent.   Attempts made to express the polarity in terms of dielectric constant, dipole moment, or other properties of the solvent have not been very successful, largely due to the simplifications used.[2]

The polarity of a solvent is determined by its solvation behaviour, which in turn depends on the action of intermolecular forces (coulomb, directional, inductive, dispersion, and charge transfer forces as well as hydrogen bonding forces) between the solvent and the solute.   The macroscopic property, the dielectric constant, does not provide a direct measure of the interactions on the molecular scale, i.e., the solvating power of a solvent cannot be measured by a single parameter.   Over the past few years, solvatochromic comparison method which is based on the effect of solvent polarity on electronic excitation energy of indicator dyes has been used to

successfully characterize various solvents. This method has also been applied to the characterization of systems such as mixed solvents,[3] dry solid surfaces such as silica, silicalite[4] and zeolites,[5] and alumina[6] and also 'wetted' or 'solvated' solid surfaces, such as liquid chromatographic stationary bonded phases.[7] This method has also been extended to supercritical fluids[8] and to organized media such as cyclodextrins and micelles.

4.2.1.1. History and Development of Solvatochromic Methods

The lack of comprehensive theoretical expressions for the calculation of solvent effects and the inadequacy of defining solvent polarity in terms of simple physical characteristics led to the introduction of empirical parameters of solvent polarity. Based on the assumption that carefully selected and well-understood solvent dependent chemical reactions or spectral absorptions may serve as suitable model processes, various empirical solvent polarity scales have been developed.

The first empirical parameter of 'solvent ionizing power' was the Y-scale introduced by Winstein in 1948 and derived from the rate of the S_N1 solvolysis reaction of *t*-butyl chloride.[9] In 1951, Booker was the first to suggest that solvatochromic dyes might be useful as indicators of solvent polarity, but Kosower was the first to set up a real spectroscopic solvent polarity scale in 1958. This was called the *Z*-scale and was based on the shift of the wavelength of the maximum absorption of the intermolecular charge transfer band of 1-ethyl-4-methoxycarbonylpyridinium iodide.[10]

Dimroth *et al.* proposed a pyridinium *N*-phenoxide betaine indicator dye in 1963 as a new UV/visible spectroscopic probe of solvent polarity. This dye, by virtue of its exceptionally large negative solvatochromism (i.e., a blue shift of the UV-visible absorption band with increasing solvent polarity), overcame some practical limitations of other solvatochromic indicator dyes.

The E$_T$(30) scale developed by Reichardt is based on the spectroscopic behaviour of this betaine indicator dye, 4-(2,4,6-triphenylpyridinium)-2,6-diphenylphenoxide (ET-30).[11] The ET-30 molecule shows pronounced solvent-dependent spectral shifts, i.e., it is pink in methanol (λ_{max} = 515 nm), green in acetone (λ_{max} = 677 nm), and blue in acetonitrile (λ_{max} = 620 nm). The range of colours exhibited by this dye is shown in Figure 4.1.

Figure 4.1: *Colours of solutions of Reichardt's betaine (ET-300. From left: n- butanol, n-propanol, ethanol, methanol, acetophenone, acetonitrile and acetone.*

The E$_T$(30) scale has been shown to give an indication of both dipolarity and hydrogen bonding donating acidity of the solvent.[1] In applying solvent polarity scales based on a single empirical parameter, it is assumed that the combination of solute-solvent interactions between the indicator dye and the solvent is the same as the particular solute under consideration. In many cases, this becomes an oversimplification. To overcome this problem, multiparameter correlation equations have been introduced that consist of up to four single empirical parameters, each of them measuring a certain aspect of the overall solvation capability of a given solvent such as the polarizability, dipolarity, Lewis acidity, and Lewis basicity.

4.2.1.2. Physical Basis of Solvatochromism

Theoretical treatments of electronic spectra start by assuming the presence of isolated molecules. This can be achieved experimentally only in

gas phase at low pressures or when the spectrum is recorded in very dilute solutions of the dye probe in 'non-interacting' solvents. In experiments, spectra are recorded in a variety of environments and at reasonable solute concentrations. Thus, both solute-solute and solute-solvent interactions must be considered. The effect of the medium on the spectral properties of the solute molecules can be broadly divided into two categories as *"general solvent-solute interactions"* and *"specific interactions"*.

4.2.1.2.1. General Solvent-Solute Interactions

General solvent-solute interactions involve electrostatic forces and are of three types: dipole-dipole, dipole-induced dipole, and induced dipole-induced dipole. If the dipole moment of the molecule increases upon excitation, as is the case for $\pi \rightarrow \pi^*$ transitions, then a more dipolar or polarisable solvent will serve to stabilize the excited state more than the ground state (Figure 4.2a). In that case, the separation between the ground and excited state energies is decreased and the absorption spectrum is red-shifted. This effect is called *positive solvatochromism* or a *bathochromic shift*, and the magnitude of this shift depends on the change in the probe molecule's dipole moment during the excitation process.

On the other hand, a *hypsochromic* (blue) shift is observed for molecules whose dipole moment decreases in the excited state as compared to the ground state, stabilizing the ground state energy in polar solvents (Figure 4.2b); this is *negative solvatochromism*, often seen for molecules with $n \rightarrow \pi^*$ transitions. Mention may be made in this connection that such solvatochromic behaviour forms the basis of Kasha's Test to differentiate between $\pi \rightarrow \pi^*$ and $n \rightarrow \pi^*$ transitions.
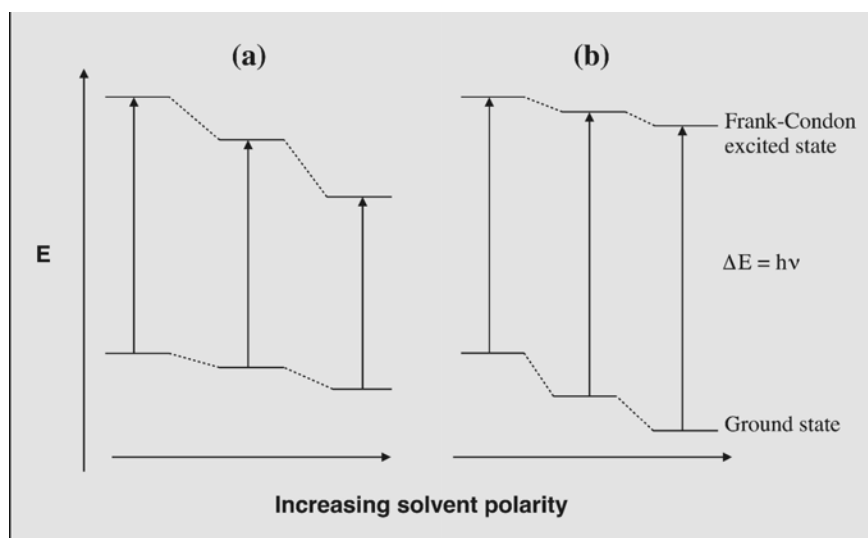
Figure 4.2: *Schematic qualitative representation of solvent effects on the electronic transition energy of dipolar solutes in polar solvents. (a) Positive solvatochromism: the UV-visible transition energy shifts to lower energy (longer wavelength) as the solvent polarity is increased because the dipole moment in the ground state is smaller than the dipole moment in the excited state. (b) Negative solvatochromism: the UV-visible transition energy shifts to higher energy (shorter wavelength) as the solvent polarity is increased because the dipole moment in the ground state is larger than the dipole moment in the excited state.*

4.2.1.2.2. Specific Interactions

These are specific chemical interactions between the chromophores and the solvent, such as hydrogen bonding, complexation, acid base chemistry, and charge transfer interactions. These interactions can lead to substantial changes in the electronic spectrum of the molecule. In HBD interactions (hydrogen bond donating), the electronic state energy is lowered by the electrostatic interaction of a positively polarized hydrogen atom of the solvent with a lone pair of electrons on a basic atom of the solute in the ground or the excited state. During the excitation process, if the electron density migrates

away from the basic atom, formation of the hydrogen bond opposes this migration.

As a result, a blue shift is observed with an increase of the HBD capacity of the solvent. Conversely, if the charge migration occurs towards the basic atom upon excitation, a red shift is observed with the increasing HBD capacity of the solvent. It should be noted that these are H-bonding interactions, as opposed to actual proton transfer reactions.

4.2.1.3. Solvent Effects on Fluorescence Spectra

When the excited state of a molecule is created in solution by continuous or flash excitation, the excited state molecule interacts to a varying degree with the surrounding solvent molecules, depending on their polarity, before relaxing to the ground state. These excited-state solute-solvent interactions found in fluorescent molecules are often reflected in the spectral position and shape of the emission bands. The time scale for fluorescence emission is much longer than that for absorption, and over this period of time, the solvent molecules have a chance to rotationally reorient to stabilize an excited state dipole moment. This effect is called solvent relaxation, and the magnitude of this effect varies with the nature of the solvent. Solvent relaxation leads to a lowering of the energy of the excited state of the molecule in a dipolar solvent. Upon emission of radiation, the excited molecule returns to the ground state electronic configuration.

Although the electronic configurations of the solvent molecules in the solvation sphere have had a chance to reorient, the solvent molecules themselves do not have time to rotationally reorganize over the time scale of fluorescence emission. The energy of this "initial" ground state ($S_0^{!}$) is therefore usually larger than the equilibrium ground state (S_0), (Figure. 4.3).[12]
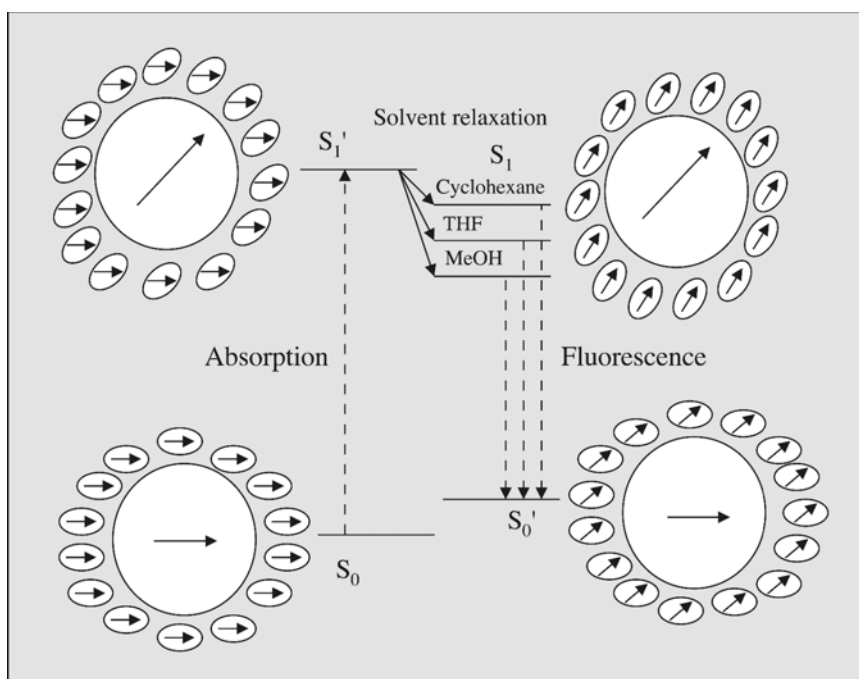
Figure 4.3: *Solvent effects on electronic state energies. S_0 is the ground state, S_1 is the excited state, dashed line: radiative process, solid lines: non-radiative processes. This figure is adapted from Cecil and Rutan.*

If the ground state has a smaller dipole moment than the excited state, then this stabilization effect will not be as pronounced as that observed for the excited state. Thus, in this case, the primary effect in fluorescence emission spectra is the observation of a red shift in polar solvents. Fluorescence offers additional means for characterizing molecular motions and interactions within the fluorophore environment, thus offering an estimation of the polarity of the environment of the fluorophore. The lifetime of an excited fluorophore molecule reflects the rate of competing processes for the relaxation of the excited state. The excess energy of the fluorophore can be lost by energy transfer to other species (typically impurities). This process is known as quenching. If a fluorophore is in an environment that is protected from collisions with quenchers, a longer lifetime will result. A related phenomenon

is the formation of excimers. Upon the formation of an excited state of the fluorophore, it may collide and interact with a second fluorophore molecule that is in the ground state to form an excited state dimer, or excimer. This excimer has its own characteristic emission response, distinct from the emission of the monomer. In the case where the excited state fluorophore collides with a different ground state species, the complex formed is known as an exciplex. Changes in charge-transfer characteristics of excimers and exciplexes can be a sensitive probe of local dielectric constants. All of these phenomena have been thoroughly discussed by Lakowicz.[12]

A wide range of different solvents and organized media has been characterized using fluorescent spectroscopic probes. The use of these probes has revealed important information regarding the polarity of the medium surrounding the probe molecules. One of the most commonly used fluorescent probes of solvent polarity is pyrene.[13] The basis for the so-called 'Py' scale of solvent polarity is the change in the intensity of the highest energy emission band. In non-polar solvents, this transition is highly symmetry forbidden, but in polar solvents, the symmetry is disrupted and the intensity of the band is increased. The numerical values for the Py scale are obtained by dividing the intensity of the lower energy 'III' band by the intensity of the high energy 'I' band. These ratios range from 0.5 for non-polar solvents to about 1.5 for polar solvents.[13] The spectroscopic characteristics of other polyaromatic hydrocarbons have also been catalogued as a function of solvent polarity.[14]

One limitation of many of the fluorescent probes is that they do not allow specific interactions such as hydrogen bonding, dipolarity, and dispersion to be identified and only give an overall indication of the overall polarity of the probe environment. The polarity of a medium, as determined by an individual fluorescent species, is usually considered to be an unspecified composite of various interactions between the probe and its surroundings. In contrast, the use of appropriate solvatochromic indicators with UV-visible

spectroscopy results in the identification and quantification of the specific interactions.

Centro-symmetric molecules show solvatochromic shifts of their absorption and fluorescence spectra in a series of solvents of different static dielectric constants. These shifts have been explained by the existence of small dipole moments of such molecules in excited states or by the "solvent Stark effect" which results from fluctuations of the electric field produced by the polar solvent. Thus solvatochromic shifts of the electronic absorption and emission spectra of molecules are often used for the estimation of the dipole moments in various excited states.

4.2.1.4. Applications

(i) **Mixed Solvents:** Mixed solvents (binary or ternary mixtures) are used in a variety of situations (i.e., chromatography and chemical synthesis) to afford better control over the polarity of the system. This allows for fine-tuning of chromatographic selectivities or reaction yields. Solvatochromic methods aid in characterizing these mixed solvent systems.

(ii) **Polymers and Chemical Sensors:** Another area where solvatochromic methods have been found to be useful is in the characterization of polymers.

(iii) **Supercritical Fluids:** One of the issues of importance to investigators studying the theoretical and practical behaviour of solute-solvent interactions in supercritical fluids is that of the local density around the solute molecule. Solvatochromic indicator dyes are very sensitive to these density fluctuations.

(iv) **Organized Media:** Over the past several years, there has been increasing interest in using microscopic or nanoscopic assemblies in solution to confer a local structure. One of the most extensively studied microstructures of this type is micelles.   Other investigators have explored solvatochromic approaches for understanding microscopic polarities in micelles.

(v) **Solid Surfaces:** The solvatochromic method has been shown to be most useful in the characterization of these types of solid surfaces, bare and bonded silica stationary phases.

4.3. Results and Discussion

4.3.1. Synthesis and Characterization

Bispyrene systems with cycloalkenone connecter, **4a-d** synthesized by us are given in Chart 4.1.

4a   **4b**   **4c**   **4d**
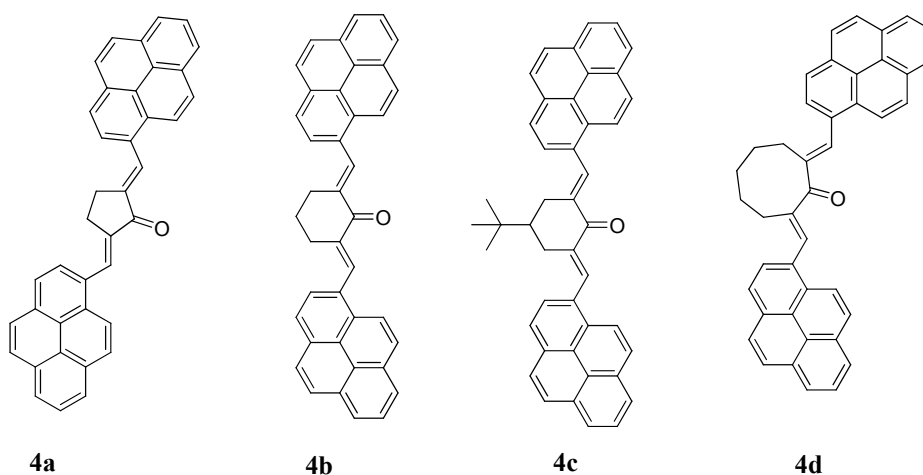
Chart 4.1

We employed Claisen-Schmidt condensation[15] for the preparation of desired (2*E*,*mE*)-2,*m*-bis(pyren-1-ylmethylene)cycloalkanones **4a-d**. Condensation of 1-pyrenecarboxaldehyde **1** and various cyclic ketones **2a-d** of varying ring size or substitution pattern in the presence of potassium hydroxide afforded novel (2*E*,*mE*)-2,*m*-bis(pyren-1-ylmethylene)cycloalkanones **4a-d** in good yields (60-83%) (Scheme 4.1 and 4.2). Cyclic ketones of our choice include cyclopentanone **2a**, cyclohexanone **2b,** *t*-butylcyclohexanone **2c** and cyclooctanone **2d.**
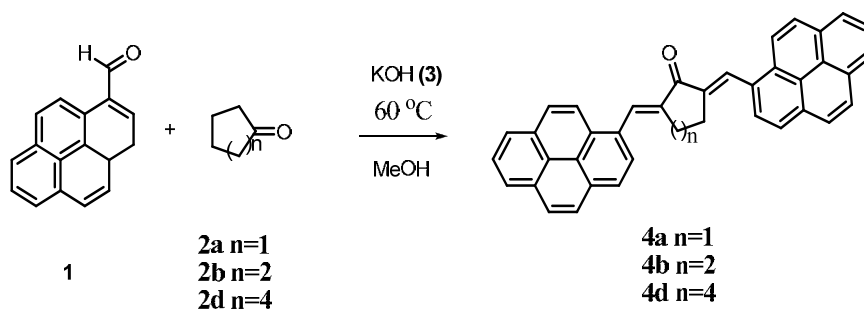
Scheme 4.1. *Synthesis of Bispyrenes* **4a,b** *and* **d.**
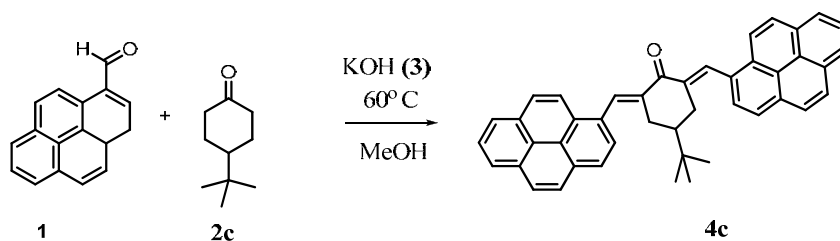
Scheme 4.2. *Synthesis of Bispyrene* **4c.**

Refluxing a mixture of cyclic ketone and 1-pyrenecarboxaldehyde (1:2) in methanol with potassium hydroxide for 6 h gave the bispyrene **4a-d** as a yellow precipitate which was filtered and further purified by recrystallization from chloroform-methanol mixture.

The molecular structures of **4a-d** were established on the basis of spectral and analytical data. Detailed explanation regarding the structure of the compound **4a** is given in Chapter **2**. The UV absorption spectra of **4b** indicated the presence of extended conjugation to pyrene residues in the bispyrene sample. The α,β-unsaturated keto group in **4b** is indicated in the IR spectrum; by the strong peak at 1658 cm^{-1} and the peak at 1593 cm^{-1} is indicative of conjugated olefinic bond. The ^{1}H NMR spectrum exhibited a multiplet from δ 1.77 to δ 1.75, denoting the two geminal hydrogens at position 4 of cyclohexanone moiety. The geminal hydrogens at position 3 and

5 of cyclohexanone appear as multiplet from δ 2.93 to δ 2.65. The multiplets from δ 7.88 to 8.75 establish aromatic protons and vinylic proton of **4b**. The molecular ion peak at *m/z* 523.19 (M$^+$+1) in the FAB mass spectrum, ascertains the structural identity of bispyrene **4b.** Satisfactory elemental analysis data also supported the formation of the adduct.

Similarly, the compound **4c** showed strong IR absorptions at 1662 cm^{-1} and 1595 cm^{-1} due to the carbonyl group and C=C group respectively. The UV absorption spectra of **4c** indicated the presence of extended conjugation to pyrene residues in the bispyrene sample. The ^{1}H NMR shows a singlet at δ 0.75 corresponds to the *t*-butyl protons and a multiplet from δ 1.62 to δ 1.60 denoting the hydrogen at 4-position of *t*-butyl cyclohexanone moiety. The geminal hydrogens at position 3 of cyclohexanone appear as multiplet from δ 1.99 to δ 2.42. The signals from δ 7.49 to 8.62 denote aromatic protons of **4c**. The molecular ion peak at *m/z* 579.36 (M$^+$+1) in the FAB mass spectrum, ascertains the structural identity of bispyrene **4c.** Satisfactory elemental analysis data also supported the formation of the adduct.

Similarly, the UV absorption spectra of **4d** indicated the presence of pyrene residues in the bispyrene sample indicating less extended conjugation than **4a-c.** The α,β-unsaturated keto group in **4d** is indicated in the IR spectrum; by the strong peak at 1668 cm^{-1}and the peak at 1592 cm^{-1} is indicative of conjugated olefinic bond. The ^{1}H NMR shows a multiplet from δ 1.67 to 1.55 denoting the two hydrogens at position 5 of cyclooctanone moiety. The geminal hydrogens at positions 3,4,6 and 7 of cyclooctanone, appear as multiplet from δ 2.72 to δ 2.81. The singlet at δ 7.87 indicates the vinylic proton of dienone moiety of cyclooctanone, further proving that **4d** is a symmetric molecule. The multiplets from δ 7.91 to 8.24 establish the aromatic protons of **4d.** The molecular ion peak at *m/z* 551.33 (M$^+$+1) in the FAB mass spectrum, ascertains the structural identity of bispyrene **4d.**

Satisfactory elemental analysis data also supported the formation of the adduct.

Due to poor solubility of bispyrenes in common organic solvents, we could not record ^{13}C NMR spectra of these compounds. We could not generate diffraction quality crystals either. So, the structural information on **4a-d** including their geometry is somewhat speculative in nature.

4.3.2. Photophysical Studies

4.3.2.1. Absorption and Fluorescence Studies

The absorption and fluorescence emission spectra of the bispyrenes **4a-d** were recorded in various solvents of increasing solvent polarity. The absorption spectrum of compound **4a** is quite different from that of pyrene. Substantial red shift is observed here and vibrational fine structure is missing here. With **4b** and **4c**, a small red shift (with respect to pyrene absorption) and vibrational fine structure are evident. For **4a-c**, small solvent shifts were observed. On the other hand, **4d** exhibited pyrene like absorption with negligible solvent shift. This observation suggests that **4a-d** posses geometry similar to the corresponding bisanthracenes connected through cycloalkanone spacers. However, the similarity in structure cannot be over emphasized and a few subtle differences deserve special mention. Unlike bisanthracenes, bispyrene **4a-c** exhibited noticeable solvent shift in their absorption spectra. However, the solvent dependence does not exhibit a definite trend (Table 4.1). For comparison, $E_T(30)$ value for the solvents employed in this study is also presented in Table 4.1. On the first look, comparison with Py values appears more relevant. But determination of Py value is possible only with vibronically resolved spectra. So, we decided to take $E_T(30)$ value as the benchmark. There is a perfect match between $E_T(30)$ values and emission maxima of **4a** while shift in absorption maxima follows a more complex

pattern. We conclude that emission maxima for bispyrenes such as **4a** are strongly influenced by solvent polarity.   Absorption maxima of these compounds are also influenced by the nature of the solvent, but solvent polarity is not the only deciding factor.   It is interesting to note that bisanthracenes having similar structural features exhibited similar trends. Here, absorption maximum was almost independent of the nature of the solvent while emission maxima were controlled by solvent polarity.
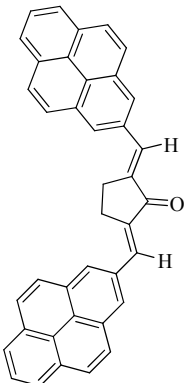
Solvent	λ_{max}(abs)	λ_{max}(emn)	E_T (30) values
THF	440 nm	530 nm	37.4
Ethyl acetate	440 nm	531 nm	38.1
Chloroform	453 nm	548 nm	39.1
Dichloromethane	449 nm	557 nm	40.7
Acetonitrile	443 nm	576 nm	45.6
Methanol	458 nm	634 nm	55.4

Table 4.1. *Solvent effect on absorption and emission maxima for* **4a**

Our observations suggest that, factors other than solvent polarity play important role on deciding the absorption maxima of these compounds. At the same time, substantial difference in the absorption and emission characteristics (including absorption/emission maxima and solvent dependence) of **4a** and **4d** conclusively demonstrates the effect of cycloalkanone spacers on the ground and excited state makeup of these bispyrenes.
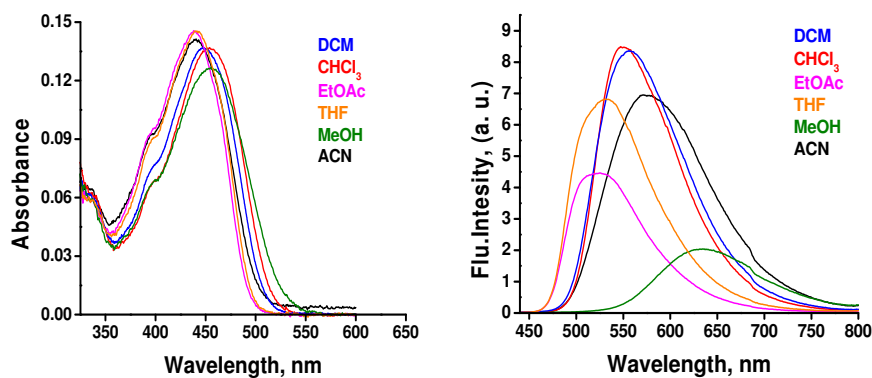
Figure 4.4: *Absorption and emission spectra of the compound 4a in various solvents.*

Fluorescence emission spectra in different solvents were structureless and exhibited positive solvatochromic shift with increasing solvent polarity. Bispyrene **4a** showed pronounced solvent-dependent spectral shifts, it emits red in methanol (λ_{max} 634 nm), yellow in chloroform (λ_{max} 548 nm), and green in tetrahydrofuran (λ_{max} 530 nm). The range of colours exhibited by molecule **4a** is shown in Figure 4.5.

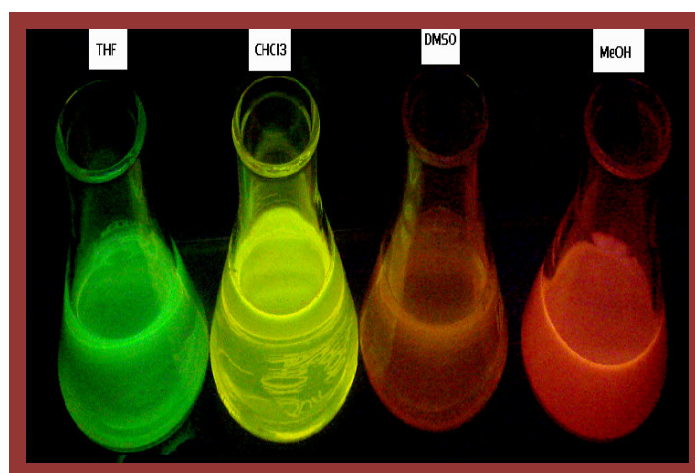
Figure 4.5: *The ''naked eye'' detection of bispyrene, 4a. All are irradiated at 365 nm with a laboratory UV lamp.*
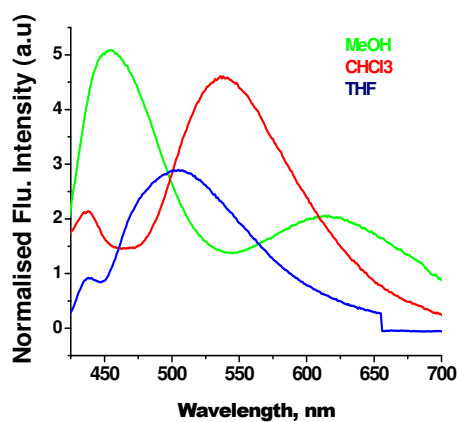
Figure 4.6: *Absorption and emission spectra of the compound 4b in various solvents.*
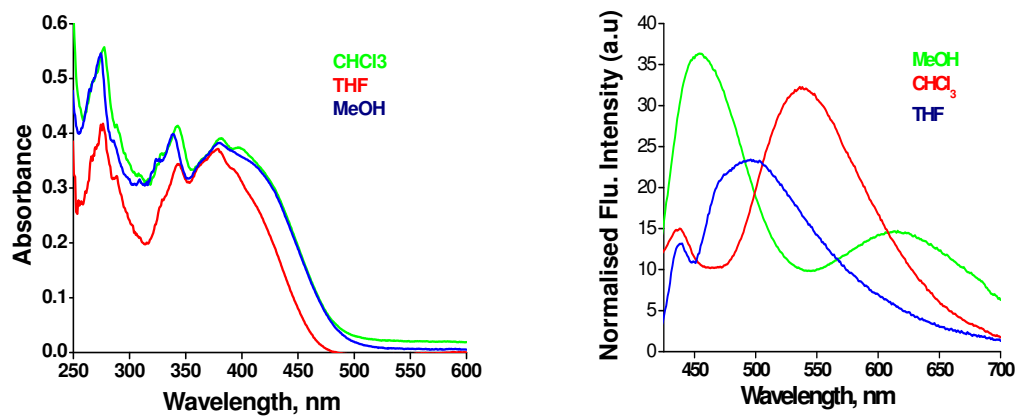

Figure 4.7: *Absorption and emission spectra of the compound 4c in various solvents.*
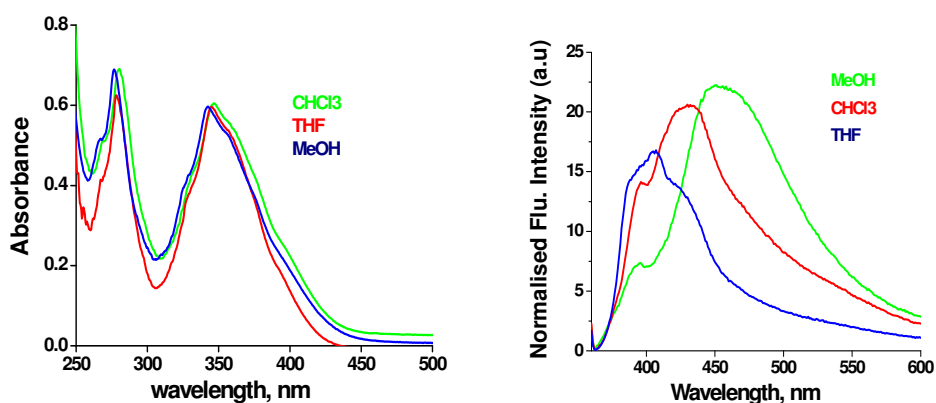

Figure 4.8: *Absorption and emission spectra of the compound 4d in various solvents.*

Interestingly, for **4a-d**, a hypsochromic shift by 45–50 nm of the absorption band in the UV-region was observed by increasing the cycloalkenone ring size. Compound **4a** exhibited simple emission spectrum which was found to be solvent dependent. The peak observed at 531 nm in the fluorescence emission spectrum of compound **4a** showed a red shift of 100 nm with increasing solvent polarity from ethyl acetate to methanol. This wide variation with polarity of solvent may be due to intramolecular charge transfer excited state. But with compound **4b,c** with increasing the solvent polarity from THF to methanol, the first peak remained unchanged in position, but the second peak observed at 503 nm showed a red shift of ~110 nm with increasing solvent polarity. Compound **4d** also showed similar effects, but with substantially reduced red shift. The dual emission of **4b-d** indicates the formation of some extra excited state complexes other than the emitting monomer. As these compounds are found associated in the ground state these excimers can be called as static excimers. The excitation spectra recorded at different emission wavelength for compounds **4a–d** showed spectra identical with the absorption spectra.

The absence of dual fluorescence in the case of **4a** was confirmed through fluorescence lifetime measurement of the sample.

4.3.2.2. Fluorescence Lifetimes

The fluorescence lifetime is one of the most important characteristics of a fluorophore. The lifetime of a fluorophore is the average time between its excitation and return to the ground state and moreover it determines the time available for the fluorophore to interact or diffuse in its environment, and hence the information available from its emission.

In the excited singlet states, the electron in the excited orbital is paired to the second electron in the ground-state orbital. Consequently, return to the ground state is spin allowed and occurs rapidly by emission of a photon. The

emission rates of fluorescence are typically 10^8 s^{-1} so that a typical fluorescence lifetime is of the order of 10 ns (10 X 10^{-9} s). Due to the short time scale of fluorescence, measurement of time-resolved emission requires sophisticated optics and electronics. In spite of the added complexity, time-resolved fluorescence is widely because of the increased information available from the data, as compared with steady-state measurements.

A general property of the fluorescence is that the same fluorescence emission spectrum is generally observed irrespective of the excitation wavelength. This is known as Kasha's rule. An important concept is that the lifetime is a statistical average and the fluorophores emit randomly throughout the decay. The fluorophore do not all emit at a time delay equal to life time. For a large number of fluorophore some will emit quickly following the excitation, and some will emit at times longer that the lifetime. This time distribution of the emitted photons is the intensity decay. The biexponential and triexponential decay of the excited species of these molecule suggest complex processes involved in their deactivation, which could be explained through further mechanistic investigations. The intensity decay of the sample **4a** is shown as a histogram of dots. The height of the dots y-axis represents the number of photons that were detected within the time interval t_k to $t_k + \Delta t$, where Δt is the width of the timing channel.

Fluorescence decay profiles of the sample **4a** in solvents of varying polarity are shown in Figure 4.9. It can be seen that the lifetime increases from **a** to **d.** The monoexponential decay suggests the deactivation process is simple; and also the non-radiative rate is slow. The curve L in the Figure is the instrument response function, i.e. the response of the instrument to a zero lifetime sample. This curve is typically collected using a dilute scattering solution such as colloidal silica (Ludax) and no emission filter. This decay represents the shortest time profile that can be measured by the instrument.
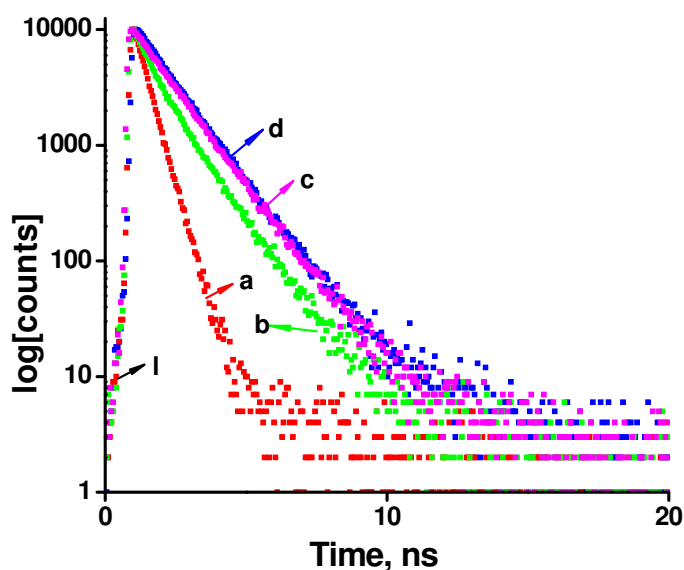
Figure 4.9: *The fluorescence decay profiles of **4a** in (a) MeOH, (b) THF, (c) DMSO, (d) CHCl$_3$. 'l' is the lamp profile.*

4.4. Applications

These bispyrene systems have several potential applications. For example, excitations of above systems are usually associated with increase in dipole moment. The properties of such system depend on solvent polarity, and these can be exploited to determine polarity of unknown solvent mixtures or even find application as "molecular nose".

4.5. Conclusions

(***i***) Effect of the cycloalkanone ring size on the absorption maxima: Absorption spectra of bispyrenes exhibited noticeable dependence on the nature of the cyclic ketone spacer. This noticeable bathochromic shift may be due to reduced interaction between chromophore components present in these molecules. Possible interactions include extended conjugation and exciton coupling as observed for similar bisanthracenes reported in Chapter IV of this thesis. As expected, both **4b** and **4c** exhibited almost identical absorption spectra. These results clearly indicated that the effect of cycloalkanone spacer

on the absorption spectra of bischromophoric systems is universal in nature. However, certain amount of caution should be applied while comparing the structure of bispyrene **4a** with the structure of the corresponding bisanthracenes. Structure of bispyrenes should be compared to those of the corresponding bisnaphthalenes. Restriction for rotation around bond '*a*' in cyclopentanone-linked bischromophoric systems **5, 6** and **4a** (Chart 4.2) is archetypal of bischromophoric systems having similar structural features.
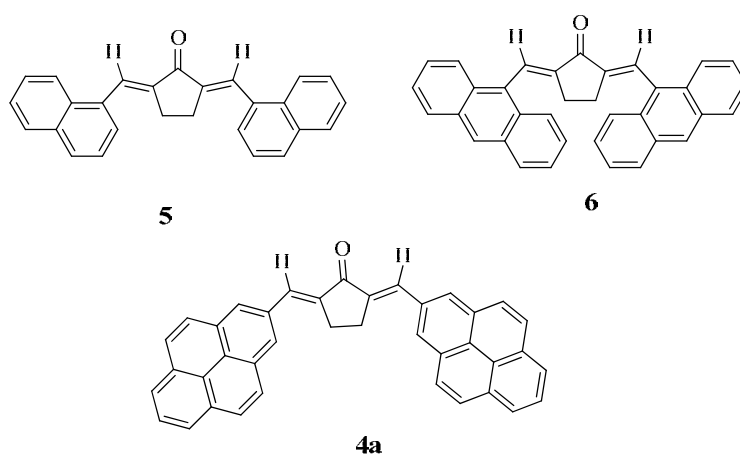

Chart 4.2

In all the three compounds, restricted rotation is observed, but for different reasons. With **5** and **4a**, rotation is restricted due to extended conjugation and resultant partial double bond character of bond '**a**'. With **6**, restricted rotation stems from adverse interaction between anthracene ring and methylene group of the cyclopentanone residue. Thus, extended conjugation between the enone and aromatic chromophores is possible for bispyrenes and bisnaphthalenes whereas bisanthracenes are destined to have a roof-like geometry. Extended conjugation will be reduced in the case of compounds having cyclohexanone spacer and completely absent for compounds having cyclooctanone spacer – here the carbonyl group is almost orthogonal to the π-system present in them. Consequently, a) substantial solvent effect on

absorption maxima is anticipated for a bispyrene having cyclopentanone spacer, b) reduced solvent effect is expected for bispyrene having cyclohexanone spacer, and c) no solvent effect should be exhibited by a bispyrene having cyclooctanone spacer. This is borne out by experiment.

(ii) Dependence of emission characteristics of bispyrenes having cycloalkanone spacers confirmed the conclusions regarding the bisanthracenes on the effect of cycloalkanone ring size on geometry and photophysical behaviour of bisaromatic compounds. Fluorescence emission studies and lifetime studies of **4a** confirmed its highly conjugated single excited state. Increasing ring size of spacer from cyclopentanone to cyclooctanone greatly affected the properties of bispyrene systems.

(iii) Solvatochromic shifts of pyrene excimer fluorescence were obtained in both polar and non-polar solvents. The observed shifts were explained in terms of solute-solvent dispersion interactions, a solute transition dipole moment term and the *solvent stark effect* (for polar solvents). The observed shifts are due to changes in the polarizability between the excimer and the dissociative ground state. The magnitudes of the shifts in the pyrene excimer are larger, indicating that the pyrene excimer is more polarizable.

(iv) Solvent dependent shift in the fluorescence spectra can be attributed to factors such as:

(1) dipole-dipole interaction between solvent and solute

(2) change in the nature of emitting state induced by solvent

(3) Specific solvent-solute interactions such as H-bonding.

Solvatochromic methods have been used to probe a wide range of chemical systems with good success. Application to an even broader range of systems can be anticipated. While the original investigators developed the approaches assuming that the indicator-dye surroundings consisted of a homogeneous solvent, an increasing number of applications are being reported for heterogeneous systems such as surfaces and organized media. While these systems may not meet the requirement of the ideal 'reaction field' described

by theory, they can still provide a wealth of information about these microenvironments. New opportunities will result from design and synthesis of specific probes for specific chemical systems and the adaptation of these macroscopic approaches for studying microscopic and nanoscopic systems, where the effects of these environments on the nature of the indicator dye absorption process will need to be reconsidered. All in all, there is a bright future for this 'colourful' field.

4.6. Experimental Section

4.6.1. General Techniques

General information about the experiments is given in section **2.5.1** of Chapter **2**. Recrystallization was done by slow evaporation method from a 1:2 mixture of chloroform-methanol at room temperature. Absorption and emission spectra were recorded at 25 ^{o}C in a 1 cm quartz cuvette. Absorption spectra were measured using Shimadzu-3101PC UV/Vis/NIR scanning spectrophotometer. Emission spectra were recorded on a SPEX Fluorolog F112X Spectrofluorimeter. HPLC grade solvents were used for all photophysical experiments. All fluorescence spectra were corrected for detector response. Fluorescence lifetimes were measured using IBH (FluoroCube) time-correlated picoseconds single photon counting (TCSPC) system. Solutions were excited with a pulsed diode laser (<100 ps pulse duration) at a wavelength of 375nm (NanoLED-11) with a repetition rate of 1 MHz. The detection system consisted of a microchannel plate photomultiplier (5000U-09B, Hamamatsu) with a 38.6 ps response time coupled to a monochromator (5000 M) and TCSPC electronics [Data station Hub including Hub-NL, NanoLED controller and preinstalled Fluorescence Measurement and Analysis Studio (FMAS) Software].

4.6.2. Materials

Cyclopentanone, cyclohexanone, *t*-butylcyclohexanone, cyclooctanone were purchased from Sigma-Aldrich and used as received.   Solvents were purchased from S. D. Fine Chem. Ltd. and were purified by distillation as per required.

4.6.3. Preparation of 2,5-Dipyrenilidenecycloalkanones, 4a-d

4.6.3.1. Synthesis of (2*E*,5*E*)-2,5-bis(pyren-2-ylmethyl-ene)cyclopentanone (4a)

The method of synthesis and characterization of **4a** is given in Chapter **2** in detail.

4.6.3.2. Synthesis of (2*E*,6*E*)-2,6-bis(pyren-2-ylmethy-lene)cyclohexanone (4b)

To a mixture of cyclohexanone (0.43 g, 4.4 mmol) and 1-pyrenecarboxaldehyde (2.02 g, 8.8 mmol) in methanol (25 mL) taken in a 100 mL conical flask, sodium hydroxide pellets (0.49 g, 8.8 mmol) was added and the reaction mixture was stirred at room temperature for 15 min whilst a yellow product precipitated out. The mixture was heated in a hot water bath at 60 ^{o}C for 6 h, until an appreciable amount of solid formed. The flask was then cooled in an ice chest and the precipitate that separated out was collected by vacuum filtration. The crude product was washed several times with ice-cold 1 mL portions of ethanol. The product was further purified by recrystallization from a mixture (1:2) of methanol and chloroform to give **4b**. The product separated was collected by vacuum filtration and air-dried to yield material of good quality.

Yellow Powder, Yield 80%; mp > 300 °C

UV λ_{max} (CH$_2$Cl$_2$) 260 (ε 65,900), 350 (ε 14,900), 380 (ε 30,900), 410 (ε 31,600);

IR (KBr) ν_{max} : 1658, 1593, 1160, 988, 645 cm^{-1}.;
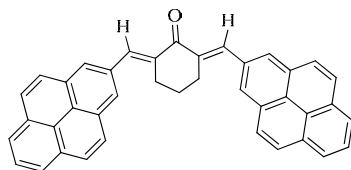
^{1}H NMR (300 MHz, CDCl$_3$) : δ 8.75 (s, 2H), 8.44-7.88 (m, 18H), 2.93-2.65 (m, 4H), 1.77-1.75 (m, 2H);

MS (FAB, [M$^+$+1]): Calcd for C$_{40}$H$_{26}$O: 522.19. Found: 523.19;

Elemental analysis calculated for C$_{40}$H$_{26}$O: C, 91.92; H, 5.01; O, 3.06. Found: C, 91.82; H, 5.03; O, 3.09.

4.6.3.3. Synthesis of (2*E*,6*E*)-4-tert-butyl-2,6-bis(pyren-2-ylmethylene)cyclohexanone (4c)
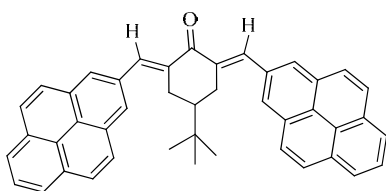
To a mixture of *t*-butylcyclohexanone (0.67 g, 4.4 mmol) and 1-pyrenecarboxaldehyde (2.01 g, 8.7 mmol) in methanol (25 mL) taken in a 100 mL conical flask, potassium hydroxide pellets (0.50 g, 8.7 mmol) was added and the reaction mixture was stirred at room temperature for 15 min whilst a yellow product precipitated out. The mixture was heated in a hot water bath at 60 °C for 6 h, until an appreciable amount of solid formed. The flask was then cooled in an ice chest and the precipitate that separated out was collected by vacuum filtration. The crude product was washed several times with ice-cold 1 mL portions of ethanol. The product was further purified by recrystallization from a mixture (1:2) of methanol and chloroform to give **4c**. The product separated was collected by vacuum filtration and air-dried to yield material of good quality.

Yellow Powder, Yield 82%; mp > 300 °C

UV λ_{max} (CH$_2$Cl$_2$) 260 (ε 65,900), 350 (ε 14,900), 380 (ε 30,900), 410 (ε 31,600);

IR (KBr) ν_{max} : 1662, 1595, 1098, 750 cm^{-1}.;

^{1}H NMR (300 MHz, CDCl$_3$) : δ 8.62 (s, 2H), 8.45 (s, 2H), 8.11-8.02 (m, 8H), 7.51-7.49 (m, 8H), 2.42-2.37 (m, 2H), 2.04-1.99 (m, 2H), 1.62-1.60 (m, 1H), 0.75 (s, 9H);

**MS** (FAB, [M$^+$+1]): Calcd for C$_{44}$H$_{34}$O: 578.26. Found: 579.36;

Elemental analysis calculated for C$_{44}$H$_{34}$O: C, 91.31; H, 5.92; O, 2.76. Found: C, 91.34; H, 5.85; O, 2.78.

4.6.3.4. Synthesis of (*2E,8E*)-2,8-bis(pyren-2-ylmethylene) cyclooctanone (4d)

To a mixture of cyclooctanone (0.60 g, 4.8 mmol) and 1-pyrenecarboxaldehyde (2.19 g, 9.5 mmol) in methanol (25 mL) taken in a 100 mL conical flask, sodium hydroxide pellets (0.53 g, 9.5 mmol) was added and the reaction mixture was stirred at room temperature for 15 min whilst a yellow product precipitated out. The mixture was heated in a hot water bath at 60 °C for 12 h, until an appreciable amount of solid formed. The flask was then cooled in an ice chest and the precipitate that separated out was collected by vacuum filtration. The crude product was washed several times with ice-cold 1 mL portions of ethanol. The product was further purified by recrystallization from a mixture (1:2) of methanol and chloroform to give **4d**.

The product separated was collected by vacuum filtration and air-dried to yield material of good quality.
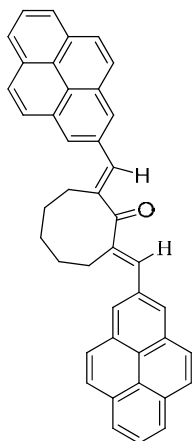
Yellow powder, Yield 75%; mp > 300 °C

UV λ_{max} (CH$_2$Cl$_2$) 260 (ε 65,900), 350 (ε 14,900), 380 (ε 30,900), 410 (ε 31,600);

IR (KBr) ν_{max} : 1668, 1592 ,1123, 756 cm^{-1};

^{1}H NMR (300 MHz, CDCl$_3$) : δ 8.24 (s, 1H), 8.22 (s, 1H), 8.14-8.10 (m, 5H), 8.08-8.05 (m, 3H), 8.02-7.97 (m, 4H), 7.95-7.91 (m, 4H), 7.87 (s, 2H), 2.81-2.79 (m, 4H), 2.74-2.72 (m, 4H), 1.67-1.55 (m, 2H);

MS (FAB, [M$^+$+1]): Calcd for C$_{42}$H$_{30}$O: 550.22. Found: 551.33;

Elemental analysis calculated for C$_{42}$H$_{30}$O: C, 91.61; H, 5.49; O, 2.91. Found: C, 91.50; H, 5.39; O, 2.94.

4.6.4. General Procedure for Photophysical Studies

Bispyrene **4a-d** (0.00101 g) were dissolved in DCM (10 mL). Then 50 μL portions of the mother solution were made up to 3 mL with corresponding solvents. These solutions were used for absorption, emission and life-time studies.

4.6.4.1. Fluorescence Lifetime Measurements

Fluorescence decay measurements of the sample **4a** were carried out using the time correlated single photon counting technique (TCSPC) with micro channel plate photomultiplier tube (MCP-PMT) as detector and picosecond laser as excitation source.

4.7. References

1.   Reichardt, C. *Solvents and Solvent Effects in Organic Chemistry,* VCH, Weinhem, 2nd ed. , **1988**.

2 .   Brady, J. E.; Carr, P. W. *J. Phys. Chem.* **1985**, *89,* 5759.

3 .   Ortega, J.; Rafols, C.; Bosch, E.; Roses, M. *J. Chem. Soc., Perkin Trans. 2* **1996**, 1497. (b) Buhvestov, U.; Rived, F.; Rafols, C.; Bosch, E.; Roses, M. *J. Phys. Org. Chem.* **1998,** *11,* 185. (c) Herodes, K.; Leito, I.; Koppel, I.; Roses, M.; *J. Phys. Org. Chem.* **1999,** *12,* 109. (d) Cheong, W. J.; Carr, P. W. *Anal. Chem.* **1988**, *60,* 820. (e) Krygowski, T. M.; Wrona, P. K.; Zielkowska, U. *Tetrahedron* **1985,** *41,* 4519. (f) Cattana, R.; Silber, J. J.; Anunziata, J. *Can. J. Chem.* **1992,** *70,* 2677. (g) Nigam, S.; Juan, A. de.; Stubbs, R. J.; Rutan, S. C. *Anal. Chem.* **2000,** *72,* 1956.

4 .   Lindley, S. M.; Flowers, G. C.; Leffler, J. E. *J. Org. Chem.* **1985**, *50,* 607. (b) Li, Z.;. Rutan, S. C. *Anal. Chim. Acta* **1995,** *312,* 127.

5 .   Handreck, G. P.; Smith, T. D. *J. Chem. Soc., Faraday Trans. 1 ,* **1988,** *84,* 1847.

6 .   Michels, J. J.; Dorsey, J. G. *Langmuir* **1990,** *6,* 414.

7.   (a) Jones, J.; Rutan, S. C. *Anal. Chem.* **1991**, *63,* 1318. (b) Men, Y.-D.; Marshall, D. B. *Anal. Chem.* **1990**, *62,* 2606. (c) Lu, H.; Rutan, S. C. *Anal. Chem.* **1996,** *68,* 1387. (d) Lu, H.; Rutan, S. *Anal. Chim. Acta.* **1999***, 388,* 345. (e) Spange, S.; Reuter, A.; Vilsmeir, E. *Colloid Polym. Sci.* **1996,** *274,* 59. (f) Kosmulski, M. *J. Coll. Interf. Sci.* **1996,** *179,* 128. (g) Bartels, M. J.; Koeberg, M.; Verhoeven, J. W. *Eur. J. Org. Chem.* **1999,** 2391. (h) Spange, S.; Vilsmeir, E.; Zimmermann, Y. *J. Phys. Chem. B,* **2000***, 104,* 6417. (i) Nigam, S.; Juan, A. de.; Cui, V.; Rutan, S. C. *Anal. Chem.* **1999***, 71,* 5225. (j) Nigam, S.; Juan, A. de.; Stephens, M.; Rutan, S. C. *Anal. Chem.* **2001,** *73,* 290.

8.   (a) Biswas, R.; Lewis, J. E.; Maroncelli, M. *Chem. Phys. Lett.* **1999,** *310,* 485. (b) Egorov, S. A. *J. Chem. Phys.* **2000**,*113,* 1950. (c) Lemert, R. M.; DeSimone, J. M. *J. Supercritical Fluids.* **1991***, 4,* 186. (d) Yonker, C. R.; Smith, R. D. *J. Phys. Chem.* **1988***, 92,* 2374.

9.   Bentley, T. W.; Llewellyn, G. *Progr. Phys. Org. Chem.* **1990***, 17,* 121.

10.   (a) Buncel, E.; Rajagopal, S. *Acc. Chem. Res.* **1990***, 23,* 226. (b) Taft, R. W.; Abboud, J. L. M.; Kamlet, M. J.; Abraham, M. H. *J. Sol. Chem.* **1985***, 14,* 153.

11.   Reichardt, C. *Leibigs Ann. Chem.* **1969***, 727,* 93.

12.   (a) Cecil, T. L.; Rutan, S. C. *Anal. Chem.* **1990***, 62,* 1998. (b) Lakowicz, J. R. *Principles of Fluorescence Spectroscopy,* Kluwer Academic/ Plenum, New York, **1999**, 2nd ed.

13.   Dong, D. C.; Winnik, M. A. *Can. J. Chem*. **1984,** *62,* 2560.

14.   Acree, W. E.; Tucker, S. A.; Fetzer, J. C. *Polycyclic Aromat. Compd.* **1991***, 2,* 75.

15.   (a) Claisen, L.; Claparede, A. *Ber.* **1881**, *14,* 2460. (b) Schmidt, J. G. *Ber*. **1881**, *14,* 1459. (c) Bhagat, S.; Sharma, R.; Chakrabarti, A. K. *J. Mol. Cat. A* **2006***, 260*, 235. (d) Russel, A.; Happoldt, W. B. Jr. *J. Am. Chem. Soc*. **1942**, *64*, 1101.

SYNTHESIS OF A FEW BISDIBENZOBARRELENE SYSTEMS

5.1. Abstract

This chapter deals with the photochemical studies of bisdibenzobarrelenes, we have synthesised. Dibenzocyclooctatetraene and dibenzosemibullvalene are the photoproducts obtained respectively through the singlet excited state and triplet excited state of dibenzobarrelenes. Dibenzobarrelene having alkenone appendage at the 9-position are also found to undergo condition-dependent photochemical rearrangements. So, examining the photochemical behavior of novel bisdibenzobarrelenes with alkenone spacer is interesting. Our attempts and results are explained in this chapter. This chapter can also be considered as an extension to our studies on effects on geometry of photochemical and photophysical behaviour of bischromophoric systems having tunable geometry.

5.2. Introduction

The [4+2] cycloaddition between a conjugated diene and a alkene commonly termed the dienophile, to form a cyclohexene system is more commonly known as the *Diels-Alder reaction,* named after O. Diels and K. Alder, who shared the 1950 Nobel Prize in chemistry for developing this reaction. This reaction occupies a very important place among the tools of the synthetic organic chemist because it provides a method for the construction of six membered rings from acyclic precursors with excellent control of

stereochemistry. Diels-Alder reaction[1] is one of the major synthetic strategies employed to generate bicyclic compounds. Bicyclic compounds[2] have gained much importance in the recent past since they constitute the basic structural frame work of several compounds which are used as potential therapeutic agent against HIV and metastasis,[3] anticancer drugs,[4] anti-thrombotic compounds,[5] therapeutic agents for diseases of the central nervous system, and so on.

Anthracene can undergo both thermal and photochemical Diels–Alder cycloadditions with a variety of dienophiles across the 9 and 10 positions due to the electron rich nature at these positions. The types of dienophile used in the Diels–Alder reactions of anthracene fall broadly into four classes, namely

- (i)   α,β unsaturated carbonyls,
- (ii)   alkenes attached to a heteroatom or halogen,
- (iii) alkenes and alkynes and
- (iv)   heterodienophiles.

The first reported cycloaddition of a dienophile, the reaction of maleic anhydride **2**, to anthracene **1** *via* a fusion reaction to give **3** at 260 °C was by Diels and Alder in 1931 (Scheme 5.1).[6]

1   **2**   **3**
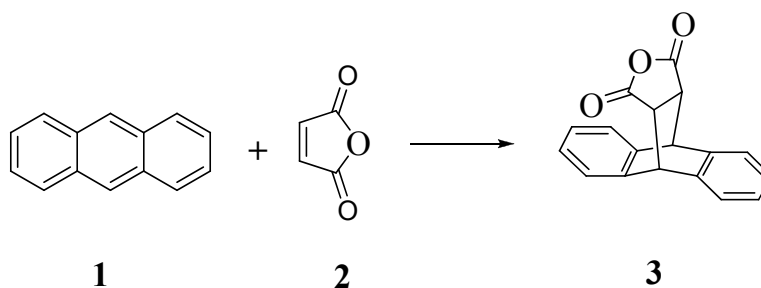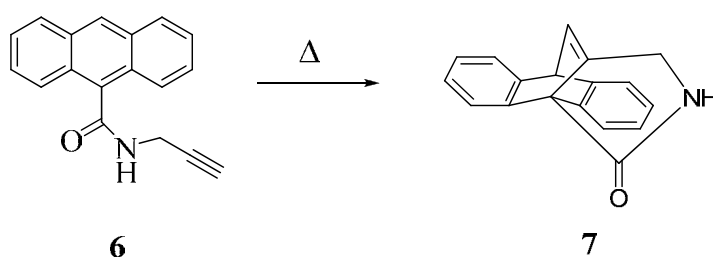
Scheme 5.1

The reaction can proceed even if some of the atoms in the newly-formed ring are not carbon. If diene or dienophile contains one or more heteroatoms, then Diels-Alder adduct formed will be a heterocyclic system. Such Diels-Alder reactions are then called as **Hetero-Diels Alder reactions**

(Scheme 5.2).[7] The hetero Diels–Alder reaction of anthracene has been used to 'trap' unstable transient compounds as stable cycloadducts.
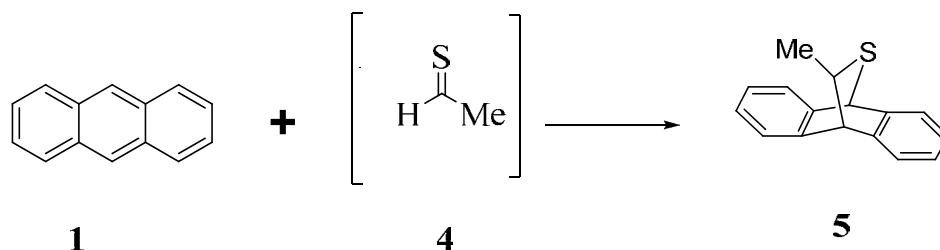
Scheme 5.2

Diels-Alder reaction can take place within a molecule if the two reacting functionalities are within the same molecule. Such Diels–Alder reactions are called **intramolecular Diels–Alder (IMDA) cycloadditions**. This exhibits less negative entropies of activation and so reaction rates will be higher under mild conditions. The intramolecular Diels–Alder cycloadditions of the 'tethered' alkynes **6** to yield a wide variety of 9,12-bridged ethenoanthracenes **7** has been performed at temperatures ranging from 25 to 220 $^\circ$C (Scheme 5.3).[8]
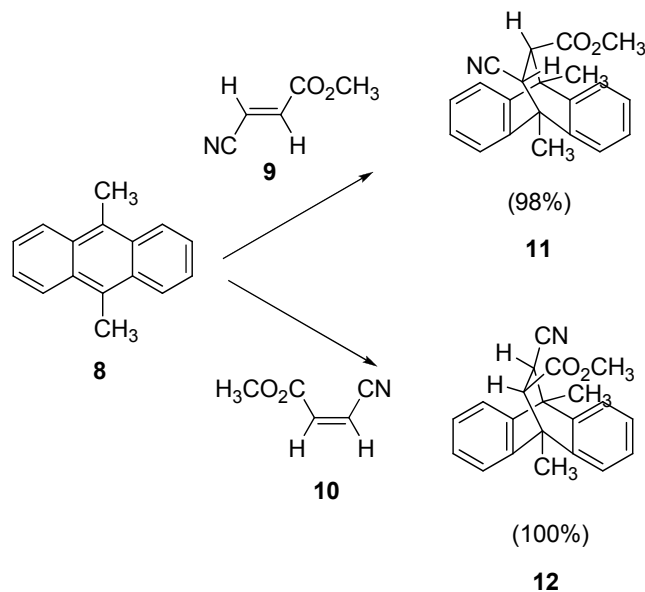

Scheme 5.3

5.2.1. Stereochemistry of the Reaction

Diels-Alder reactions can lead to formation of a variety of structural isomers and stereoisomers (enantiomers and diastereomers). Stereochemistry of Diels-Alder adducts depends on *"cis principle"* or *"endo addition rule"*.[9]

5.2.1.1. *Cis* principle

According to the ***cis* principle** or the **Alder-Stein rules** formulated by Alder and Stein in 1937, the stereochemistry of substituents in the starting material is retained in the product. This means that if a *cis*-dienophile is reacted, both of the *cis*-substituents will end up on same side (face) of the product ring. *Trans*-dienophile will yield a product where both of *trans*-substituents (that came originally from the dienophile) will be on different sides of the product ring. The same principle applies to dienes. *Trans*, *trans* or *cis*, *cis* 1,4-substituents will end up on same side of the ring, whereas *trans*, *cis* 1,4-substituents will be oriented towards different faces of the ring. An illustrative example is shown for the reactions of the isomeric methyl β-cyanoacrylates **9** and **10** with 9,10-dimethylanthracene **8** (Scheme 5.4).[10]

Scheme 5.4

5.2.1.2. *Endo* addition rule

Using the *'cis principle'* it is understood that *cis*-substituents on dienophile, for example, will end up on same side of the molecule. It is not obvious where the substituents on both diene and dienophile will end up

relative to each other. To predict the *cis* or *trans* orientation of substituents that are coming from different molecules we have to examine possible transition states. The most stable transition state will lead to the major product. Transition states will also dictate the relative orientation of the diene's and dienophile's substituents on the product ring. In some cases another rule can be applied: the endo addition rule. According to this rule, the most stable transition state results when there is a 'maximum accumulation of double bonds'. This rule is not always followed. It most often applies when dealing with cyclic dienes and dienophiles. For example, the Diels-Alder reaction of cyclopentadiene and maleic anhydride yields over 95% of the *endo* product. It is important to note that labels "*exo*" and "*endo*" relate to the orientation of substituents in the transition state and not to a specific orientation of substituents in the product molecule. In each individual case, the transition state has to be examined to see the most favored relative orientation of substituents. It is not true for the *endo* transition state that the substituents on dienophile and 1,4-substituents on diene will always point towards the same side of the newly formed ring. "*Endo*" and "*exo*" define specific transition states, not orientation of substituents. In the case of maleic anhydride and cyclopentadiene the endo product will have the R groups of the diene and dienophile oriented toward the opposite sides of the newly formed ring. IMDA cyclization of a 9-substituted anthracene derivative reported by Meek and Dann who obtained the cyclic acetal **13** (Figure 5.1) in 2% yield on attempted preparation of 9-anthraldehyde diallyl acetal is an example of endo addition.[11]
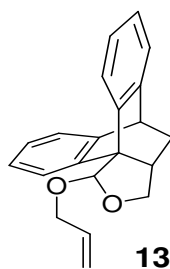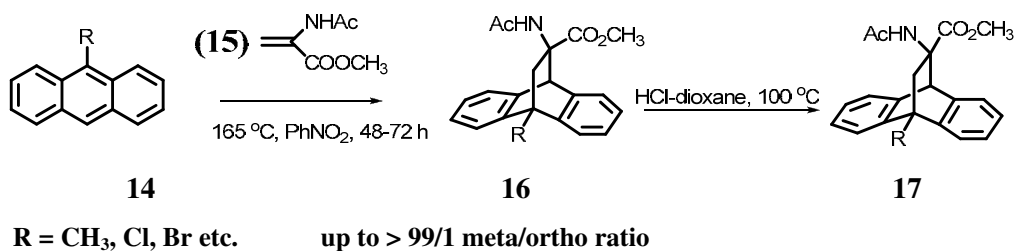

13

Figure 5.1

5.2.2. Regioselectivity of the Reaction

Synthesis of conformationally constrained bicyclic bisaryl α-amino acids, from 9-substituted anthracenes and 2-acetamidoacrylate is an example for regio-selective Diels–Alder reaction (Scheme 5.5).


R = CH₃, Cl, Br etc.   **up to > 99/1 meta/ortho ratio**

Scheme 5.5

Thus, a variety of dibenzobarrelenes can be synthesized by the Diels-Alder reaction between suitably substituted anthracenes and reactive acetylenes. IMDA reactions add a whole new dimension to the variety of multicyclic systems that be generated from anthracene derivatives. Our group is actively interested in the generation of barrelene derivatives by Diels Alder reactions. Our primary interest is in examining intramolecular quenching of barrelene excited state and deciphering factors controlling regioselectivity in barrelene-semibullvalene rearrangement. Hence, a brief overview of the diverse photochemistry of barrelenes is deemed appropriate here.

## 5.3. An Overview on the Photochemistry of Dibenzo-barrelenes

Zimmerman and co-workers[12] have shown that barrelene **18** which contains π moieties within rigidly structured environments, rearranges by the di-π-methane pathway to semibullvalene **18** solely by acetone sensitization. The triplet excited states of bicyclic systems are incapable of "free rotor" energy dissipation due to their rigid structures, thus paving way for the

conversion of the triplets to π-substituted cyclopropanes. The singlet excited states of many cyclic systems have potentially available facile alternative pericyclic processes which compete with di-π-methane rearrangement. Direct irradiation of barrelene **19** leads to cyclooctatetraene **20** by an electrocyclic [2π + 2π] addition followed by a retro [2π + 2π] fission (Scheme 5.6).
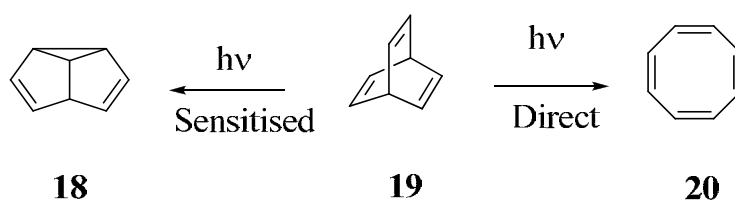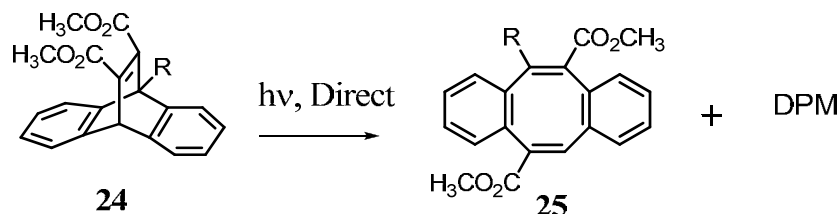

Scheme 5.6

The solution phase photochemistry of 9,10-ethenoanthracene **21** is multiplicity-dependent. Irradiation of dibenzobarrelenes **22** in the presence of triplet sensitizers leads to dibenzosemibullvalene **21**,[13] whereas direct irradiation (i.e., irradiation in the absence of triplet sensitizers) affords mainly dibenzocyclooctatetraene **23** (Scheme 5.7)[14]
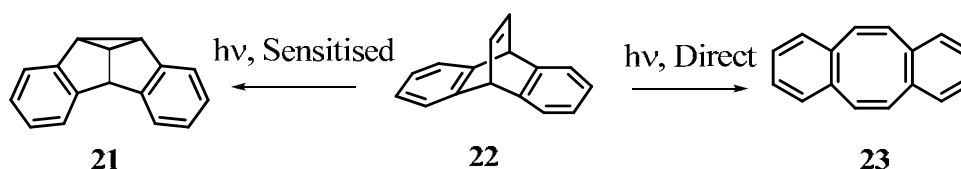
Scheme 5.7

Earlier studies have shown that direct irradiation of 9,10-ethenoanthracene derivatives **24**, which have ester substituents attached to vinyl double bond, leads to triplet (di-π–methane or more appropriately tri-π-methane in this case) reactivity, a result that is presumably due to rapid

intersystem crossing of the initially formed singlet excited state (Scheme 5.8).[15]

Scheme 5.8

5.3.1. Regioselectivity Exhibited by Dibenzobarrelenes

The photochemical studies conducted on several dibenzobarrelenes by Ciganek[13] and Friedman[16] indicated that electronic effects are important in determining the course of initial bonding in di-π-methane (DPM) rearrangement.

Iwamura *et al.* have shown that substituents at the methane position on the bridging position determine the bridging selectivity in di-π-methane systems. There exists two possible competitive vinyl-benzo bridging in the triplet excited states (Scheme 5.9).[17]

$(E = CO_2CH_3)$

$(R = CN, CO_2CH_3, CHO, OCH_3)$
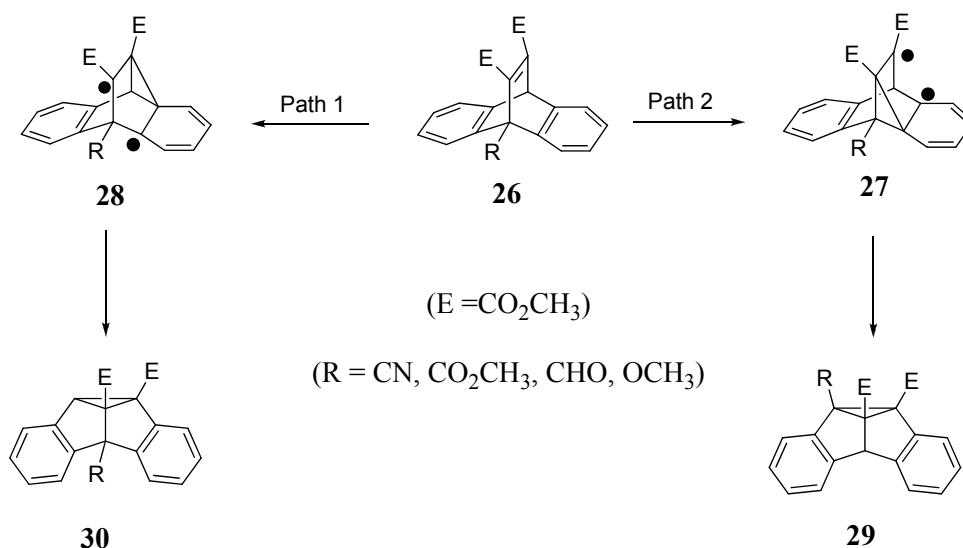
Scheme 5.9

π-Electron accepting substituents such as CN, CO_2CH_3 and CHO at the bridgehead position should stabilize the cyclopropane ring, favours bridging through path 1, while π-electron donors such as OCH_3 should destabilize the cyclopropane ring favour path 2.

Richards *et al*. have shown that bridgehead hydroxy- and acetoxy-dibenzobarrelene have hydrogen bonding and electronegativity effects in forming the product. Irradiation products of hydroxydibenzobarrelene and acetoxy-dibenzobarrelene are given in Scheme 5.10.[18] These results were further supported by the findings by George *et al*.[21c] Thus steric effects as well as electronic effect of bridgehead substituents determine the photoproduct of dibenzobarrelene.
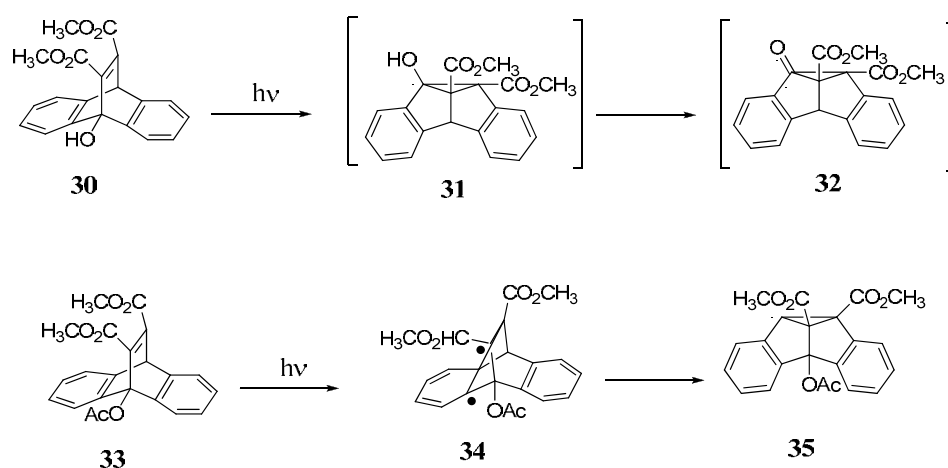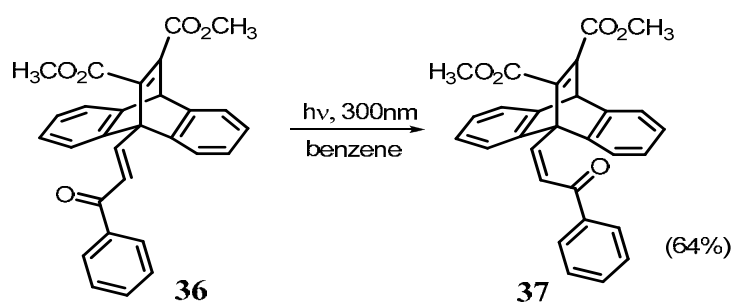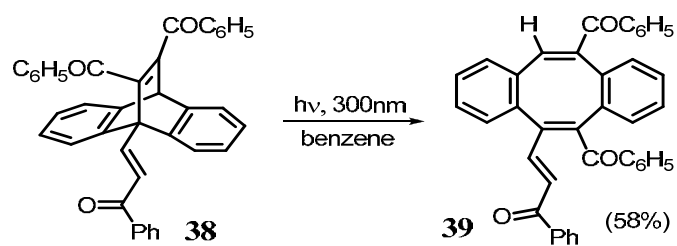

Scheme 5.10

Thus steric effects as well as electronic effect of bridgehead substituents determine the photoproduct of dibenzobarrelene.

5.3.2. Photochemistry of Enone-appended Barrelenes

On irradiation, dimethyl 9-(1-phenylprop-2-en-1-one)-9,10-dihydro-9,10-ethenoanthracene-11,12-dicarboxylate, **36** is found to undergo *cis-trans*

isomerization (*Case I*, Scheme 5.11), while 11,12-dibenzoyl-9-(1-phenylprop-2-en-1-one)-9,10-dihydro-9,10-ethenoanthracene,   **38**   underwent   DPM rearrangement to give dibenzocyclooctatetraene derivative (*Case II*, Scheme 5.11).

Case I

Case II
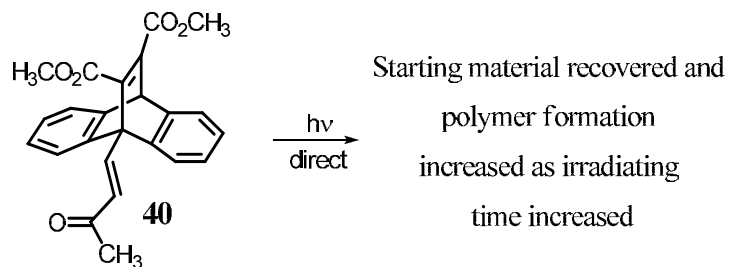
Case III
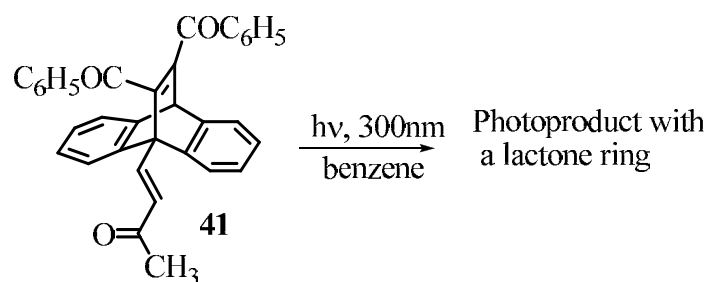
Case IV

Scheme 5.11

Irradiation of dimethyl 9-(1-methylprop-2-en-1-one)-9,10-dihydro-9,10-ethenoanthracene-11,12-dicarboxylate, **36** gave starting material unchanged (*Case III*, Scheme 5.11), while barrelene having benzoyl group at the 11,12 positions underwent rearrangement to give an unidentified lactone (*Case IV*, Scheme 5.11).

All the above interesting photochemistry prompted us for the synthesis of enone appended bisdibenzobarrelenes (Chart 5.I).

5.4. Results and Discussion

For the synthesis of dibenzobarrelenes several methods were described in the literature. Paquette *et al*. synthesized dimethyl 9-deuterio-9,10-dihydro-9,10-ethenoanthracene-11,12-dicarboxylate **44**, through neat reaction of anthracene-*9-d* **42** and dimethyl acetylenedicarboxylate (DMAD) **43** at 180 °C, in appreciable yield (Scheme 5.12).[19]
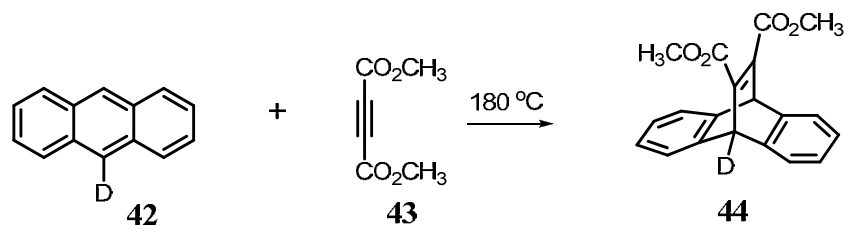
Scheme 5.12

Richards *et al.* prepared a series of 9-substitued dimethyl 9,10-dihydro-9,10-ethenoanthracene-11,12-dicarboxylates **46a-f,** by refluxing a solution of the appropriate 9-substituted anthracene **45** and dimethyl acetylenedicarboxylate **43** in a suitable solvent[20] (Scheme 5.13).

X = a) Br, b) OCH$_3$, c) OC$_2$H$_5$, d) NH$_2$, e) NHAc, f) CH$_3$
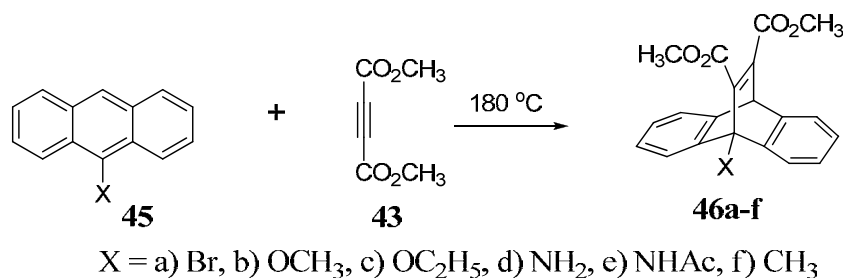
Scheme 5.13

George *et al.* prepared several 11,12-dibenzoyl substituted dibenzobarrelenes, through the Diels-Alder addition of appropriately substituted anthracenes **47** with dibenzoylacetylene (DBA) **48**, either thermally or in the presence of Lewis acid catalysts such as aluminium chloride.[21] Depending on the substituents and reaction conditions, the reaction yields either 11,12-dibenzoyl-substituted dibenzobarrelene **49** or a mixture of **49** and dibenzoyl-substituted naphthobarrelene **50** (formed through addition across the 1,4 positions of anthracene)[22] (Scheme 5.14).
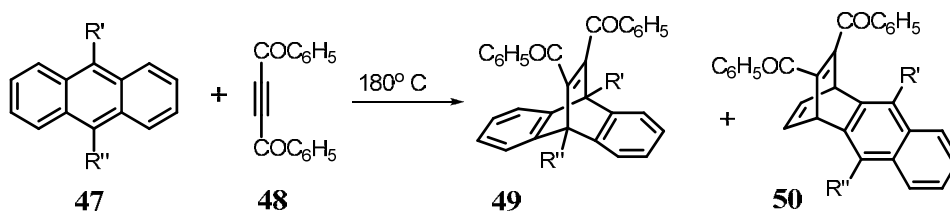
Scheme 5.14

So, by employing Diels–Alder reactions of bisanthracenes as dienes and dimethyl acetylenedicarboxylate (DMAD) and dibenzoylacetylene (DBA)

as dienophiles we have synthesized a few bisdibenzobarrelenes, **51a-f**.   The
dibenzobarrelenes synthesized by us are given in Chart 5.I.

5.4.1. Synthesis and Characterization

5.4.1.1. Diels-Alder Reaction of Bisanthracenes (51a-e) with Dimethyl Acetylenedicarboxylate (DMAD)

The bisdibenzobarrelenes **51a-e** were synthesized *via* Diels-Alder
reaction of the bisanthracenes **52a-e** with the dienophile DMAD (**43,** excess)
in dry xylene under reflux.   The bisadducts were formed in appreciable yield
accompanied by polymerisation of DMAD (Scheme 5.15).
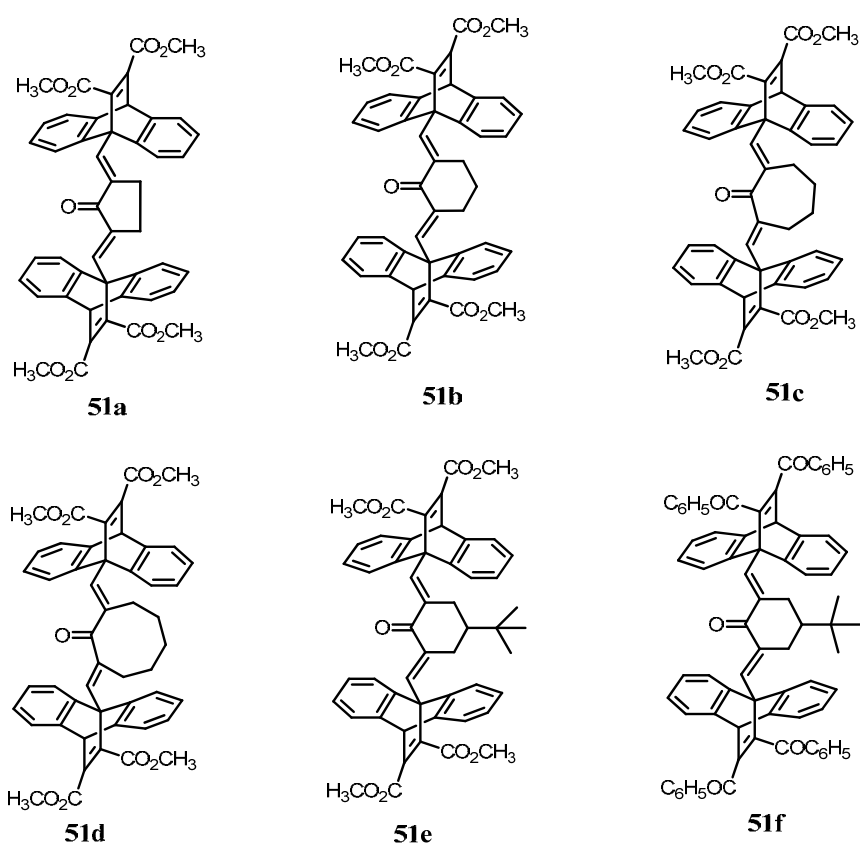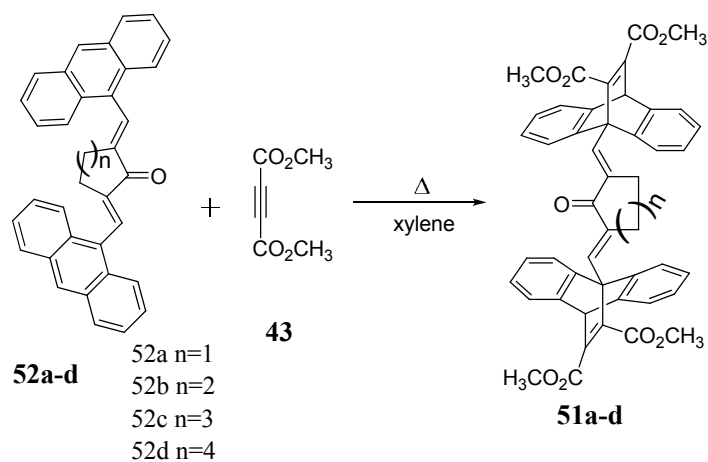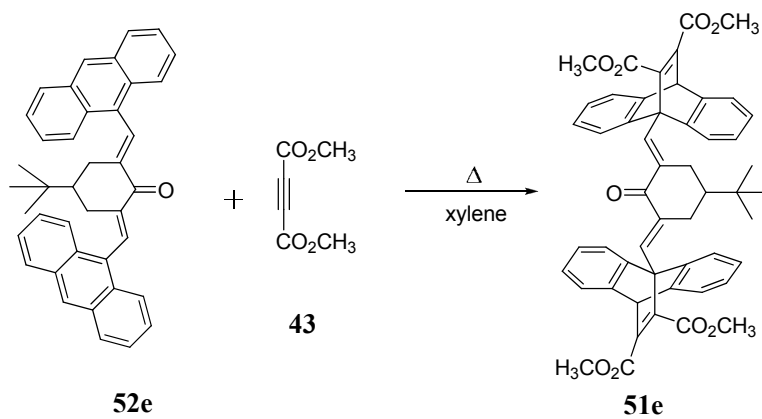

Chart 5.I

Scheme 5.15

The poor solubility of **51a-d** led us to the preparation of potentially more soluble analogues **51e** (Scheme 5.16) and **51f** (Scheme 5.17).

Scheme 5.16

The structures of the bisbarrelenes **51a-e** were established through the comparison of their spectral data with that of monodibenzobarrelenes and *via* analytical data.

The product **51a** was identified as the [4+2] biscycloadduct between bisanthracene **52a** and two DMAD units, where the anthracene moieties functioned as the dienes, by spectroscopic methods. The IR spectrum showed strong carbonyl absorption at 1728 cm^{-1} and a shoulder peak at 1684 cm^{-1}, which were assigned to the ester carbonyls and ring carbonyl respectively. The ^{1}H NMR spectrum of **51a** provided clear indications of the formation of a symmetrical cycloadduct. The salient features of the spectrum pointing towards this were (a) the appearance of aliphatic protons as singlet at δ 2.44, (b) the methoxy groups of DMAD part as two singlets at δ 3.77 and 3.83, (c) appearance of bridgehead proton as singlet at δ 5.68 and (d) appearance of aromatic protons and a vinylic proton as multiplet from δ 7.06 to δ 7.72. The salient features of the ^{13}C NMR spectrum include the peaks at (a) δ 27.7 and 28.8 which were assigned to the bridging methylene carbon and aliphatic carbon, (b) δ 50.9 due to the quaternary carbons, (c) δ 52.2 and 52.9 corresponding to the two methoxy carbons, (d) δ 167.2 and 163.8 due to the two ester carbonyl groups and (e) δ 194.4 due to the cyclopentanone carbonyl carbon respectively. The proposed structure was further supported by the FAB mass spectrum which showed the [M$^+$+1] ion peak at 745.36 and satisfactory elemental analysis.

Similarly, the IR spectrum of **51b** showed strong carbonyl absorption at 1729 cm^{-1} and a shoulder peak at 1683 cm^{-1}, which were assigned to the ester carbonyls and ring carbonyl respectively. In the ^{1}H NMR spectrum, the multiplet from δ 1.67 to δ 1.62 indicates the two geminal hydrogens at the 4-position of cyclohexanone moiety. The four geminal hydrogens at 3 and 5 positions appear as multiplet from δ 2.37 to δ 2.34. The singlets at δ 3.76 and δ 3.90 depicts the methoxy protons. The bridgehead proton appears as singlet at δ 5.68. The aromatic protons and a vinylic proton appear as multiplet from δ 7.06 to δ 7.46. In the ^{13}C NMR spectrum, the saturated carbons of cyclohexanone moiety appear at δ 28.7 and at δ 31.3. The signals of methoxy

carbon appear at δ 51.0 and δ 51.9. The two bridgehead carbons appear at δ 50.7 and 59.6. The signals from δ 111.4 to δ 143.8 denote the aromatic and vinylic carbon. The signals of the ester carbonyls appear at δ 162.9 and δ 166.2. The cyclohexanone carbonyl appears at δ 170.1. The peak at *m/z* 759.90 (M^+ + 1) in the FAB spectrum, ascertains the identity of the molecule.

Similarly, the IR spectrum of **51c** showed strong carbonyl absorption at 1729 cm^{-1} which is assigned to the ester carbonyl and the stretching frequency of the carbonyl group of cycloheptanone moiety lies embedded in the ester carbonyl region. In the ^1H NMR spectrum, the multiplets from δ 1.74 to δ 1.72 and from δ 2.42 to δ 2.40 indicates the four geminal hydrogens at 3 and 6 positions and 4 and 5 positions of cycloheptanone moiety respectively. The singlets at δ 3.76 and δ 3.87 depicts the methoxy protons. The bridgehead proton appears at δ 5.68. The aromatic protons and a vinylic proton appear as multiplet from δ 7.07 to δ 7.47. In the ^{13}C NMR spectrum, the saturated carbons of cycloheptanone moiety appear at δ 27.6, δ 29.2, δ 30.2 and at δ 30.9. The signals of methoxy carbon appear at δ 53.0 and δ 53.1. The two bridgehead carbons appear at δ 47.5 and 58.1. The signals from δ 123.4 to δ 155.6 denote the aromatic and vinylic carbon. The signals of the ester carbonyls appear at δ 163.5 and δ 166.6. The cycloheptanone carbonyl appears at δ 202.7. The peak at *m/z* 773.20 (M^++1) in the FAB spectrum, ascertains the identity of the molecule.

Similarly, the IR spectrum of **51d** showed strong carbonyl absorption at 1732 cm^{-1} and a shoulder peak at 1688 cm^{-1}, which were assigned to the ester carbonyls and ring carbonyl respectively. In the ^1H NMR spectrum, the multiplets from δ 1.70 to δ 1.68 indicates the six geminal hydrogens at 4,5 and 6 positions and from δ 2.47 to 2.45 indicates four geminal hydrogens at 3 and 7 positions of cyclooctanone moiety. The singlets at δ 3.75 and δ 3.80 depicts the methoxy protons. The bridgehead proton appears at δ 5.68. The aromatic

protons and a vinylic proton appear as multiplet from δ 7.08 to δ 7.52. In the ^{13}C NMR spectrum, the saturated carbons of cyclooctanone moiety appear at δ 25.1, 26.4, 28.9, 29.3, 29.6. The signals of methoxy carbon appear at δ 52.6 and 52.4. The two bridgehead carbons appear at δ 47.5 and 60.3. The signals from δ 121.5 to 155.9 denote the aromatic and vinylic carbon. The signals of the ester carbonyls appear at δ 163.7 and 166.9. The cyclooctanone carbonyl appears at δ 206.3. The peak at *m/z* 787.39 (M^{+} + 1) in the FAB spectrum, ascertains the identity of the molecule.

The IR spectrum of **51e** showed strong carbonyl absorption at 1729 cm^{-1} and a shoulder peak at 1683 cm^{-1}, which were assigned to the ester carbonyls and ring carbonyl respectively. In ^{1}H NMR spectrum, singlet at δ 0.73 corresponds to the *t*-butyl protons and multiplet from δ 1.57 to δ 1.54 denotes the hydrogen at 4-position of *t*-butyl cyclohexanone moiety. The geminal hydrogens at position 3 of cyclohexanone appear as multiplet from δ 1.94 to 2.41 respectively. The singlets at δ 3.75 and δ 3.88 depicts the methoxy protons. The bridgehead proton appears at δ 5.68. The aromatic protons and a vinylic proton appear as multiplet from δ 7.09 to δ 7.46. The peak at *m/z* 815.31 (M^{+} + 1) in the FAB spectrum, ascertains the identity of the molecule.

5.4.1.2. Diels-Alder Reaction of Bisanthracenes (51f) with Dibenzoylacetylene (DBA)

The bisdibenzobarrelene **51f** were synthesized *via* Diels-Alder reaction of the bisanthracene **52e** with the dienophile DBA (**48**, excess) in dry xylene under reflux. The bisadducts were formed only in appreciable yield accompanied by polymerisation of DBA (Scheme 5.17).
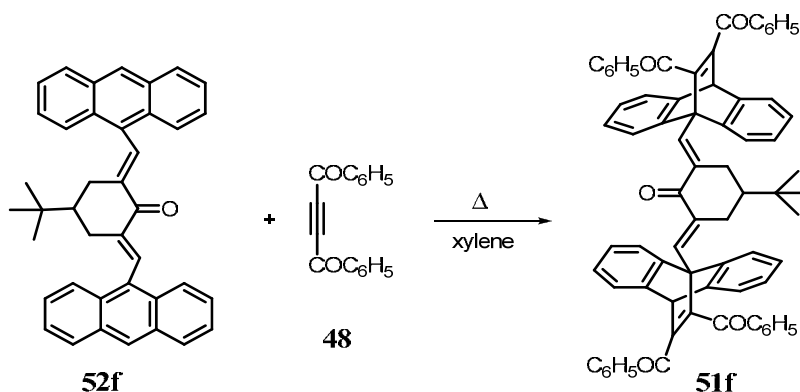
Scheme 5.17

The spectral analysis of the bisadduct **51f** matched with compound **51e**, except it showed some extra aromatic peaks in ^{1}H NMR.

5.4.2. Photochemistry of Bisdibenzobarrelenes

Based on the reports that dibenzobarrelenes undergo interesting phototransformations, we carried out the irradiation experiments on the above bisdibenzobarrelene samples. We anticipated the flowing possibilities here:

1) barrelene-semibullvalene rearrangement

2) barrelene-cyclooctatetraene rearrangement

3) *cis-trans* isomerization around the enone component

4) hitherto unknown reaction pathways

All irradiations were done in benzene purged with nitrogen at 300 nm using a Rayonet Photochemical Reactor. The criterion for the selection of 300 nm lamps for irradiation was based on a simple Beer-Lambert calculation which reveals that for bulk reactivity, photolysis wavelength near the absorption tail should be used or else the incident radiation will be absorbed near the surface.

Bisdibenzobarrelene posses $S_0 \rightarrow S_1$ transition at 280 nm region. Due to the solubility of the bisdibenzobarrelenes in benzene, and its transparency at the 300 nm region, led us to opt benzene as ideal solvent for photochemical studies. Studies have shown that sensitizers transfer their triplet energy to the acceptor bisdibenzobarrelenes, thereby quenching the singlet excited state of the substrate promoting the triplet mediated pathway. Even after 20 hours no new products were observed, where starting compound remained as such along with some polymeric material. Since bisbarrelenes exhibited strong absorption in the 200-350 nm region, we could not use a suitable sensitizer to examine triplet reactivity of these molecules. The best we could do was to irradiate very dilute solutions of **51a-f** in acetone. We fixed the concentration of acetone solution to the level where acetone absorbed most of the light. However, the new product were formed under these sensitized irradiation conditions as well.

5.4.3. Conclusion

The bisdibenzobarrelenes **51a-f** was found to be mostly stable under irradiation condition employed by us. The presence of intractable mixture confirms slight photochemical conversion. The UV absorption spectrum of monobarrelene connected to alkenone is having more or less similar in absorption spectra to bisbarrelenes prepared by us. So some radiationless energy dissipations are occurring in the excited state of bisdibenzobarrelenes in the excited state making it different from the reactions of monobarrelene. The vibrational motion of dibenzobarrelene system connected to highly complicated system can dissipate energy, which in turn can prevent the system largely from undergoing reactions in larger amounts. In other words, fast radiationless decay (less fluorescence) from the excited state can prevent it from undergoing reactions.

5.5. Experimental Section

5.5.1. General Techniques

General information about the experiments is given in section **2.5.1** of Chapter **2**. Photochemical reactions were carried out in a Rayonet reactor fitted with sixteen lamps.

5.5.2. Starting Materials

Dimethyl acetylenedicarboxylate (DMAD) was purchased from Sigma-Aldrich and was used as received. Solvents were distilled and dried as per requirements.

5.5.2.1. Dibenzoylacetylene (48)

Dibenzoylacetylene was prepared by a known method (72%, mp 109-112 °C).[23]

5.5.3. Synthesis of Bisdibenzobarrelenes 51a-f

5.5.3.1. Synthesis of Bisdibenzobarrelene 51a

Bisanthracene **52a** (1.00 g, 2.2 mmol) was dissolved in dry xylene (8 mL) under inert atmosphere. DMAD **43** (1.39 g, 9.8 mmol) was added to it and stirred under reflux for 12 h. Solvent was removed under vacuum and the residue subjected to silica gel column chromatography to remove the excess dienophile using 85:15 hexane-ethyl acetate solvent mixture to afford **51a** as a white powder. mp decomposed > 300 °C.
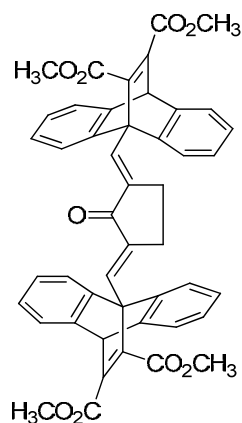
Yield 55%;

UV λ_{max} (CH$_2$Cl$_2$) 198 (ε 20,900), 250 (ε 34,900), 300 (ε 2900); **IR** (KBr) ν_{max} 1728, 1684, 1201, 894 cm^{-1};

^{1}H NMR (300 MHz, CDCl$_3$) : δ 7.72 (s, 2H), 7.47-7.44 (m, 4H), 7.32-7.31 (m, 4H), 7.09-7.06 (m, 8H), 5.68 (s, 2H), 3.83 (s, 6H), 3.77 (s, 6H), 2.44 (s, 4H);

^{13}C NMR (75 MHz, CDCl$_3$) : δ 194.4, 167.2, 163.8, 52.9, 52.2, 50.9, 28.8, 27.7;

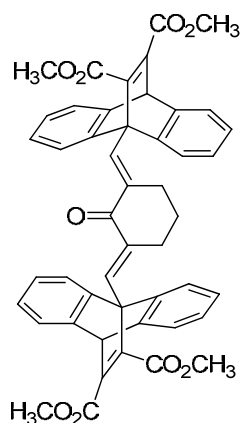**MS** (FAB, [M$^+$+1]): Calcd for C$_{47}$H$_{36}$O$_9$: 744.23; Found: 745.36;

Elemental analysis calculated for C$_{47}$H$_{36}$O$_9$: C, 75.79; H, 4.87; O, 19.33. Found: C, 75.77; H, 4.77; O, 19.23.

5.5.3.2. Synthesis of Bisdibenzobarrelene 51b

Bisanthracene **52b** (1.00 g, 2.1 mmol) was dissolved in dry xylene (8 mL) under inert atmosphere. DMAD **43** (1.35 g, 9.5 mmol) was added to it and stirred under reflux for 12 h. The solvent was removed under vacuum and the residue subjected to silica gel column chromatography to remove the excess dienophile using 85:15 hexane-ethyl acetate solvent mixture to afford **51b** as a white powder. mp decomposed > 300 °C.

Yield 55%;

UV λ_{max} (CH$_2$Cl$_2$) 198 (ε 18,900), 250 (ε 86,900), 300 (ε 2900); **IR** (KBr) ν_{max} 1729, 1683, 1234, 1045, 769 cm^{-1}; **^{1}H NMR** (300 MHz, CDCl$_3$) : δ 7.46-7.37 (m,10H),

7.09-7.06 (m, 8H), 5.68 (s, 2H), 3.90 (s, 6H), 3.76 (s, 6H), 2.37-2.34 (m, 4H), 1.67-1.62 (m, 2H); ^{13}**C NMR** (75 MHz, CDCl$_3$) : δ 170.1, 166.2, 162.9, 143.8, 111.4, 59.6, 51.9, 51.0, 50.7, 31.3, 28.7;

MS (FAB, [M$^+$+1]): Calcd for C$_{48}$H$_{38}$O$_9$: 758.25; Found: 759.90;

Elemental analysis calculated for C$_{48}$H$_{38}$O$_9$: C, 75.98; H, 5.05; O, 18.98.   Found: C, 75.87; H, 5.07; O, 18.90.

5.5.3.3. Synthesis of Bisdibenzobarrelene 51c

Bisanthracene **52c** (1.00 g, 2.0 mmol) was dissolved in dry xylene (8 mL) under inert atmosphere. DMAD **43** (1.31 g, 9.2 mmol) was added to it and stirred under reflux for 12 h. The solvent was removed under vacuum and the residue subjected to silica gel column chromatography to remove the excess dienophile using 85:15 hexane-ethyl acetate solvent mixture to afford **51c** as a white powder. mp decomposed > 300 °C.

Yield 40%;
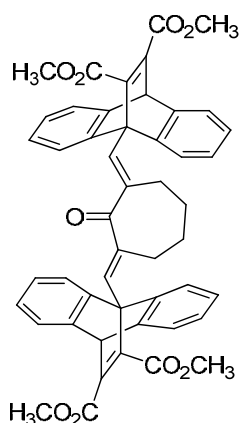
UV λ$_{max}$ (CH$_2$Cl$_2$) 198 (ε 37,900), 250 (ε 98,900), 300 (ε 2800); **IR** (KBr) ν$_{max}$ 1729, 1200, 1008, 798 cm^{-1};

^{1}**H NMR** (300 MHz, CDCl$_3$) : δ 7.47-7.37 (m, 10H), 7.09-7.07 (m, 8H), 5.68 (s,2H), 3.87 (s, 6H), 3.76 (s, 6H), 2.42-2.40 (m, 4H), 1.74-1.72 (m, 4H);

^{13}**C NMR** (75 MHz, CDCl$_3$) : 202.7, 166.6, 163.5, 155.6, 123.4, 58.1, 53.1, 53.0, 47.5, 30.9, 30.2, 29.2, 27.6;

MS (FAB, [M$^+$+1]): Calcd for C$_{49}$H$_{40}$O$_9$: 772.26; Found: 773.20;

Elemental analysis calculated for C$_{49}$H$_{40}$O$_9$: C, 76.15; H, 5.22; O, 18.63. Found: C, 76.25; H, 5.12; O, 18.67.

5.5.3.4. Synthesis of Bisdibenzobarrelene 51d

Bisanthracene **52d** (1.00 g, 2.0 mmol) was dissolved in dry xylene (8 mL) under inert atmosphere. DMAD **43** (1.27 g, 9.0 mmol) was added to it and stirred under reflux for 12 h. The solvent was removed under vacuum and the residue subjected to silica gel column chromatography to remove the excess dienophile using 85:15 hexane-ethyl acetate solvent mixture to afford **51d** as a white powder. mp decomposed > 300 °C.

Yield 40%;

UV λ_{max} (CH$_2$Cl$_2$) 198 (ε 57,900), 250 (ε 99,900), 300 (ε 2600); IR (KBr) ν_{max} : 1732, 1688, 1210, 1021,789 cm^{-1};

^{1}H NMR (300 MHz, CDCl$_3$) : δ 7.52-7.45 (m, 10H), 7.10-7.08 (m, 8H), 5.68 (s, 2H), 3.80 (s, 6H), 3.75 (s, 6H), 2.47-2.45 (m, 4H), 1.70-1.68 (m, 6H);

^{13}C NMR (75 MHz, CDCl$_3$) : δ 206.3, 166.9, 163.7, 155.9, 121.5, 60.3, 52.6, 52.4, 47.5, 29.6, 29.3, 28.9, 26.4, 25.1;

MS (FAB, [M$^+$+1]): Calcd for C$_{50}$H$_{42}$O$_9$: 786.28; Found: 787.39;

Elemental analysis calculated for C$_{50}$H$_{42}$O$_9$: C, 76.32; H, 5.38; O, 18.30. Found: C, 76.34; H, 5.28; O, 18.40.
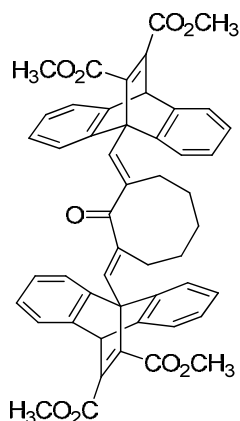
5.5.3.5. Synthesis of Bisdibenzobarrelene 51e

Bisanthracene **52e** (1.00 g, 1.9 mmol) was dissolved in dry xylene (8 mL) under inert atmosphere. DMAD **43** (1.21 g, 8.5 mmol) was added to it and stirred under reflux for 12 h. The solvent was removed under vacuum and the residue subjected to silica gel column chromatography to remove the excess dienophile using 85:15 hexane-ethyl acetate solvent mixture to afford **51e** as a white powder. mp decomposed > 300 °C.
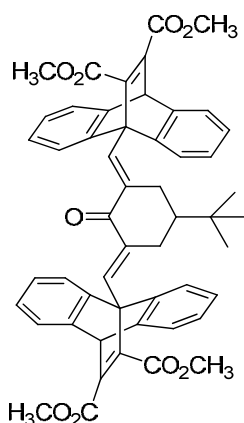
Yield 57%;

UV λ_{max} (CH$_2$Cl$_2$) 198 (ε 61,900), 250 (ε 99,900), 300 (ε 2600)**; IR** (KBr) ν_{max}: 1729, 1683,898, 769 cm^{-1};

^{1}H NMR (300 MHz, CDCl$_3$) : δ 7.46-7.38 (m, 10H), 7.12-7.09 (m, 8H), 5.68 (s, 2H), 3.88 (s, 6H), 3.75 (s, 6H), 2.41-2.36 (m, 2H), 2.01-1.94 (m, 2H), 1.57-1.54 (m, 1H), 0.73 (s, 9H);

^{13}C NMR (75 MHz, CDCl$_3$) : δ 195.0, 141.3, 132.7, 129.0, 128.9, 127.3, 124.8, 23.9;

MS (FAB, [M$^+$+1]): Calcd for C$_{52}$H$_{46}$O$_9$: 814.31; Found: 815.31;

Elemental analysis calculated for C$_{52}$H$_{46}$O$_9$: C, 76.64; H, 5.69; O, 17.67. Found: C, 76.54; H, 5.78; O, 17.49.

5.5.3.6. Synthesis of Bisdibenzobarrelene 51f

A sample of bisanthracene **52e** (1.00 g, 1.9 mmol) was dissolved in minimum quantity of dry xylene and DBA **48** (1.99 g, 8.5 mmol) was added and the mixture was refluxed for about 12 h under inert atmosphere. The solvent was removed under vacuum and the residue subjected to silica gel

column chromatography to remove the excess dienophile using 85:15 hexane-ethyl acetate solvent mixture to afford **51f** as a white powder. mp decomposed > 300 °C.
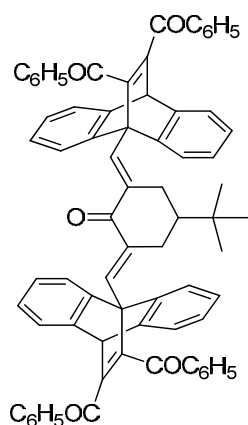
Yield 50%;

UV λ_{max} (CH$_2$Cl$_2$) 198 (ε 37,900), 250 (ε 98,900), 300 (ε 2800); **IR** (KBr) ν_{max} : 1729, 1683,1110, 987, 759 cm^{-1};

^{1}H NMR (300 MHz, CDCl$_3$) : δ 7.87-7.48 (m, 10H), 7.42-7.33 (m, 12H), 7.14-6.92 (m, 16H), 5.51 (s, 2H), 2.31-2.26 (m, 4H), 1.56-1.53 (m, 1H), 0.71 (s, 9H);

^{13}C NMR (75 MHz, CDCl$_3$) : δ 195.2, 145.5, 142.3, 141.2, 131.7, 129.8, 127.9, 126.3, 125.8, 23.2;

MS (FAB, [M$^+$+1]): Calcd for C$_{72}$H$_{54}$O$_5$: 998.39; Found: 999.43;

Elemental analysis calculated for C$_{72}$H$_{54}$O$_5$: C, 86.55; H, 5.45; O, 8.01. Found: C, 86.54; H, 5.48; O, 8.03.

5.5.4. Irradiation of Bisdibenzobarrelenes 51a-f

5.5.4.1. Irradiation of Bisdibenzobarrelene 51a

A solution of **51a** (40 mg, 0.05 mmol) was dissolved in dry benzene (80 mL) and was irradiated in a Rayonet photochemical reactor (RPR) at 300 nm for 12 h after purging with dry N$_2$ gas. The solvent was removed and the residue was purified by column chromatography on silica gel. Elution with a

mixture (4:1) of hexane and ethyl acetate gave the starting compound **51a** (50%) along with some intractable material.

In a repeat run, an acetone solution of **51a** was irradiated using RPR (300 nm) for 5h gave the starting compound (50%) along with some intractable mixture.

In another run, an acetone solution of **51a** was irradiated using RPR (254 nm) for 5h gave the starting compound (50%) along with some intractable mixture.

5.5.4.2. Irradiation of Bisdibenzobarrelene 51b

A solution of **51b** (40 mg, 0.05 mmol) was dissolved in dry benzene (80 mL) and was irradiated in a photochemical reactor at 300 nm for 12 h after purging with dry N_2 gas. The solvent was removed and the residue was purified by column chromatography on silica gel. Elution with a mixture (4:1) of hexane and ethyl acetate gave the starting compound **51b** (50%) along with some intractable material.

In a repeat run, an acetone solution of **51b** was irradiated using RPR (300 nm) for 10h gave the starting compound (50%) along with some intractable mixture.

5.5.4.3. Irradiation of Bisdibenzobarrelene 51c

A solution of **51c** (40 mg, 0.05 mmol) was dissolved in dry benzene (80 mL) and was irradiated in a photochemical reactor at 300 nm for 12 h after purging with dry N_2 gas. Removal of the solvent under reduced pressure gave a residual solid, which was chromatographed over silica gel. Elution with a mixture (4:1) of hexane and ethyl acetate gave the starting compound **51c** (50%). Further elution with a mixture of hexane and ethyl acetate (1:1) gave some intractable mixture.

In a repeat run, an acetone solution of **51c** was irradiated using RPR (300 nm) for 10h to get the starting compound (50%) along with some intractable mixture.

5.5.4.4. Irradiation of Bisdibenzobarrelene 51d

A solution of **51d** (40 mg, 0.05 mmol) was dissolved in dry benzene (80 mL) and was irradiated in a photochemical reactor at 300 nm for 12 h after purging with dry N_2 gas. The solvent was removed and the residue was purified by column chromatography on silica gel. Elution with a mixture (4:1) of hexane and ethyl acetate gave the starting compound **51d** (50%) along with some intractable material.

In a repeat run, an acetone solution of **51d** was irradiated using RPR (300 nm) for 10h yielding the starting compound (50%) along with some intractable mixture.

5.5.4.5. Irradiation of Bisdibenzobarrelene 51e

A solution of **51e** (40 mg, 0.04 mmol) was dissolved in dry benzene (80 mL) and was irradiated in a photochemical reactor at 300 nm for 12 h after purging with dry N_2 gas. The solvent was removed and the residue was purified by column chromatography on silica gel. Elution with a mixture (4:1) of hexane and ethyl acetate gave the starting compound **51e** (50%) along with some intractable material.

In a repeat run, an acetone solution of **51e** was irradiated using RPR (300 nm) for 10h to get the starting compound (50%) along with some intractable mixture.

5.5.4.6. Irradiation of Bisdibenzobarrelene 51f

A solution of **51f** (40 mg, 0.04 mmol) was dissolved in dry benzene (80 mL) and was irradiated in a photochemical reactor at 300 nm for 12 h after purging with dry N_2 gas. The solvent was removed and the residue was

purified by column chromatography on silica gel. Elution with a mixture (4:1) of hexane and ethyl acetate gave the starting compound **51f** (50%) along with some intractable material.

In a repeat run, an acetone solution of **51f** was irradiated using RPR (300 nm) for 10h to get the starting compound (50%) along with some intractable mixture.

5.6. References

1.   Kloetzel, M. *Organic Reactions.* **1967**, *4*, 1.

2.   Shea, K. J. *Tetrahedron.* **1980**, *36*, 1683.

3.   Acena, J. L.; Alba, de E.; Arjona, O.; Plumet, J. *Tetrahedron Lett.* **1996**, *37*, 3043.

4.   Wiseman, J. R.; French, N. I.; Hallmark, R. K. *Tetrahedron Lett.* **1978**, 3765.

5.   Pecanha, E. P.; Fraga, C. A. M.; Barreiro, E. J. *Heterocycles.* **1998**, *48*, 2621.

6.   Diels, O.; Alder, K. *Ann.* **1931**, *486*, 191.

7 .   Baldwin, J. E.; Lopez, R. C. G. *Tetrahedro*n. **1983**, *39,* 1487.

8.   Ciganek, E. *J. Org. Chem.* **1980***, 45*, 1497.

9.   Alder, K.; Stein, G. *Angew. Chem.* **1937**, *50*, 510.

10.   Sauer, J.; Wiest, H.; Mielert, A. *Chem. Ber.* **1964**, *97*, 3183.

11.   (a) Meek, J. S.; Dann, J. R. *J. Org. Chem.* **1956**, *21*, 968. (b) Meek, J. S.; Wilgus, D. R.; Dann, J. R. *J. Am. Chem. Soc.* **1960**, *82*, 2566.

12 .   (a) Zimmerman, H. E. In *Rearrangements in Ground and Excited States*; de Mayo, P., Ed.; Academic Press: New York, **1980**; *3*, Chapter 16, pp 131. (b) Zimmerman, H. E. In *Organic Photochemistry*; Padwa, A, Ed.; Marcel Dekker: New York, **1991**; *11*, 1.

13.   Ciganek, E. *J. Am. Chem. Soc.* **1966**, *88*, 2882.

14.   Adam, W.; de Lucchi.; Peters, K.; Peters, E. M.; von Schering, H. G. *J. Am. Chem. Soc.* **1982**, *104*, 5747.

15.   Chen, J.; Scheffer, J. R.; Trotter, J. *Tetrahedron.* **1992,** *48,* 3251.

16.   Rabideau, P. W.; Hamilton, J. B.; Friedmann, L. *J. Am. Chem. Soc.* **1968**, *90*,   4465.

17.   Chen, J.; Scheffer, J. R.; Trotter, J. *Tetrahedron.* **1992**, *48*, 3251.

18.   Richards, K. E.; Tillman, R. W.; Wright, G. J. *Aust. J. Chem.* **1975**, *28*, 1289.

19.   Paquette, L. A.;Bay, E. *J. Am. Chem. Soc.* **1984**, *106*, 6693.

20.   Paddick, R. G.; Richards, K. E.; Wright, G. J. *Aust. J. Chem.* **1976**, *29*, 1005.

21.   (a) Kumar, S. A.; Rajesh, C. S.; Das, S.; Rath, N. P.; George, M. V. *J. Photochem. Photobiol. A.* **1995**, *86*, 177. (b) Kumar, S. A.; Ramaiah, D.; Eldho, N. V.; Das, S.; Rath, N. P.; George, M. V. *J. Photochem. Photobiol. A.* **1997**, *103*, 69. (c) Murthy, B. A. R. C.; Prathapan, S.; Kumar, C. V.; Das, P. K.;George, M. V. *J. Org. Chem.* **1985**, *50*, 2533. (d) Sajimon, M. C.; Ramaiah, D.; Muneer, M.; Rath, N. P.; George, M. V. *J. Photochem. Photobiol. A. 2000*, *136*, 209.

22.   Sajimon, M. C.; Ramaiah, D.; Ajayakumar, S.; Rath, N. P.; George, M. V. *Tetrahedron.* **2000,** *56,* 5421.

23.   Lutz, R. E.; Smithy, W. R. *J. Org. Chem.* **1951**, *16*, 648.